A Passive Pediatric Exoskeleton to Improve the Walking Ability of Children with Neuromuscular Disorders

Jessica Zistatsis

A thesis

submitted in partial fulfillment of the

requirements for the degree of

MASTER OF SCIENCE IN MECHANICAL ENGINEERING

University of Washington

2018

Committee:

Katherine M. Steele

Kristie Bjornson

Patrick Aubin

Mark Ganter

Program Authorized to Offer Degree:

Mechanical Engineering

University of Washington

Abstract

A Passive Pediatric Exoskeleton to Improve the Walking Ability

of Children with Neuromuscular Disorders

Jessica Zistatsis

Chair of the Supervisory Committee:
Katherine M. Steele, Ph.D.
Assistant Professor
Mechanical Engineering

Children with neuromuscular disorders, such as cerebral palsy (CP) often have walking limitations. Assistive devices for home use, such as walkers and crutches, may not provide optimal participation opportunities or lead to effective walking dosage. Even with therapy and assistive devices, children with CP get significantly less walking practice than typically developing peers. Recent research has shown that passive exotendon driven exoskeletons are effective for improving walking outcomes for adults with neurologic injury. A passive pediatric exoskeleton using exotendons was developed and evaluated for improving gait of children with CP and other forms of hemiparesis. Three typically developing (TD) children and two children with hemiparesis walked on level ground with the exoskeleton at three stiffness settings. Motion capture and electromyography data were collected to evaluate changes in joint kinematic symmetry, walking speed, and step width. The exoskeleton had no significant impact on gait

outcome measures for TD participants, but for participants with hemiparesis the exoskeleton significantly improved kinematic joint symmetry at the hip or the ankle depending on the participant's natural gait pattern. These results suggest that exotendon-based designs for passive exoskeletons may provide a novel platform to improve walking for children with neurologic injuries and support community-based gait training.

Table of Contents

LIST OF FIGURES

LIST OF TABLES

ACKNOWLEDGEMENTS

I would like to acknowledge Kristie Bjornson, PhD, PT for her assistance with this work and expertise in clinical studies of cerebral palsy and Brian Glaister, COO for inspiring the development of a pediatric exoskeleton. Thank you to Katherine Steele, PhD for advising this research and to Keshia Peters, Heather Feldner, PhD, PT, Daniel Ballesteros, and Brianna Goodwin for assisting with data collection and processing. Also, thank you to Chris Richburg at the Seattle VA Hospital for assistance with 3D printing and to Andrea Willson for providing MATLAB code and assisting with OpenSim. Thanks to Alex Gong, Daniel Parrish, Jeffrey Bergeson, and Kira Newman for their excellent teamwork during initial prototype development in the University of Washington's Engineering Innovations in Health capstone course. Sections from the capstone report are included in this thesis.

Additionally, I would like to acknowledge my funding sources: the CoMotion Innovation Fund, the NEPDC and FDA award P50FD004907 and TREAT and NIH award R24HD065703 and P2CHD086841, the Orthotic and Prosthetic Education and Research Foundation, Inc. (OPERF) under grant number OPERF-2017-FA-1, and a 2017 Developmental Grant from the University of Washington Global Center for Integrated Health of Women, Adolescents, and Children (Global WACh) and the University of Washington Coulter Translational Research Partnership Program.

Chapter 1 INTRODUCTION

Hemiparesis is a neurologic condition in which half the body is affected by motor impairments. There are many causes for hemiparesis such as stroke, spinal cord injury, and viral infections such as nonpolio enterovirus-D68 (Khetsuriani et al. 2006). However, the largest cause of hemiparesis among children is cerebral palsy (CP) (NSCIS 2004, Krigger 2006, Agrawal et al. 2009). As such, the following sections provide background on CP and currently available assistive devices for children with CP since this is the largest population that informed and motivated this research.

1.1 Cerebral Palsy

Approximately 2-3.8 out of every 1000 children born in the United States (US) are diagnosed with CP (Krigger 2006, Cans et al. 2008, Yeargin-Allsopp et al. 2008). This population has been mostly steady or slightly downward trending depending on a child's birth weight since the 1980s both in the US and Europe (Cans et al. 2008). In 2013, there were 10,000 infants born in the US with CP, with an additional 1200-1500 preschoolers diagnosed (Palsy 2013).

CP is a non-progressive neurologic condition resulting from brain injury before, during, or shortly after birth that causes impaired movement (CerebralPalsy.org , Krigger 2006). Individuals with CP are typically classified into bilateral CP, in which both sides of the body are affected, or unilateral CP, in which one side of the body is affected. Subtypes of these classifications include quadriplegia, diplegia, and hemiplegia. Quadriplegia affects all four limbs, diplegia affects both legs, and hemiplegia affects both limbs on the same side of the body. A

study of nearly 500 children with CP in the US reported that quadriplegia affects 15%, diplegia affects 59%, and hemiplegia affects 23% (Wren et al. 2005).

The cost of care for individuals with CP varies by country, but was estimated to be $920,000 per individual (2003 dollars) in the US over an individual's lifetime (Honeycutt A 2004). Assistive devices for children cost at any given point in time an average of $3,416 (1989 dollars) per child across all devices used by children in the home, daycare, and school environments, with orthoses and prostheses accounting for 23.4% and personal mobility devices accounting for 26.5% of the these costs (Korpela et al. 1992).

1.2 Cerebral Palsy Gait and Activity

CP ambulation levels are typically categorized by the Gross Motor Function Classification System (GMFCS). Classification ranges from Level I (mild, requiring no assistive devices) to Level V (severe, requiring powered mobility devices, Table 1.1) (Palisano et al. 1997). In a study of children with CP in nine countries, it was found that 59.3% have mild impairment (Levels I-II), 11.5% have moderate impairment (Level III), and 29.3% have severe impairment (Levels IV-V) (Reid et al. 2011). A longitudinal study demonstrated that motor function declines through adolescence for GMFCS levels III-V, with peak function at an approximate age of 7 years (Hanna et al. 2009).

Children with CP demonstrate a wide variety of gait patterns. The most common gait abnormality is stiff knee gait, defined by Wren et al., (2005) as "decreased arc of knee motion from maximum knee extension in stance to peak knee flexion in swing, and/or delay in peak swing knee flexion to mid- or terminal swing" (Wren et al. 2005). Wren et al. reported that stiff knee gait is seen in 80% of CP patients visiting clinical motion analysis laboratories, and is

followed in prevalence by crouch (increased knee flexion during stance) at 69%. Specifically focusing on individuals with hemiplegia, the most common gait problem is equinus (70%) among children with no previous surgery and crouch (74%) in children with prior surgery. Equinus is characterized by increased plantarflexion during stance due to spasticity or contracture of the ankle plantarflexors and is often coupled with knee recurvatum and excessive hip extension (Rodda et al. 2001). Walking habitually with these gait abnormalities also increases the risk for bone deformities, especially rotational malalignments such femoral or tibial internal rotation (Wren et al. 2005).

Table 1-1: Characteristics of GMFCS Levels.

GMFCS Level	Characteristics
I	Ambulation and gross motor skills similar to typically-developing peers with limited speed, balance, or coordination.
II	Walk in most settings, use hand railings, minimal gross motor skills, may use handheld or wheeled mobility devices.
III	Walk with handheld mobility devices and use wheeled mobility for long distances.
IV	Require physical assistance or powered mobility for most mobility.
V	Require wheelchair in all settings and have difficulty controlling limb movements.

With the challenges caused by these gait abnormalities, children with CP do not engage in their communities as much as typically-developing (TD) children. Regardless of age and motor function, they participate in 13-53% less habitual physical activity than their TD peers (Carlon et al. 2013). Bjornson et al., (2014) reported that youth with CP in all GMFCS Levels spend significantly more time each day not walking compared to TD youth (Bjornson et al. 2014). For instance, TD youth spend on average 6 hours/day walking at a rate of 1-30 strides/min, while children with CP spend on average 39 min, one hour, and three hours less for GMFCS Levels I, II, and III, respectively. Of those who can walk with assistance, 56% don't use

that assistance at home, one third do not walk at school, and 59% do not ambulate in the community (Tieman et al. 2004).

A key to improving functional ability is practice (Adolph et al. 2003, Valvano 2004, Garvey et al. 2007). For example, after studying activity-focused motor interventions, Valvano (2004) reported that with repeated practice the coordination of the ankle and pelvis changed in children with spastic diplegia. This increased movement coordination was also associated with improvements in walking speed and efficiency. She further noted that generalizing the practiced movement of meaningful functional tasks to many situations is important, especially for children with CP in school and community environments. Garvey et al. (2007) similarly found through a neuroscience approach that children with CP require more practice to demonstrate a small level of learning compared to TD peers and thus need more "off-line learning" (Garvey et al. 2007). Bjornson et al. (2007) discussed that "interventions aimed at improving daily ambulation activity performance appear to have the most potential for change in youth with CP in GMFCS levels II and III" (Bjornson et al. 2007). These results point to a need for youth with CP to have assistive devices that offer them the same opportunities for activity in the home, school, or community as their TD peers.

1.3 Current Rehabilitation and Assistive Device Solutions

1.3.1 Clinical Solutions

Children with CP often see a therapist at least twice a week either in school or through private therapy. Physical therapists focus on improving walking activity and performance, but the goal is not on normal movement quality (Valvano 2004). However, many clinics incorporate gait training and robotic exoskeletons to facilitate movement patterns more similar to TD peers.

Gait training, such as bodyweight-supported treadmill training, is one of the most widely available treatments and supports walking practice as the participant practices movement patterns with or without therapist assistance. Treadmill training has been shown to have small, positive effects for providing repetitive, task-specific walking practice (Damiano et al. 2009) In a systematic review, Damiano & DeJong (2009) reported that the strength of evidence is weak for the effectiveness of treadmill training in pediatric populations with CP as there have been no randomized trials, but individual studies in the review demonstrated significant positive outcomes. For example, Chan et al., (2004) investigated two types of treadmill training and reported significant increases in gross motor function measure (GMFM) scores for standing, walking, running, and jumping along with significantly increased gait speed during a ten-meter walk test after 4 weeks of training. However, this study did not include a no-treatment group for comparison. Similarly, Dodd & Foley (2007) reported that bodyweight supported treadmill training effectively increased self-selected gait speed for children with CP (Dodd et al. 2007).

Robotic-assisted gait training (RAGT) has more recently been developed and can help to guide an individual's limb movements instead of the therapist needing to support or guide positioning (Lefmann et al. 2017). In a systematic review, eight of nine studies using RAGT (*e.g.*, Lokomat, Gait Trainer GT1, and ReoAmbuator) demonstrated statistically significant improvements in standing (identified through the GMFM-66: Item D) after RAGT and six of nine studies showed statistically significant improvements in walking (identified through the 10 m walk test) after RAGT. While treadmill training and RAGT are beneficial, they can only be used in the clinic and require large commitments in time and resources. Many clinics cannot offer RAGT due to the high cost of the machinery.

More recently, robotic exoskeletons that can be used to walk around the clinic and are not constrained to a treadmill have been developed. While several commercial adult exoskeletons are now available on the market, primarily for individuals with spinal cord injury and stroke (Westlake et al. 2009, Esquenazi et al. 2012, Glaister et al. 2015), no pediatric devices are currently available outside of research settings. However, initial results with robotic exoskeletons are promising. Lerner et al. (2017) developed a robotic knee exoskeleton to assist with crouch gait and tested it with eight children with spastic diplegic CP (Lerner et al. 2017, Lerner et al. 2017). With this exoskeleton, knee extension improved on average 18% during stance and total knee range of motion increased by 21°; changes in gait that are similar to outcomes after orthopedic surgery (Stout et al. 2008, De Mattos et al. 2014). Furthermore, the exoskeleton elevated muscle activity during late stance phase in the rectus femoris and semitendinosus muscles. Laubscher et al., (2017) published a conference abstract outlining the preliminary assessment of a powered pediatric lower limb orthosis for children with neurologic impairments consisting of hip, thigh, and shank segments with actuators at the hip and knee. Initial testing with a dummy representing a 32 kg child indicated the orthosis could successfully track representative predefined pediatric hip and knee trajectories (Laubscher et al. 2017). While these devices demonstrate promise for improving gait in CP, they are active devices, requiring heavy and bulky motors and batteries. The increased weight and cost of these devices largely restricts their use to clinical settings.

Treadmill training, RAGT training, and robotic exoskeletons have shown merit for improving important gait metrics, such as improved GMFM scores and walking speed, for children with CP, yet their restriction to clinical settings limits the amount of repetitious walking practice children can obtain. Thus, a need emerges to provide gait training in home and

community settings so children with CP and other neurologic injuries have the maximum opportunity to improve ambulation.

1.3.2 Home and Community Solutions

Outside of therapy, children with CP are prescribed assistive mobility devices. These include walkers (front- and rear-facing), crutches, and orthoses. While walkers and crutches often provide critical support to balance and improve mobility (Park et al. 2001), they occupy the child's hands, are difficult to navigate in tight spaces, and present challenges for traversing uneven terrain. Orthoses are braces and other such devices used to provide a base of support, facilitate training in skills, and improve efficiency of gait (Condie et al. 1995). They are fabricated by certified orthotists for each child. While orthoses can be designed to cross and assist with motion across multiple joints, children with CP are commonly prescribed ankle foot orthoses (AFOs) which cross the ankle joint, providing mediolateral ankle support and assisting with dorsiflexion and/or plantarflexion. There are many types of AFOs with the most common types in CP including hinged, leaf spring, ground reaction, or solid AFOs (Rodda et al. 2001). However, customizing these AFOs to each child's unique gait pattern remains challenging and improvements in gait are highly variable (Ries et al. 2015). Other types of orthoses for assisting with gait include the knee-ankle orthosis (KAFO) and the hip-knee-ankle orthosis (HKAFO), which is similar to the reciprocating gait orthosis (RGO) – a rigid bilateral device used to assist polio survivors. However, these multi-joint orthoses are rarely prescribed. While there is continuous research and development of powered orthoses spanning the ankle or knee, there are no passive devices that cross and provide assistance at the ankle, knee, and hip that are commonly prescribed in CP.

1.4 Exotendon-Based Exoskeletons

Passive orthoses such as AFOs have traditionally relied upon the form or structure of the device to assist motion. For example, the thickness of the material used in a solid AFO will dictate the resistance to ankle dorsiflexion as a function of ankle angle. Alternatively, passive exoskeletons rely on the energy stored in the device from the user's actions to assist motion. Collins et al., (2015) designed a passive ankle exoskeleton to reduce energy cost of walking in unimpaired populations by placing an elastic mechanism in parallel with the calf muscles to offload muscle energy that would otherwise be consumed in muscle contractions. Energy was stored in the elastic mechanism through a spring that was loaded during stance. This system reduced the metabolic cost during walking by 7% (Collins et al. 2015). In biological systems, ligaments, tendons, and other passive structures are used to assist and constrain movement (Wilson et al. 1998, Kawakami et al. 2008). These passive elements can be important contributors to efficient motion. For example, horses possess extremely efficient leg locomotion as they have long muscle tendon units spanning multiple joints (Van den Bogert 2003), whereas human lower-extremity muscle tendon units primarily span one or two joints. In systems with long tendons, energy can be saved during movement such that the negative power required at one joint may be transferred to a joint requiring positive power.

Recent research has suggested that drawing inspiration from these biological systems may enhance exoskeleton design and function. Simulations by van den Bogert (2003) suggested that using exotendons, long spring-like devices that can be integrated into exoskeletons, could assist human locomotion and reduce energy costs (Van den Bogert 2003). From simulations, he suggested that in human locomotion the most efficient exotendon system that minimized residual joint moments and residual joint power, was an exotendon spanning three joints in one leg: the

hip, knee, and ankle. This system reduced joint moments by 46% when simulated with unimpaired human walking. Van Dijk et al. (2011) applied this theory to an experimental exoskeleton with unimpaired adults and found the reduction in energy expenditure was negligible and hypothesized this was due to a required learning effect with the device and increased mass and mechanical movement constraints (Van Dijk et al. 2011). This exoskeleton idea was further investigated by Glaister et al. (2015) with their invention of Kickstart®, a mobility training tool for adults recovering from neurological injuries. Kickstart uses pulleys at the hip, knee, and ankle to provide assistive flexion moments through the exotendon. In a case series, they demonstrated increased walking speed and endurance for three adults with neurologic injury due to incomplete spinal cord injury or stroke – such a dramatic increase that patients achieved community ambulation levels (Glaister et al. 2015). Passive exotendon-based exoskeletons spanning the entire lower extremities thus provide a promising framework for reducing energy cost of walking and improving gait outcomes for individuals with neurologic injury in settings outside the clinic, and should be investigated with pediatric populations.

1.5 Thesis Objective

The long-term goal for this research is to address a gap in the therapy of children with hemiparesis, primarily by addressing the deficit of quality repetitious walking practice with a community-accessible device solution. The goal of this thesis was to develop and test a passive pediatric exoskeleton that spans the hip, knee, and ankle joints using exotendon technology. The principal contributions of this work included:

1. Design of a passive pediatric exoskeleton for children with hemiparesis

2. Analysis of the impacts of a passive exotendon-based exoskeleton on the gait of children with cerebral palsy and TD peers

Chapter 2 DEVICE DEVELOPMENT

Exotendon technology as a means of passive energy storage and return to assist with walking for people with neurological injury has previously only been investigated for adults with the Kickstart, an adult exoskeleton developed by Cadence Biomedical (Figure 2-1). Kickstart features a large hip pulley to provide a hip flexion moment, a small pulley at the knee to guide the exotendon along the exoskeleton frame, and an ankle pulley to provide a dorsiflexion moment. An extension spring in series with the exotendon is enclosed in a protective pouch between the knee and ankle joints. Challenges of the Kickstart design include its bulkiness, difficulty adjusting height due to hardware used, and its inability to assist pediatric populations. To adapt exotendon-based designs for pediatric populations safety, adjustability, and ease of use were important considerations. The following sections detail the design of PlayGait, the pediatric exoskeleton designed and tested through this thesis. The following sections identify the core functions and design specifications, document PlayGait's design features, and evaluate how well the final design meets these specifications.

Figure 2-1: Kickstart®, a passive adult exoskeleton produced by Cadence Biomedical.

2.1 Core Functions and Design Specifications

To identify the core functions and design specifications for an exotendon-based exoskeleton, we conducted phone interviews and surveys with pediatric physical therapists and parents of children with CP. These interviews and surveys were conducted to discuss current

treatment practice for CP, assistive devices used, and the challenges in achieving mobility goals for children with neuromuscular disorders. Questions included:

- What do you see as the strengths and weaknesses of current treatment options to improve walking ability for cerebral palsy and other neuromuscular disorders?
- What are the biggest challenges or unmet needs in helping children learn to walk?
- What gaps are present in your current treatment options that if met would improve your patients' functional abilities? (*e.g.*, features of assistive devices or other treatment options, amount of therapy time, amount of in-home practice time, etc.)

Parents noted that their children's walkers do not work in many environments such as on the playground or climbing school bus stairs. Further, balance and stamina are limited with these devices and occupy their children's hands, limiting participation in daily activities. Their children want to keep up with their peers and siblings, but are limited by current devices. Common themes in the PTs responses included that it is difficult for therapy to carryover from the therapy to the clinic, that there is a need for high quality repetitious walking practice, and that the lack of in-home walking practice is a huge gap in therapy.

Based upon these interviews and prior research, the following set of core functions were identified to guide the development of the pediatric exoskeleton:

- Fit children just learning to walk, as young as three years old, to support early walking practice and prevent bone deformities
- Be easily adjustable for growth (changes in height, waist size)
- Be easily don/doffed by the therapist and/or parent
- Increase walking time outside of therapy
- Promote fluid movement (minimize jerk during gait transitions)

- Fail in a predictable manner
- Prevent scratching or breaking of skin
- Remain durable

From these core functions, a set of design specifications was developed (adapted from a previous report provided in Appendix A) to guide development and provide metrics for evaluation:

- Fit / Growth: Leg length adjustable between 17.4 – 24.5 in (Kuczmarski 2002)
- Fit / Range of motion: hip abduction/adduction 13°, hip flexion/extension 45°, hip rotation 16° (Ounpuu et al. 1991)
- Don/doff and adjust within 5 minutes
- Fluid movement: Tibial accelerations of -2.09 g's peak negative anterior-posterior, 0.90 g's peak lateral, and 1.70 g's peak axial (LaFortune 1991)

2.2 PlayGait Design

To address these core functions and design specifications, this research led to the development of PlayGait, a passive pediatric exoskeleton spanning the hip, knee, and ankle that utilizes an exotendon to assist with walking for children with neuromuscular walking impairments (Figure 2-2). PlayGait was designed such that the leg supports may be removed independently so the device accommodates unilateral or bilateral users. For unilateral configurations, PlayGait allows 5 degrees of

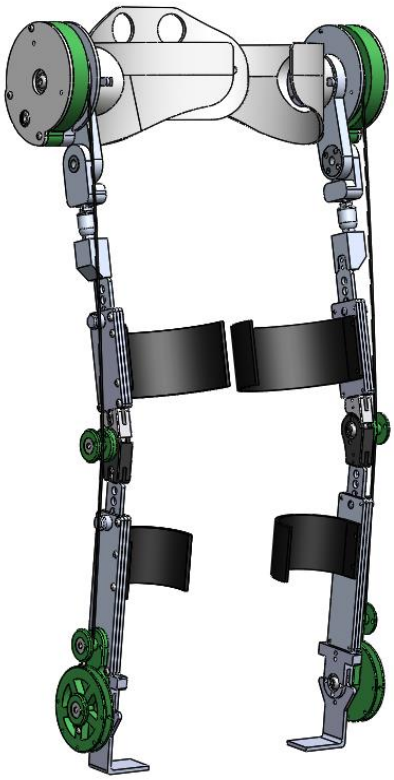

Figure 2-2: A CAD rendering of PlayGait, a passive pediatric exoskeleton, demonstrating the bilateral configuration.

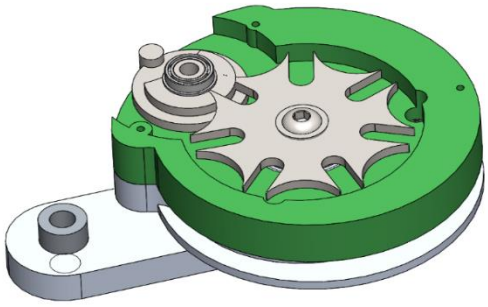

Figure 2-3: Section view of an assembled hip pulley mechanism featuring the Geneva mechanism.

freedom: knee and ankle flexion/extension in the sagittal plane and full hip range of motion (3 degrees of freedom including flexion/extension, ab/adduction, and internal/external rotation).

For an exotendon-based system, a key component is the energy storage and return mechanism. For the design of PlayGait, enclosing the energy storage and return mechanism inside the hip pulley via a spiral torsion spring was an innovation to improve safety by protecting the design from users' fingers and enabling a compact design. The spiral torsion spring connects to a Geneva mechanism for two-way ratcheting, further improving the adjustability of the device's assistance level (Figure 2-3). The Geneva mechanism consists of a circular ratchet and a pin. A user can turn the pin while the device is fully assembled to increase or

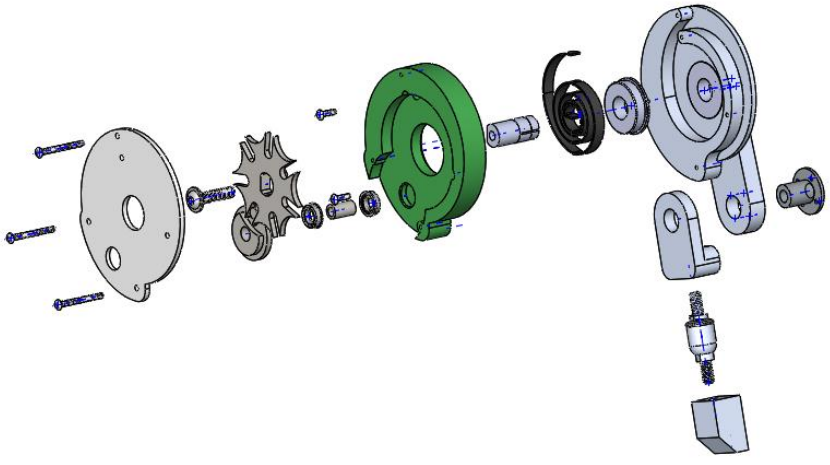

Figure 2-4: An exploded view of PlayGait's hip pulley mechanism. The spiral torsion spring (black) shares an axis of rotation with the geneva mechanism (gray disk and pin).

Figure 2-5: A unilateral assembly of PlayGait showcasing the spiral torsion spring in the hip assembly (top) connected to an exotendon wrapping anteriorly around the hip and knee pulleys and wrapping posteriorly around the ankle pulley.

decrease the winding of the spiral torsion spring, which is aligned with the ratchet (Figure 2-4). This spring is in series with an exotendon, or cable, that connects the hip, knee, and ankle pulleys (Figure 2-5). To adjust the slack length of the exotendon, a spool was enclosed in the hip pulley mechanism and secured along the same axis as the Geneva mechanism (Figure 2-6). For experimental testing with easy adjustment of the spring stiffness, the internal spiral torsion spring may be substituted with an external extension spring, as shown with the Kickstart design.

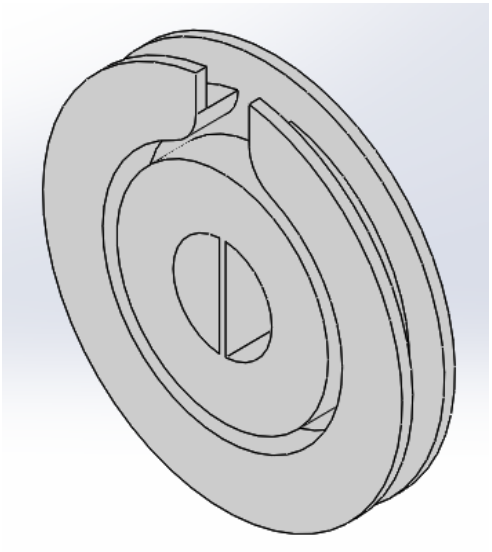

Figure 2-6: The spool used to store extra exotendon length while preloading the spring.

To address adjustability for rapidly growing children and challenges with hardware used in prior adult designs, a low-profile pin mechanism was used to allow leg length to be adjusted between 17.75 - 28.0 in (Figure 2-7). These dimensions are characteristic of the leg length for 5th percentile three-year olds and 95th percentile six-year olds, when leg length is approximately half of a child's height (Kuczmarski 2002). The pin pulls outward and swivels to lock in an open position for easy adjustment. To accommodate the full height range, the exoskeleton has two lengths of telescoping thigh struts that may be easily substituted depending on the user.

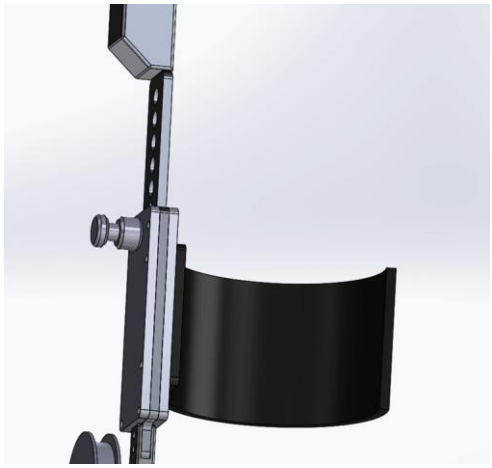

Figure 2-7: Leg strut featuring a telescoping mechanism.

Another adaptation for pediatric use was redefining the biomechanical impact of the exotendon by sizing the hip, knee, and ankle pulleys. While an optimization can be run to

optimize pulley size, similar to that presented by van den Bogert (Van den Bogert 2003) for passive adult exoskeletons, since joint moments can vary greatly between children with hemiparesis, this research focused upon selecting a baseline set of pulleys to test with a range of springs of varying stiffness. For the initial testing, PlayGait pulleys were manufactured with radii of 34.0 mm, 4.8 mm, and 26.9 mm for the hip, knee, and ankle, respectively. This design provided a baseline set of measures for evaluation with children and future research could optimize the size of pulleys and path of the exotendon based upon a child's specific gait pattern and joint moments.

Additional design components for PlayGait included the footplate and tendon spool. For community use, PlayGait would include a custom foot orthosis (Figure 2-8) replacing the flat metal stirrup shown in Figure 2-4 to allow maximum biomechanical benefit to each user through a unique fit inside their shoe. For experimental testing and clinical therapy with multiple users, PlayGait was initially designed and tested with a standard footplate that could use Velcro to secure the device around the user's shoe (Figure 2-9).

PlayGait was manufactured using steel cable for the exotendon, 7000 series aluminum for

Figure 2-8: Example custom foot orthosis attaching to PlayGait's ankle joint.

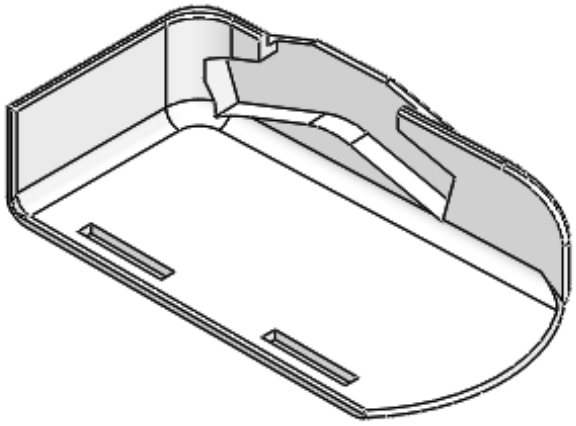

Figure 2-9: A footplate design featuring slots through which to loop Velcro. The inset area holds the stirrup which connects the footplate to the ankle.

the leg struts, polylactic acid (PLA) for the hip pulley, belt, and leg cuffs, and acrylonitrile butadiene styrene (ABS) for the footplate, tendon spool, and ankle pulley. 3D-printing was used for the PLA and ABS fabrication using FlashForge 3D Printer Creator Pro for PLA and both a Stratasys Connex 3 and a Stratasys Fortus 250mc for ABS. PlayGait's design was created in a computer-aided design (CAD) software (SolidWorks, Dassault Systems) for evaluating the design and assembly.

2.3 Device Evaluation

The PlayGait prototype was evaluated through mechanical testing to compare with the design specifications. Range of motion and leg segment adjustability measurements indicated the final PlayGait design allowed 9 in of height change and range of motion needed for walking and sitting. A pendulum test was conducted to identify tibial accelerations and demonstrated PlayGait met required peek accelerations in the anterior-posterior and lateral directions. A 3-point bend test was used to evaluate whether PlayGait's knee joint could withstand lateral loading. These test results are detailed in Appendix B.

Compared to current assistive walking devices on the market, PlayGait is the only device that meets the needs specified by therapists and parents of children with CP (Table 2.1).

Table 2-1: Comparison of PlayGait and other assistive devices.

	AFOs	Walkers	Crutches	PlayGait
Fit children age 3+	✓			✓
Don/doff with ease				✓
Increase "correct" walking outside therapy	✓ (variable results)	✗	✗	✓ (expected)
Adjust for growth	✗	✓	✓	✓
Promote fluid movement	✓			✓
Durable		✓	✓	✓
Fail predictably		✓	✓	✓
Skin health	✓	✓	✓	✓

Chapter 3 PARTICIPANT TESTING

To evaluate the PlayGait's impact on walking, a case series study was conducted with three TD children and two children with gait impairments. The protocols described were approved by the Institutional Review Board at the University of Washington and all participants and parents provided informed consent and/or assent.

3.1 Aim & Hypotheses

Aim: Determine whether PlayGait impacts gait in children with hemiparesis and TD peers.

The primary goal of this research was to analyze the impacts of a passive exotendon-based exoskeleton on the gait of children with hemiparesis and TD peers. Specifically, we sought to evaluate the impact of PlayGait on four primary outcome measures (1) gait symmetry, (2) walking speed, (3) step width, and (4) muscle activity. Gait symmetry was evaluated as the correlation of the average right and left limb kinematics in the sagittal plane. Walking speed was evaluated as average nondimensionalized walking speed (Equation 1) (Hof 1996, Vaughan et al. 2003), where V is velocity in m/s, g is acceleration due to gravity (9.8 m/s^2), and LL is leg length in meters (Vaughan et al. 2003). Leg length was defined as the vertical distance from the greater trochanter to the ground (Hof 1996). Step width was evaluated as the average step width normalized by leg length. Muscle activity during walking was evaluated from four muscles using surface electromyography (EMG) recordings.

$$\beta = \frac{V}{\sqrt{g \; x \; LL}} \qquad \text{Equation 1}$$

Among TD children, we sought to evaluate the magnitude of change of these outcome measures while walking with the PlayGait. Ideally, PlayGait would have minimal impact on walking symmetry or stability (i.e., step width) for TD children, but may increase walking speed

or reduce muscle activity due to the potential energy-savings provided by the exotendon. For children with hemiparesis, we hypothesized that:

1.1: Joint angle symmetry would increase with PlayGait compared to unassisted walking.

1.2: Walking speed would increase with PlayGait compared to unassisted walking.

1.3: Step width would decrease with PlayGait compared to unassisted walking.

1.4: Muscle activity during gait would be reduced compared to unassisted walking

While this small case series was not designed or powered to definitively address these hypotheses, this research sought to investigate and document the first observed changes with an exotendon-based pediatric exoskeleton. The results from this case series can be used to inform future design iterations and power analyses for clinical evaluation. Further, since children with hemiparesis represent a heterogeneous population with varying gait patterns, we anticipated that different stiffness levels would be most beneficial for each individual participant.

3.2 Methods

3.2.1 Participant Demographics

Data were collected for five participants (age 5 ± 2 yr, height 1.15 ± 0.10 m, weight 25.68 ± 10.84 kg): three TD children, one child with CP, and one child with hemiparesis from the D68 virus (Table 3.1).

3.2.2 Data Collection

Five participants were recruited through Seattle Children's Hospital and private physical therapy clinics in the greater Seattle area based on the inclusion criteria listed below. This study was approved by the UW Institutional Review Board (IRB) (STUDY00001789). Researchers emailed flyers to patients, colleagues, and posted notices on Facebook. Each child visited the

data collection facility, the Amplifying Movement and Performance (AMP) Lab, at the University of Washington for one data collection visit. If the participant was not a patient of the recruiting physical therapist, an additional visit was conducted or a video of the child walking was reviewed to assess the child's gait pattern and determine if he/she met the following inclusion criteria:

- For all participants:
    - Over 3 years of age
    - Ankle range of motion to neutral position
    - Hip extension range of motion ≥ 10 degrees
    - No surgery, hospitalization, or musculoskeletal injury in the past year
    - Cognitive ability to follow simple instructions in English with parent and therapist assistance
- For children with CP:
    - GMFCS Levels I-III
    - No dystonia or other restrictive muscle tone
    - Modified Ashworth Scale Levels 0-1 (pharmacological spasticity management permitted)

During the data collection session, participants were tested for three hours on average with a four-hour maximum. The full protocol is provided in Appendix C. The consent form was explained to parents and their participating children and willing parents documented written consent. Children under 7 years of age did not document written assent (verbal assent was given), but children ages 8 years and older documented assent. In a small exam room with a physical therapist or kinesiologist present, the child's height, weight, and age were recorded.

Reflective markers were placed on the child following a modified Helen Hayes marker set along with EMG sensors (2000 Hz, Trigno, Delsys, Boston, MA) (Figure 3-1). For trials with the child wearing PlayGait, the ASIS and PSIS were removed to accommodate belt placement and five markers were placed on PlayGait: one centered on each of the hip, knee, and ankle pullies and one placed anywhere on each of the thigh and shank segments. Trigno snap lead sensors were used for the gastrocnemius and Trigno IM sensors were used for the rectus femoris, biceps femoris, and tibialis anterior (Table 3-2, see Appendix C for a diagram of sensor placement). Measurements were taken of body segments (see tables in Appendix C). Motion capture data were collected with an eight-camera optical motion capture system (120 Hz, Qualisys, Sweden).

Table 3-1: Demographic data.

Participant Abbreviation	Sex	Age	Height (m)	Weight (kg)	Diagnosis	Prescribed Orthosis
TD1	M	4	1.09	42.9	TD	N/A
TD2	F	4	1.12	16.06	TD	N/A
TD3	M	8	1.33	29.3	TD	N/A
H1	M	6	1.13	21.7	R sided hemiplegic CP	AFO - FC
H2	M	3	1.08	18.46	R sided hemiparesis, D68 virus	SMO, AFO, KAFO

Abbreviations: AFO - FC = Ankle Foot Orthoses Footwear Combination, SMO = Supra Malleolar Orthosis, KAFO = Knee Ankle Foot Orthosis

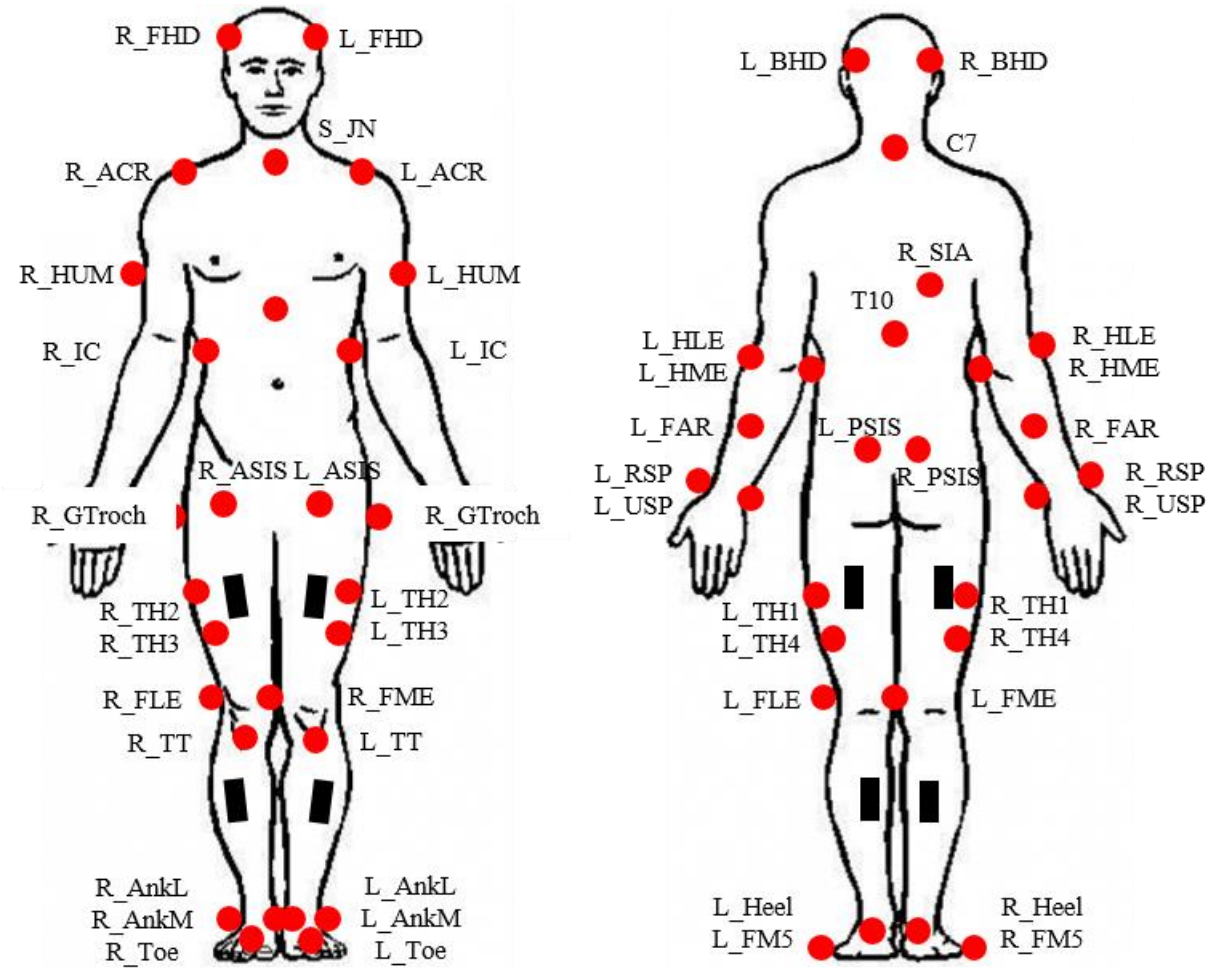

Figure 3-1: Modified Helen Hayes marker set (red dots) used for motion capture. Black boxes represent EMG sensors.

Table 3-2: Electromyography sensor placement and type.

Location	Sensor Type
Left biceps femoris long head	IM
Right biceps femoris long head	IM
Left medial gastrocnemius	Snap Lead
Right medial gastrocnemius	Snap Lead
Left rectus femoris	IM
Right rectus femoris	IM
Left tibialis anterior	IM
Right tibialis anterior	IM

Participants walked over level ground at a self-selected walking speed for three trials in each walking condition. Four walking conditions without PlayGait and with PlayGait at varying spring stiffness levels were completed in a non-randomized format (Table 3.3). In all trials, the participants wore their own tennis shoes and used no other assistive devices, such as AFOs. A static trial was completed before the first trials with and without the exoskeleton for scaling the model used for kinematic analysis and data processing. If markers fell off or moved during the trials, another static trial was completed. Medial knee and ankle markers could be removed after the static trials if the participant's gait pattern caused them to fall off.

Table 3-3 Walking trials for motion capture.

Condition	Description	Trials
1	No exoskeleton (No Exo)	1 Static + 3 Dynamic
2	Exoskeleton, low stiffness (Exo Low)	1 Static + 3 Dynamic
3	Exoskeleton, medium stiffness (Exo Med)	3 Dynamic
4	Exoskeleton, high stiffness (Exo High)	3 Dynamic

Exotendon stiffness was varied by using a series of extension springs normalized to each participant's body weight and leg length (Equation 2), where k' is the normalized spring stiffness, k is spring stiffness, LL is leg length, m is mass, and g is gravitational acceleration (Domingo et al. 2009). When selecting springs, the leg length was approximated as half the body height.

$$k' = k\,\frac{LL}{mg} \qquad \text{Equation 2}$$

Using the optimal spring stiffness from Kickstart and the average adult male body size, the normalized spring stiffness of 1.62 was selected for the medium stiffness level. The normalized stiffness for low and high settings were arbitrarily chosen as 0.62 and 2.62, respectively, to provide a wide range of stiffness values for this initial evaluation. According to the spring stiffness normalization in Equation 2, springs with a normalized stiffness closest to 0.62 for Low,

1.62 for Med, and 2.62 for High were selected for each participant out of an inventory of 14 springs with a stiffness range of 1 lb/in – 17 lb/in (Table 3.4).

Table 3-4 Spring stiffness for each participant.

	Low stiffness		Medium Stiffness		High Stiffness	
Participant	Normalized	lb/in	Normalized	lb/in	Normalized	lb/in
TD1	0.678	2.0	1.39	4.1	2.54	7.5
TD2	0.621	1.0	1.68	2.7	2.55	4.1
TD3	0.62	1.55	1.66	4.1	2.84	7.0
H1	0.721	1.55	1.67	3.6	2.33	5.0
H2	0.522	1.0	1.41	2.7	2.61	5.0

Note: Participant H2 did not advance to condition 3 and thus did not test with the high stiffness spring.

PlayGait was fit to the impaired leg of participants with hemiparesis, which was the right leg for both participants, and the right leg of all TD participants for consistency. When fitting PlayGait to each participant, the belt, femur, and tibia segments were adjusted to align the joints with the participant's joints. Foam padding was placed in the belt and cuffs for improved fit and comfort before PlayGait was strapped in place using Velcro. The exotendon and spring were slack for this step. The knee joint of the device was aligned with the participants knee center of rotation; however, this was not possible for the tallest participant (TD3) as the tibia segment could not adjust long enough for his shank and thus the femur segment was extended past the knee center of rotation and may have adversely impacted his knee kinematics. Once the device was fit to size, the exotendon was tightened to slack length (taut) using the hip ratcheting mechanism. The mechanism was ratcheted 1-2 more times to preload the spring. Each rotation click corresponds to 51.4 degrees rotation of the Geneva mechanism.

3.2.3 Data Processing

Motion capture data was processed in Qualisys by labeling all markers and gap filling marker trajectories. Each trial was truncated in length such the maximum number of steps were

included with the heel, lateral ankle, 5th metatarsal, and toe markers at or near 100%. Gaps over 100 frames were not filled, as the Qualisys-estimated marker trajectories for large gaps were inaccurate. Trials were exported into MATLAB (MathWorks, MA, USA) for post-processing and analysis.

Custom MATLAB code was used to compute spatiotemporal and muscle activation outcomes from the experimental data and to generate input files for inverse kinematic processing. OpenSim, an open-source musculoskeletal modeling software platform was used for the kinematic analysis (NCSRR, USA). See Figure 3-2 for a depiction of the MATLAB processing pipeline and Appendix D for a detailed description of the OpenSim processing pipeline.

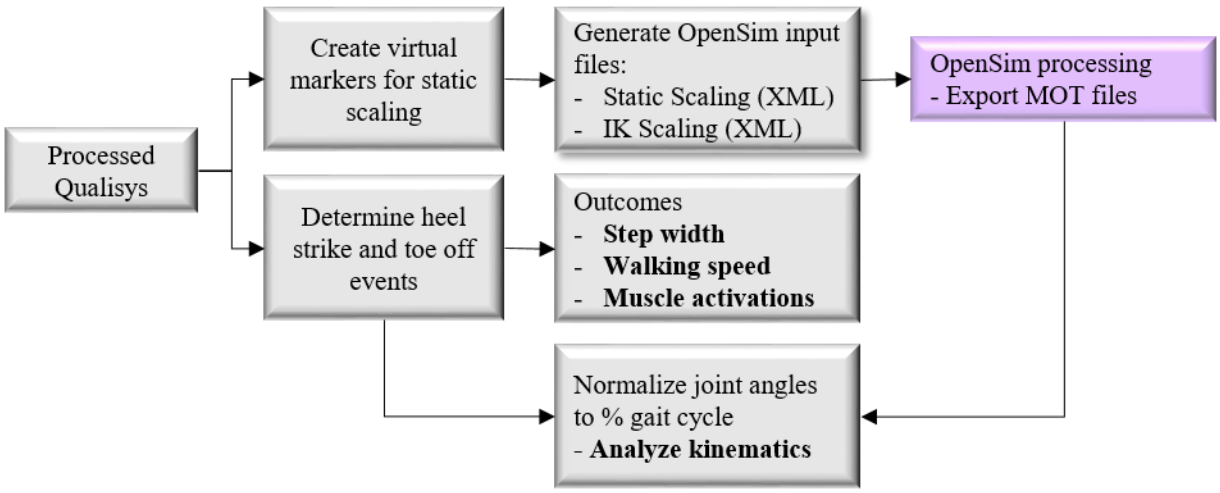

Figure 3-2: MATLAB data processing pipeline to generate outcomes of step width, walking speed, muscle activations and kinematics.

3.2.4 Outcome Measure Calculations

3.2.4.1 Kinematic Symmetry

For each participant, the average joint angles from the right and left legs of each walking condition were plotted against each other, as exemplified with the No Exo condition for P006 in

Figure 3-3. All participants were fitted with PlayGait to the right leg (the impaired leg for both participants with hemiparesis) so the horizontal axis is consistently the right/impaired leg and the vertical axis is consistently the left/unimpaired leg. MATLAB's *fitlm* function was used generate a linear fit of the joint angle comparison, and from this linear fit, the R^2 value was obtained as a measure of symmetry. Values near one indicate high symmetry between the left and right joints while values near zero indicate low symmetry based on the amount of vertical or horizontal offset between the left and right joint angle trends. Slope was also evaluated as a measure of symmetry and indicates the difference in amplitude between the left and right joint angle trends. A slope of one indicates the trend lines exhibit the same amplitude while a slope less than one indicates the left (unimpaired) joint has a higher amplitude than the right (impaired) joint.

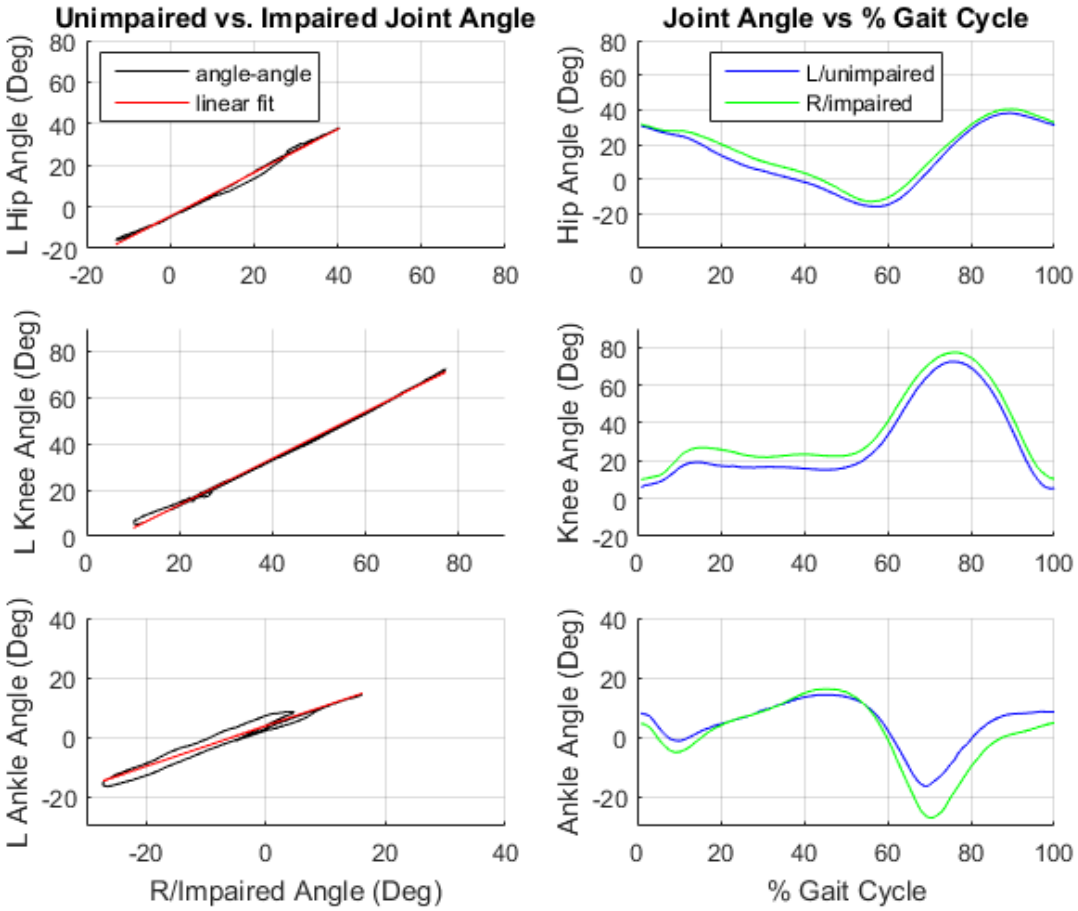

Figure 3-3: Kinematic symmetry comparison for the average of the No Exo trials for one TD subject. The left column depicts the unimpaired/left leg joint angles plotted against the impaired/right leg joint angles. High symmetry is indicated by a linear fit slope line with high correlation to the angle-angle trendline.

3.2.4.2 Spatiotemporal Parameters

Spatiotemporal changes in gait were evaluated through walking speed and step width. Walking speed was quantified by dividing the fore-aft distance traveled of the S_JN marker (Sternum – Jugular Notch) for each trial by the time to travel that distance, as velocity must be measured over a distance for subjects with unequal step lengths (Sutherland 1997). The speed was nondimensionalized for each participant according to Equation 1.

Step width was defined as the average mediolateral distance between the lateral ankle markers during double stance phase. The lateral ankle marker was chosen as it best reflects the

center of pressure with the experimental marker set. Several participants had variable in-toeing or out-toeing gait patterns so the heal and toe markers would yield variable quantification of step width. Step width was normalized by leg length (Veneman et al. 2008).

3.2.4.3 Electromyography

EMG data for each muscle was high-pass filtered at 40 Hz, rectified, low-pass filtered at 10 Hz, and then divided into gait cycles. Each gait cycle was divided into seven phases: initial loading (0-12% gait cycle), mid-stance (12-30% gait cycle), terminal stance (30-50% gait cycle), pre-swing (50-62% gait cycle), initial swing (62-75% gait cycle), mid-swing (75-87% gait cycle), and terminal swing (87-100% gait cycle). In each phase, the EMG signal was integrated to evaluate muscle activity and compared across walking conditions (Hidler et al. 2005).

3.3 Results

3.3.1 Kinematics

Overall, TD participants exhibited high symmetry across all walking conditions, but each hemiplegic participant demonstrated differing, low degrees of symmetry for each condition. Inverse kinematic plots for each participant and the corresponding correlation plots are provided in Appendix E. Average R^2 and slope values for each condition and participant are presented in Table 3.5 and Table 3-6, respectively. Averaging the R^2 values for the TD participants across conditions shows the hip had the highest level of symmetry and the ankle had the lowest level of symmetry (Figure 3-4). The differences in symmetry at each joint were similar across conditions. The average symmetry at the hip across conditions was an R^2 of 0.98 ± 0.02 with a slope of 1.08 ± 0.19 for the TD participants, versus an R^2 0.89 ± 0.08 and a slope of 1.02 ± 0.21 at the ankle. Slope values near one indicate symmetry of amplitude of the joint angles for the TD participants.

Table 3-5: R^2 correlation coefficients quantifying level of symmetry between participants' left and right legs

Condition	TD1	TD2	TD3	H1	H2
Hip					
No Exo	0.99	0.97	0.98	0.14	0.84
Exo Low	0.97	0.98	0.98	0.11	0.51
Exo Med	0.97	0.99	0.99	0.13	0.92
Exo High	0.98	0.93	0.98	0.13	
Knee					
No Exo	0.99	0.96	0.98	0.63	0.35
Exo Low	0.93	0.989	0.93	0.38	0.17
Exo Med	0.92	0.95	0.97	0.41	0.17
Exo High	0.93	0.83	0.95	0.34	
Ankle					
No Exo	0.95	0.94	0.95	0.00	0.43
Exo Low	0.88	0.94	0.93	0.08	0.31
Exo Med	0.74	0.95	0.92	0.00	0.36
Exo High	0.94	0.80	0.75	0.20	

Table 3-6: Slopes of linear fit comparing participants' left and right kinematics for each condition

Condition	TD1	TD2	TD3	H1	H2
Hip					
No Exo	1.05	0.89	1.11	0.44	1.96
Exo Low	1.32	1.06	0.90	0.46	1.62
Exo Med	1.27	1.07	0.90	0.50	2.20
Exo High	1.45	1.08	0.87	0.47	
Knee					
No Exo	1.01	0.95	1.02	0.88	0.60
Exo Low	1.21	1.20	0.96	0.84	0.66
Exo Med	1.15	1.19	0.98	0.87	0.65
Exo High	1.09	1.14	0.88	0.81	
Ankle					
No Exo	0.68	0.77	1.17	0.03	0.43
Exo Low	0.86	1.01	1.38	0.22	0.56
Exo Med	0.93	1.13	1.28	0.03	0.65
Exo High	0.86	0.96	1.19	0.29	

The participants with hemiparesis demonstrated different responses to the exoskeleton based upon their impairments and gait patterns. Among these participants the slope deviated from one, demonstrating asymmetry in the amplitude of kinematic patterns. H1 demonstrated the highest symmetry at the knee for all conditions with an average R^2 of 0.44 ± .13 and slope of 0.85 ± .0.03 (Figure 3-5). The knee symmetry was relatively constant across conditions, but there was a large increase in ankle symmetry for the Exo High condition (R^2 from 0.00 to 0.20 and slope from 0.03 to 0.29 for No Exo to Exo High). H2 demonstrated consistently higher symmetry of cyclic motion at the hip compared to other joints across conditions with an average R^2 of 0.76 ± 0.22, similar to the TD participants (Figure 3-6). However, there was an offset between the left and right sides for H2 with the left side demonstrating increased flexion based on an average slope of 1.93 ± 0.30. H2 exhibited lower symmetry at the knee and ankle for both Exo conditions compared to the No Exo condition (R^2 of 0.35 versus 0.17 ± 0.00 for the knee and 0.43 versus

0.34 ± 0.04 for the No Exo and Exo conditions, respectively), but exhibited the highest hip symmetry for the Exo Med condition (R^2 of 0.92 for Exo Med versus 0.84 for No Exo and 0.51 for Exo Low). While the cyclic motion of the knee and ankle caused decreased symmetry with Exo conditions, the offset between the left and right sides improved with PlayGait for H2 (slope of 0.60 versus 0.65 ± 0.01 for the knee and 0.43 versus 0.61 ± 0.07 for the ankle for the No Exo and Exo conditions, respectively). Due to severe fatigue, H2 could not complete the high stiffness condition. He completed the three No Exo walking trials, but only two of the three Exo Low trials and one of three Exo Med trials. Furthermore, he held the hand of an adult during the Exo conditions for stability, while he walked independently for the No Exo condition which may have also impacted his measures of symmetry.

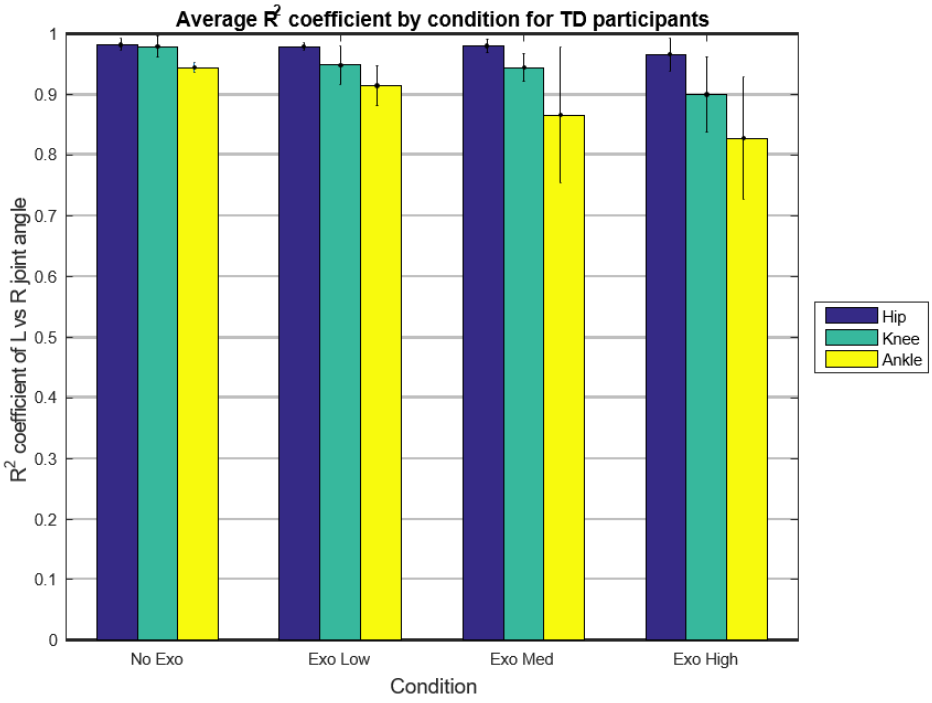

Figure 3-4: Average R^2 coefficient of each joint by condition for TD participants. Error bars represent the standard deviation of R^2 values for the three TD participants.

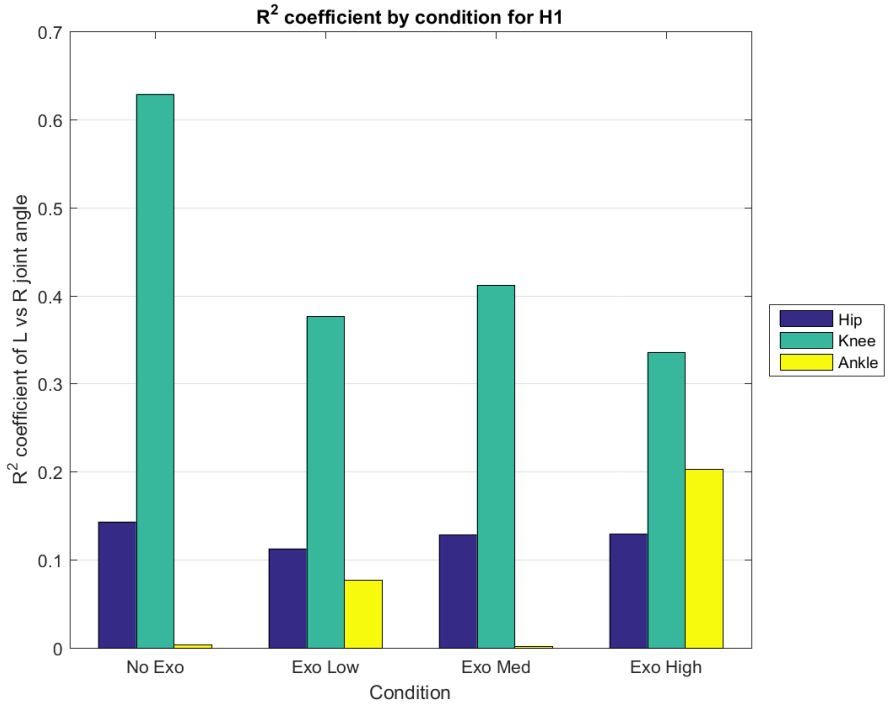

Figure 3-5: R^2 coefficient for each joint versus condition for participant H1.

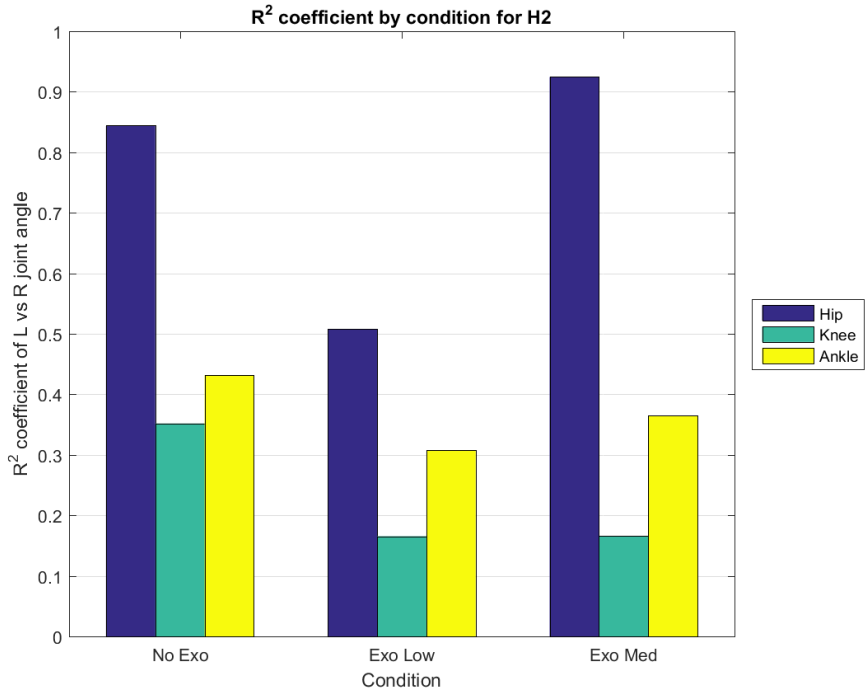

Figure 3-6: R^2 coefficient for each joint versus condition for participant H2.

3.3.2 Spatiotemporal

TD1 and TD3 had similar walking speeds across conditions, but TD2 had a lower walking speed for the No Exo condition (Figure 3-7). The average walking speed was also highly variable between the TD participants, ranging from 0.31 to 0.56 without the exoskeleton, likely due to the age range and allowing the participants to pick their self-selected speed for all trials. H1's average walking speed was 0.35 without the exoskeleton, and this speed remained similar during the Low and Med Exo conditions. However, his walking speed increased to 0.46 during the Exo High condition. H2's walking speed was 0.31 without the exoskeleton, versus 0.17 and 0.11 during the Exo Low and Med conditions. As previously noted, H2 elected to hold the therapist's hand throughout the exoskeleton conditions which likely impacted his self-selected walking speed.

Step width was similar across conditions for all participants (Figure 3-8). The average step width among the TD participants was 0.28 and 0.30 with and without the exoskeleton, respectively. H1 and H2 had an average step width of 0.42 and 0.55, respectively, without the exoskeleton. For H1, this step width remained similar across conditions, but H2 demonstrated a decreased step width (0.39) during the Exo Low condition, which may reflect his initial learning and exposure to the device.

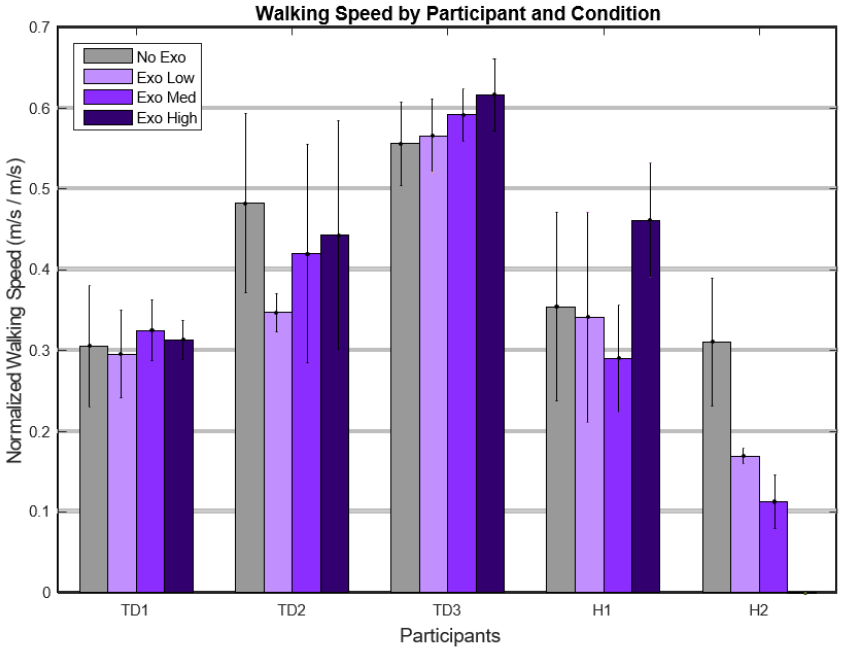

Figure 3-7: Nondimensionalized walking speed for each participant across conditions. Error bars represent standard deviations across trials.

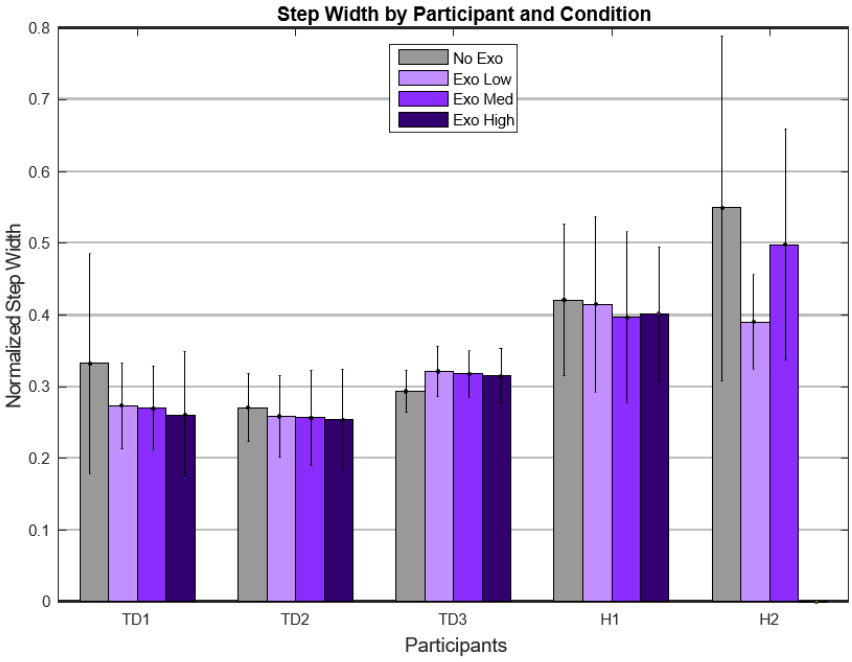

Figure 3-8: Normalized step width for each participant across conditions. Error bars represent the standard deviation across trials.

3.3.3 Electromyography

Electromyography of the rectus femoris (RF), biceps femoris (BF), medial gastrocnemius (MG), and tibialis anterior (TA) indicated variable changes in muscle activity across participants (Appendix F). The primary outcome of interest was the changes in activation in the right leg, as that was the leg receiving assistance from PlayGait. Given that the device assists with hip flexion and dorsiflexion, we anticipated that the RF (hip flexor) and ankle muscles would exhibit the greatest changes with the exoskeleton. Among the TD participants, TD1 and TD2 demonstrated similar muscle activations for all muscles with and without the exoskeleton (Figure 3-9). TD3 demonstrated increased MG activity during terminal swing and increased TA activity during terminal stance for all Exo conditions. H1 had lower activations of the RF with Exo conditions at initial loading, mid-stance, and initial swing, and in the MG with Exo Med at initial loading. H2

demonstrated lower activations in the BF with Exo Low during pre-swing and terminal swing. On the left leg, TD 3 demonstrated increased BF activity with Exo Med in initial swing and H2 demonstrated lower activity with Exo Med in initial swing. The activation patterns and magnitudes differed between TD participants and participants with hemiparesis. A representative TD activation plot for the BF and MG shows nearly zero activation during pre-swing and initial swing, but H1 demonstrated higher BF activations and H2 had higher activations in both BF and MG (Figure 3-10).

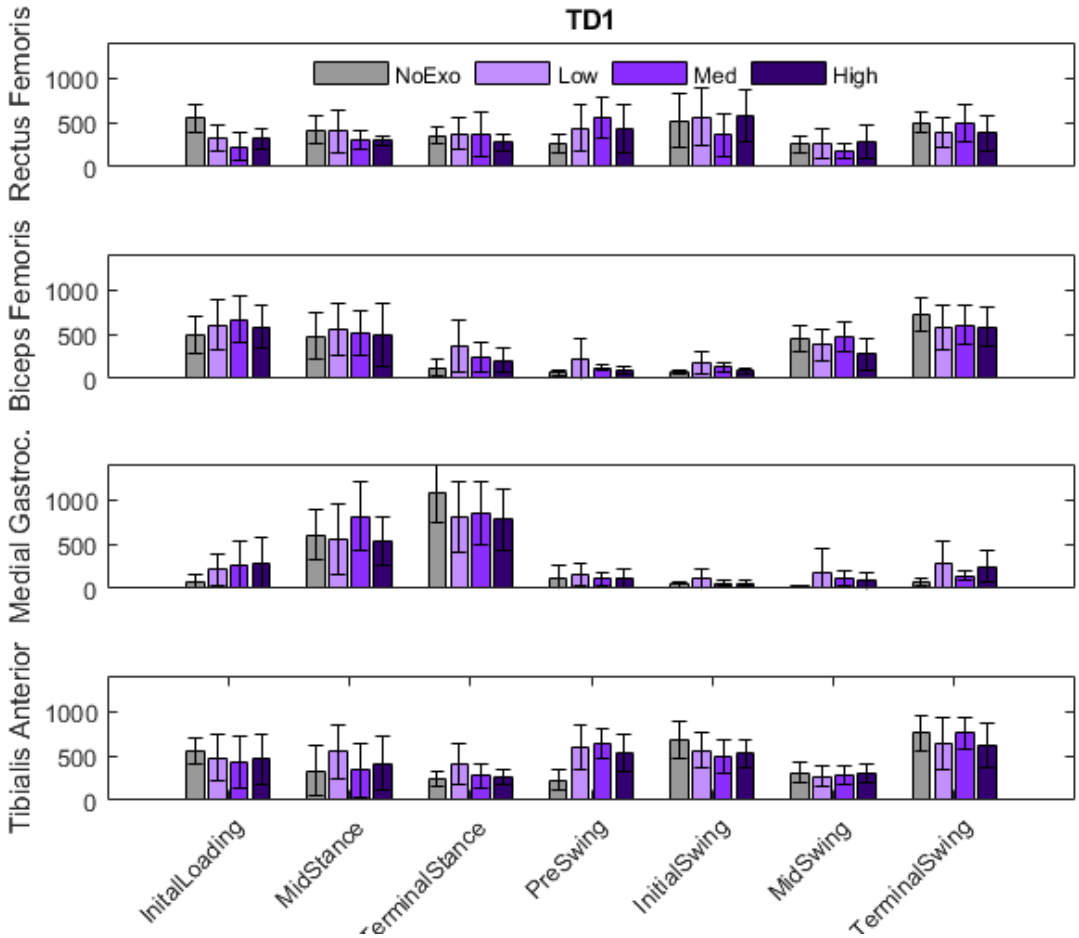

Figure 3-9: Muscle activations for a TD participant

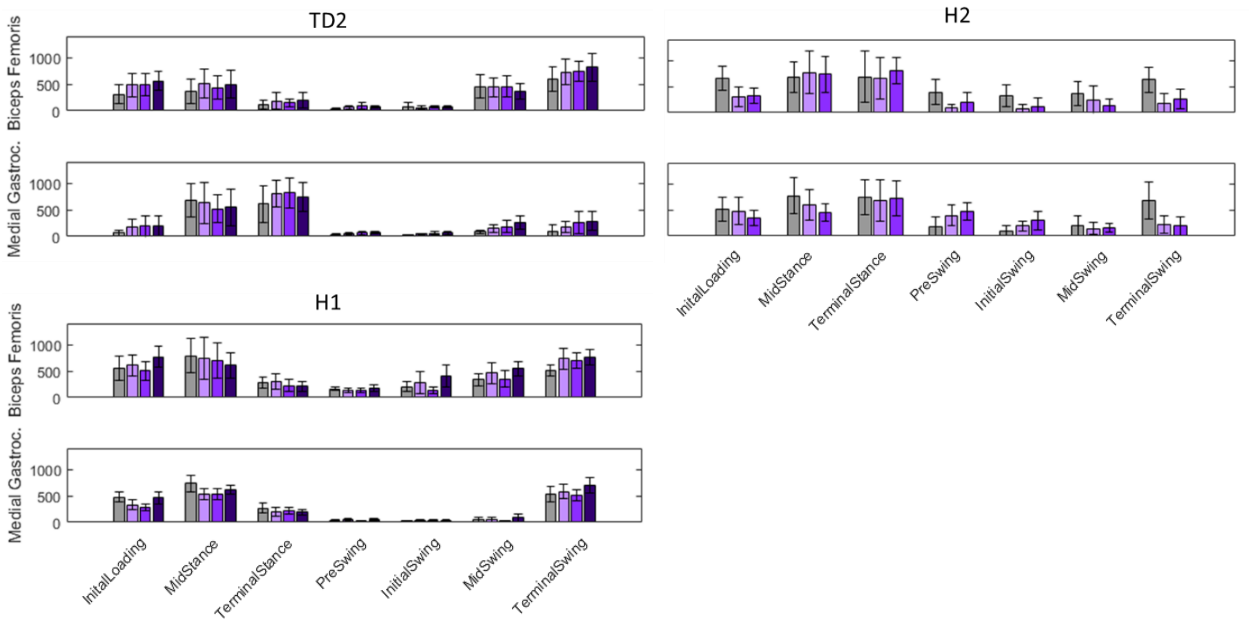

Figure 3-10: Comparison of muscle activation in the biceps femoris and medial gastric. for a representative TD participant and both participants with hemiparesis.

3.4 Discussion

The goal of this research was to evaluate changes in gait with a passive pediatric exoskeleton, specifically the impact of this device on kinematic symmetry, spatiotemporal gait parameters, and muscle activity. A functional prototype of PlayGait which used an exotendon-spring system was developed and tested with five participants. The following sections will describe the study interpretations, limitations, and recommendations for future work.

3.4.1 Kinematic Symmetry

PlayGait had minimal impact on gait symmetry for the TD participants, suggesting that the device did not hinder natural walking patterns. For participants with hemiparesis, PlayGait facilitated an increased joint correlation symmetry at one joint for each participant. H1 exhibited an increase in ankle joint symmetry for the Exo High condition while H2 increased hip symmetry for the Exo Med condition. It is interesting to note that H1 (CP) walked with an

equinus and stiff knee gait on the paretic side, and that PlayGait improved ankle symmetry, thus providing assistance to the joint seemingly most needing assistance. Additionally, H2 (D68 virus) had very low muscle tone in the paretic limb and walked by swinging his leg with the ankle plantarflexed and dropping his leg at stance. PlayGait could not address excessive plantarflexion as there is currently no locking mechanism in its ankle joint, but it facilitated improved symmetry at the hip – the joint seemingly needing the most assistance for this participant. The non-normalized spring stiffness that had the greatest improvement in joint symmetry was 5.0 lb/in for H1 (Exo High) and 2.7 lb/in for H2 (Exo Med), so no conclusions can be drawn about an optimal spring stiffness. However, H2 could not complete the study due to severe fatigue, so potentially the Exo High condition with a spring stiffness of 5.0 lb/in would have shown improved joint symmetry outcomes. These variable results between participants demonstrate that exotendon-based exoskeletons likely need to be tuned to the unique dynamics of each child's gait pattern.

3.4.2 Walking Speed and Step Width

TD participants showed similar walking speed and step width across conditions. While we hypothesized that PlayGait would increase walking speed due to the added assistance, we found that walking speed was similar across conditions for H1 and decreased for H2. H1 did increase walking speed for the Exo High condition. However, rather than attributing this to acclimatization to PlayGait or improved speed due to the assistance of PlayGait, this increase is more likely due to H1's playful behavior towards the end of the data collection session. He imagined PlayGait was a rocket booster, and would tap the hip pulley before starting each trial and "blast off" at a much higher speed than his normal walking speed. H2's significant decrease in speed for each consecutive condition may be attributed to his rapid fatigue. His parents say

this is typical during long periods of walking or standing, regardless of assistive device use. Step width was similar across conditions for all participants. Step width is often used as a rough measure of stability (Owings et al. 2004, Young et al. 2012), and thus these results suggest that wearing the rigid PlayGait device did not adversely impact walking stability, although H2 requested to hold the therapist's hand during these trials. Examining long-term changes with further instructions and gait training will be critical to understand the potential impacts of exotendon-based devices on spatiotemporal parameters of gait and walking stability for use in daily life.

3.4.3 Electromyography

Evaluation of EMG data demonstrated that muscle activation patterns differed between TD participants and participants with hemiparesis, both with and without the exoskeleton. Figure 3-10 highlights the increased muscle demand and activation commonly seen among children with hemiparesis (Unnithan et al. 1996, Crenna 1998, Damiano et al. 2000). With PlayGait, two of the three TD participants had similar muscle activity across conditions, but TD3 demonstrated increased muscle activity in the MG during terminal swing and in TA during terminal stance. Among the participants with hemiparesis, muscle activity decreased in the right leg with PlayGait, but the muscle with reduced activity and the phase of gait in which the reduction occurred was unique to each participant. These results demonstrate promise that exotendon-based exoskeletons may be able to reduce excess muscle activity among children with hemiparesis. Evaluations of EMG data without the exoskeleton may be useful to optimize the design and assistance provided by these devices. Further, monitoring EMG data while training with an exoskeleton may help to inform the guidance given by the therapist to optimize gait with assistive devices.

3.4.4 Limitations

This research represents the first evaluation of exotendon-based devices to assist gait among children. Conclusions from this study are limited by the small population of participants, but provide guidance for future design iterations and gait evaluations. To best understand how PlayGait can improve the gait of children with hemiparesis, and to make conclusions for children with specific diagnoses such as hemiplegic CP, the study should be repeated with more participants and longer training periods. TD participants should be age matched with the children with hemiparesis to serve as more accurate controls, particularly since gait patterns continue to change for children until roughly age seven (Sutherland 1997, Bril et al. 1998). As characteristic of most children, study participants often deviated from straight line walking which could impact step width outcomes (due to in-toeing and out-toeing) and joint angle symmetry (due to inconsistent joint rotation). One child (H2) held an adult's hand during trials with PlayGait which may impact step width and walking speed outcomes. Additionally, for more accurate findings from the control group, TD participants should be fitted with PlayGait on their non-dominant side (Rossi et al. 2013).

All outcome measures could be affected by the brief training period provided to the participants in this research. While time was provided for participants to walk and test the device, most participants opted to cut this period short. Their choice to cut this period short demonstrates comfort in walking with the exoskeleton, but a longer acclimation period with the device or specific instructions of gait training could impact the magnitude of changes observed with PlayGait. The exoskeleton walking conditions and spring stiffness levels were also not randomized, and could have resulted in training and improvements of outcomes with greater

practice with the device, although there was only one significant outcome associated with a later condition (hip symmetry with Exo Med for H2). The goal of this research was to provide a proof-of-concept of evaluation of the device with minimal instructions or training, but these factors will be important to examine in future research.

3.4.5 Recommendations for Future Work

The current prototype is functional for laboratory testing with human subjects, but further design advances should be considered before the exoskeleton is ready for clinical and community trials. The leg supports currently have no contour; there is a straight line from the hip to the ankle. To best fit users, the cuffs – which attach to the thigh and calf struts – should be as close as possible to the thigh and calf without interfering with clothing. This means a medially curved strut component should be added just below the hip. To improve fit of the cuffs, they should be manufactured with a more compliant material than PLA such as thermoformed plastic. This new material choice could allow a degree of customizability in the cuffs between users.

Parent and child feedback indicates PlayGait looks robotic and bulky, and that they'd be hesitant to use it unless it made a huge impact on the child's ability to ambulate. In contrast, PT's remarked that PlayGait is very lightweight, low-profile, and has potential to be a great tool in therapy. Work should be done to improve cosmetic appearance and reduce bulk, if possible. Additional considerations, such as allowing for easy use of the restroom and testing for falls that are common among children during daily life (Adolph et al. 2012) should also be evaluated.

Within the specific population of CP, crouch gait and stiff-knee gait are two of the most common gait patterns. However, the current PlayGait prototype that was based upon the adult design and analyses of unimpaired gait has minimal impact at the knee, allowing free knee flexion. Optimizing the pulley sizes and exotendon path based upon a child's unique joint

moments may increase the potential positive impacts of exotendon-based devices on gait for children with diverse gait patterns. Incorporating a knee joint that facilitates passive resistance to flexion during stance could also expand the population that this device could assist.

Chapter 4 CONCLUSION

To improve gait for children with hemiparesis, a passive pediatric exoskeleton using an exotendon was developed and tested. Our analyses of gait among three TD children suggest that a passive exotendon can be comfortable when worn during walking with minimal changes in kinematics, walking speed, step width, or muscle activity. For children with hemiparesis, the results of this research suggest that exotendon-based design hold promise for improving kinematic joint symmetry at the hip or the ankle, depending on a child's natural gait pattern, although with this initial testing we found minimal changes in walking speed or step width with PlayGait. Changes in muscle activity as measured from EMG recordings also suggest that a pediatric exoskeleton may be useful for reducing excessive muscle activity commonly observed among children with hemiparesis. Further research to identify optimal spring stiffness and improve device function should be completed, along with incorporating design features based on feedback from therapists, children with hemiparesis, and their caregivers. A need exists for novel solutions that can support early walking practice in the clinic, at home, and in the community for children with gait impairments. Passive pediatric exoskeletons may provide a novel affordable platform for enhancing daily walking practice while enabling activities of daily life and increasing community participation.

References

Adolph, K. E., W. G. Cole, M. Komati, J. S. Garciaguirre, D. Badaly, J. M. Lingeman, G. L. Chan and R. B. Sotsky (2012). "How do you learn to walk? Thousands of steps and dozens of falls per day." Psychological science **23**(11): 1387-1394.

Adolph, K. E., B. Vereijken and P. E. Shrout (2003). "What changes in infant walking and why." Child development **74**(2): 475-497.

Agrawal, N., S. C. Johnston, Y. W. Wu, S. Sidney and H. J. Fullerton (2009). "Imaging data reveal a higher pediatric stroke incidence than prior US estimates." Stroke **40**(11): 3415-3421.

Bjornson, K. F., B. Belza, D. Kartin, R. Logsdon and J. F. McLaughlin (2007). "Ambulatory physical activity performance in youth with cerebral palsy and youth who are developing typically." Physical Therapy **87**(3): 248-257.

Bjornson, K. F., C. Zhou, R. Stevenson, D. Christakis and K. Song (2014). "Walking activity patterns in youth with cerebral palsy and youth developing typically." Disability and rehabilitation **36**(15): 1279-1284.

Bril, B. and A. Ledebt (1998). "Head coordination as a means to assist sensory integration in learning to walk." Neuroscience & Biobehavioral Reviews **22**(4): 555-563.

Cans, C., J. De-la-Cruz and M.-A. Mermet (2008). "Epidemiology of cerebral palsy." Paediatrics and child health **18**(9): 393-398.

Carlon, S. L., N. F. Taylor, K. J. Dodd and N. Shields (2013). "Differences in habitual physical activity levels of young people with cerebral palsy and their typically developing peers: a systematic review." Disability and Rehabilitation **35**(8): 647-655.

CerebralPalsy.org. "Definition of Cerebral Palsy." 2018, from http://www.cerebralpalsy.org/about-cerebral-palsy/definition.

Collins, S. H., M. B. Wiggin and G. S. Sawicki (2015). "Reducing the energy cost of human walking using an unpowered exoskeleton." Nature **522**(7555): 212.

Condie, D. N. and C. B. Meadows (1995). Report of a Consensus Conference on the Lower Limb Orthotic Management of Cerebral Palsy: Held at Duke University, Durham, N. Carolina, from 10-12 November 1994, International Society for Prosthetics and Orthotics.

Crenna, P. (1998). "Spasticity andspastic'gait in children with cerebral palsy." Neuroscience & Biobehavioral Reviews **22**(4): 571-578.

Damiano, D. L. and S. L. DeJong (2009). "A systematic review of the effectiveness of treadmill training and body weight support in pediatric rehabilitation." Journal of neurologic physical therapy: JNPT **33**(1): 27.

Damiano, D. L., T. L. Martellotta, D. J. Sullivan, K. P. Granata and M. F. Abel (2000). "Muscle force production and functional performance in spastic cerebral palsy: relationship of cocontraction." Archives of Physical Medicine and Rehabilitation **81**(7): 895-900.

De Mattos, C., K. Patrick Do, R. Pierce, J. Feng, M. Aiona and M. Sussman (2014). "Comparison of hamstring transfer with hamstring lengthening in ambulatory children with cerebral palsy: further follow-up." Journal of children's orthopaedics **8**(6): 513-520.

Dodd, K. J. and S. Foley (2007). "Partial body-weight-supported treadmill training can improve walking in children with cerebral palsy: a clinical controlled trial." Developmental Medicine & Child Neurology **49**(2): 101-105.

Domingo, A. and D. P. Ferris (2009). "Effects of physical guidance on short-term learning of walking on a narrow beam." Gait & posture **30**(4): 464-468.

Esquenazi, A., M. Talaty, A. Packel and M. Saulino (2012). "The ReWalk powered exoskeleton to restore ambulatory function to individuals with thoracic-level motor-complete spinal cord injury." American journal of physical medicine & rehabilitation **91**(11): 911-921.

Garvey, M. A., M. L. Giannetti, K. E. Alter and P. S. Lum (2007). "Cerebral palsy: new approaches to therapy." Current neurology and neuroscience reports **7**(2): 147-155.

Glaister, B., J. Schoen, C. Kawahara, A. Pacanowsky, M. C. Zachar and N. P. Byl (2015). "Mobility Training for Patients Recovering from Neurological Injuries with Kickstart®: A Case Series." Physical Medicine and Rehabilitation - International **2**(8).

Hanna, S. E., P. L. Rosenbaum, D. J. Bartlett, R. J. Palisano, S. D. Walter, L. Avery and D. J. Russell (2009). "Stability and decline in gross motor function among children and youth with cerebral palsy aged 2 to 21 years." Developmental Medicine & Child Neurology **51**(4): 295-302.

Hidler, J. M. and A. E. Wall (2005). "Alterations in muscle activation patterns during robotic-assisted walking." Clinical Biomechanics **20**(2): 184-193.

Hof, A. L. (1996). "Scaling gait data to body size." Gait & posture **3**(4): 222-223.

Honeycutt A, D. L., Chen H, al Homsi G, Grosse S, Schendel D. (2004). "Economic Costs Associated with Mental Retardation, Cerebral Palsy, Hearing Loss, and Vision Impairment --- United States, 2003." Retrieved 12/22/17, 2017, from https://www.cdc.gov/mmwr/preview/mmwrhtml/mm5303a4.htm.

Kawakami, Y., H. Kanehisa and T. Fukunaga (2008). "The relationship between passive ankle plantar flexion joint torque and gastrocnemius muscle and achilles tendon stiffness: implications for flexibility." journal of orthopaedic & sports physical therapy **38**(5): 269-276.

Khetsuriani, N., A. LaMonte-Fowlkes, S. Oberst, M. A. Pallansch, C. f. D. Control and Prevention (2006). "Enterovirus surveillance—United States, 1970–2005." MMWR Surveill Summ **55**(8): 1-20.

Korpela, R. A., T. O. Siirtola and M. J. Koivikko (1992). "The cost of assistive devices for children with mobility limitation." Pediatrics **90**(4): 597-602.

Krigger, K. W. (2006). "Cerebral palsy: an overview." American family physician **73**(1).

Kuczmarski, R. J. (2002). "2000 CDC growth charts for the United States; methods and development."

LaFortune, M. A. (1991). "Three-dimensional acceleration of the tibia during walking and running." Journal of biomechanics **24**(10): 877881-879886.

Laubscher, C. A., R. J. Farris and J. T. Sawicki (2017). Design and Preliminary Evaluation of a Powered Pediatric Lower Limb Orthosis. ASME 2017 International Design Engineering Technical Conferences and Computers and Information in Engineering Conference, American Society of Mechanical Engineers.

Lefmann, S., R. Russo and S. Hillier (2017). "The effectiveness of robotic-assisted gait training for paediatric gait disorders: systematic review." Journal of neuroengineering and rehabilitation **14**(1): 1.

Lerner, Z. F., D. L. Damiano and T. C. Bulea (2017). "A lower-extremity exoskeleton improves knee extension in children with crouch gait from cerebral palsy." Science translational medicine **9**(404): eaam9145.

Lerner, Z. F., D. L. Damiano, H.-S. Park, A. J. Gravunder and T. C. Bulea (2017). "A robotic exoskeleton for treatment of crouch gait in children with cerebral palsy: Design and initial application." IEEE Transactions on Neural Systems and Rehabilitation Engineering **25**(6): 650-659.

NSCIS, C. (2004). "The 2004 annual statistical report for the model spinal cord injury care systems." University of Alabama at Birmingham, Birmingham.

Ounpuu, S., J. Gage and R. Davis (1991). "Three-dimensional lower extremity joint kinetics in normal pediatric gait." Journal of Pediatric Orthopaedics **11**(3): 341&hyhen.

Owings, T. M. and M. D. Grabiner (2004). "Step width variability, but not step length variability or step time variability, discriminates gait of healthy young and older adults during treadmill locomotion." Journal of biomechanics **37**(6): 935-938.

Palisano, R., P. Rosenbaum, S. Walter, D. Russell, E. Wood and B. Galuppi (1997). "Development and reliability of a system to classify gross motor function in children with cerebral palsy." Developmental Medicine & Child Neurology **39**(4): 214-223.

Palsy, U. C. (2013). Fact Sheet.

Park, E. S., C. I. Park and J. Y. Kim (2001). "Comparison of anterior and posterior walkers with respect to gait parameters and energy expenditure of children with spastic diplegic cerebral palsy." Yonsei medical journal **42**(2): 180-184.

Rajagopal, A., C. L. Dembia, M. S. DeMers, D. D. Delp, J. L. Hicks and S. L. Delp (2016). "Full-body musculoskeletal model for muscle-driven simulation of human gait." IEEE Transactions on Biomedical Engineering **63**(10): 2068-2079.

Reid, S. M., J. B. Carlin and D. S. Reddihough (2011). "Using the Gross Motor Function Classification System to describe patterns of motor severity in cerebral palsy." Developmental Medicine & Child Neurology **53**(11): 1007-1012.

Ries, A. J., T. F. Novacheck and M. H. Schwartz (2015). "The efficacy of ankle-foot orthoses on improving the gait of children with diplegic cerebral palsy: a multiple outcome analysis." PM&R **7**(9): 922-929.

Rodda, J. and H. Graham (2001). "Classification of gait patterns in spastic hemiplegia and spastic diplegia: a basis for a management algorithm." European journal of neurology **8**(s5): 98-108.

Rossi, S., A. Colazza, M. Petrarca, E. Castelli, P. Cappa and H. I. Krebs (2013). "Feasibility study of a wearable exoskeleton for children: is the gait altered by adding masses on lower limbs?" PloS one **8**(9): e73139.

Stout, J. L., J. R. Gage, M. H. Schwartz and T. F. Novacheck (2008). "Distal femoral extension osteotomy and patellar tendon advancement to treat persistent crouch gait in cerebral palsy." JBJS **90**(11): 2470-2484.

Sutherland, D. (1997). "The development of mature gait." Gait & posture **6**(2): 163-170.

Tieman, B. L., R. J. Palisano, E. J. Gracely and P. L. Rosenbaum (2004). "Gross motor capability and performance of mobility in children with cerebral palsy: a comparison across home, school, and outdoors/community settings." Physical therapy **84**(5): 419-429.

Unnithan, V., J. Dowling, G. Frost, B. A. Volpe and O. Bar-Or (1996). "Cocontraction and phasic activity during GAIT in children with cerebral palsy." Electromyography and clinical neurophysiology **36**(8): 487-494.

Valvano, J. (2004). "Activity-focused motor interventions for children with neurological conditions." Physical & occupational therapy in pediatrics **24**(1-2): 79-107.

Van den Bogert, A. J. (2003). "Exotendons for assistance of human locomotion." Biomedical engineering online **2**(1): 17.

Van Dijk, W., H. Van der Kooij and E. Hekman (2011). A passive exoskeleton with artificial tendons: Design and experimental evaluation. Rehabilitation Robotics (ICORR), 2011 IEEE International Conference on, IEEE.

Vaughan, C. L., N. G. Langerak and M. J. O'malley (2003). "Neuromaturation of human locomotion revealed by non-dimensional scaling." Experimental Brain Research **153**(1): 123-127.

Veneman, J. F., J. Menger, E. H. van Asseldonk, F. C. van der Helm and H. van der Kooij (2008). "Fixating the pelvis in the horizontal plane affects gait characteristics." Gait & posture **28**(1): 157-163.

Westlake, K. P. and C. Patten (2009). "Pilot study of Lokomat versus manual-assisted treadmill training for locomotor recovery post-stroke." Journal of neuroengineering and rehabilitation **6**(1): 18.

Wilson, D., J. Feikes and J. O'connor (1998). "Ligaments and articular contact guide passive knee flexion." Journal of biomechanics **31**(12): 1127-1136.

Wren, T. A., S. Rethlefsen and R. M. Kay (2005). "Prevalence of specific gait abnormalities in children with cerebral palsy: influence of cerebral palsy subtype, age, and previous surgery." Journal of Pediatric Orthopaedics **25**(1): 79-83.

Yeargin-Allsopp, M., K. V. N. Braun, N. S. Doernberg, R. E. Benedict, R. S. Kirby and M. S. Durkin (2008). "Prevalence of cerebral palsy in 8-year-old children in three areas of the United States in 2002: a multisite collaboration." Pediatrics **121**(3): 547-554.

Young, P. M. M. and J. B. Dingwell (2012). "Voluntarily changing step length or step width affects dynamic stability of human walking." Gait & posture **35**(3): 472-477.

Appendix A: Design Specifications

Stakeholders	Core Functions	Design Specifications	Evaluation
Patients and Physical Therapists/Orthotists	Patient can easily don/doff the device	Don/Doff and adjust within 5 minutes	- Record the amount of time it takes to open/close each type of proposed fastener. - Therapists/orthotists can practice donning and doffing the device with a pediatric sized model.
	Promote fluid movement (minimize jerks at the transition between toe off and swing phase)	Adult male walking in shod conditions (tibial accelerations) (m/s^2): *anterior-posterior* Peak positive acceleration 2.33 g. Peak negative acceleration -2.09 g. *Lateral max accel* 0.90g. *Axial max accel* 1.70g. [1] From double differentiating normative joint angles, peak sagittal plane accelerations are (deg/sec^2): -Ankle 2720.6 -Knee 5730.7 -Hip 1920.4 (% stride was converted to sec) During walking, we want to keep these accelerations similar.	- To test tibial acceleration, fix the belt and thigh bracing, weight the foot, and let the foot/tibia bracing swing like a pendulum while measuring the acceleration of the ankle. - Clinical study in which patients walk with accelerometers. Peak accelerations and maximum changes in accelerations will be computed.* - Compare accelerations achieved with and without our device.*
		Pediatric Range of motion: -Hip abduction/adduction 13° -Hip flexion/extension 45° (90° for sitting) -Hip rotation 16° [2] These measures should be achieved so that the device does not compromise movement.	- Fix the belt and rotate the femoral bracing about the hip joint while recording the minimum and maximum rotation achieved.
Patients and Physical Therapists/Orthotists and Cadence Biomedical	Durability	Fatigue failure	ISO 22675 [3] and ASTM E399 [4] Waistband: Abrasion testing on the material used as padding for the waistband.
		Impact Testing	Metals: ISO/DIS 148-1 [5]

			Plastic Pulley: Charpy impact test to determine the force at failure.
		Bending Failure	Metals: ISO 7438:2016 [6] Bend the knee joint laterally with an Instron.
	Increase walking time outside of therapy	Normative data indicates 7,998 steps per day for 2-3 year olds, 9,069 steps for 4-5 year olds, and 9,794 steps for 6-7 year olds [7]. see also [8]	- Place a pedometer on the device and verify it counts the number of steps properly. - Clinical study trials with a pedometer, such as Step Watch. - Measure steps per day for one week without the exoskeleton and one week with the exoskeleton.*
Industry Partners	Fail in a predictable manner	The components that would not compromise safety should fail first (i.e. tendon, ankle joint, pulley). The bracings should not fail.	For the final design, test the whole device with an instron or a 3 point bending test (with load applied in various configurations) to the point of failure
	Does not scratch or break skin	Rounded edges on metal and plastic components (no perfect 90° corners)	Using a material with toughness similar to that of skin, run the material over all surfaces watching for abrasion. Also swing the device into the material and watch for snagging.
Patients, Physical Therapists/Orthotist, Industry Partners, and Insurers	Easily be adjusted or modified for growth (changes in height, waist size)	Total height must adjust 13”-22” Total width must adjust 18.07”-25.8”	- Record the time it takes to reconfigure the device from its smallest size to its largest size. - Measure the maximum and minimum height and width achieved.

* Future evaluation plans recommended for preparing a device for clinical use.

References:

[1] Lafortune, Mario A. "Three-Dimensional Acceleration Of The Tibia During Walking And Running". *Journal of Biomechanics* 24.10 (1991): 877-886. Web.

[2] Ounpuu, S., J. R. Gage, and R. B. Davis. "Three-Dimensional Lower Extremity Joint Kinetics In Normal Pediatric Gait". *Journal of Pediatric Orthopaedics* 11.3 (1991): 341-349. Web.

[3] Iso.org,. "ISO 22675:2006(En) Prosthetics — Testing Of Ankle-Foot Devices And Foot Units — Requirements And Test Methods". N.p., 2016. Web. 12 Feb. 2016. https://www.iso.org/obp/ui/#iso:std:iso:22675:ed-1:v1:en

[4] ASTM Compass,. "Standard Test Method For Linear-Elastic Plane-Strain Fracture Toughness Kic Of Metallic Materials1". N.p., 2016. Web. 12 Feb. 2016. http://compass.astm.org/EDIT/html_annot.cgi?E399+12e3#s00001

[5] Iso.org,. "ISO/DIS 148-1 - Metallic Materials -- Charpy Pendulum Impact Test -- Part 1: Test Method". N.p., 2016. Web. 12 Feb. 2016. http://www.iso.org/iso/home/store/catalogue_tc/catalogue_detail.htm?csnumber=63802

[6] Iso.org,. "SO 7438:2016(En) Metallic Materials — Bend Test". N.p., 2016. Web. 12 Feb. 2016. https://www.iso.org/obp/ui/#iso:std:iso:7438:ed-3:v1:en

[7] Measurement of Walking Activity Throughout Childhood:Influence of Leg Length. K Bjornson

[8] Kristie F. Bjornson, Chuan Zhou, Richard Stevenson, Dimitri Christakis & Kit Song (2014) Walking activity patterns in youth with cerebral palsy and youth developing typically, Disability and Rehabilitation, 36:15, 1279-1284, DOI: 10.3109/09638288.2013.845254

Note: This material is from in the Engineering Innovations in Health final report created by Jessica Zistatsis, Kira Neuman, Alex Gong, Jeffrey Bergeson, and Daniel Parrish (2016).

Appendix B: Mechanical Testing

Range of Motion & Adjustability

Both range of motion and adjustability were tested by manually moving the device and measuring the minimum and maximum values. For adjustability, the design specification required 9 in (228.6 mm) for vertical adjustment as well as 8 in (203.2 mm) of adjustment around the waist. The device was measured in both its shortest and tallest configurations to confirm the leg struts will accommodate the desired range of patients and found to allow 9.67 in (245.6 mm) of change (Table B.1). The hip belt adjusts 5.5 in (139.7 mm) circumferentially, with the largest circumference at 25.5 in (647.7 mm). The angular ranges of motion allowed at each joint are recorded in Table B.2, with the primary reference for average unimpaired range from Ounpuu et al., (1991) [1]. Though PlayGait slightly restricts motion in many directions, it meets the range required for both walking and sitting.

Table B.1: Leg segment adjustability.

Shortest tibia length (ankle center to knee center)	183.0 mm
Shortest femur length (knee center to screw connecting the hip pulley to ball joint)	196.0 mm
Longest tibia length	289.0 mm
Longest femur length	345.0 mm

Table B.2: Angular range of motion at the knee and hip joint.

Joint	Type of Motion	Average Unimpaired Range (Children ages 2- 8)	PlayGait Range
Hip Joint	Flexion	136°	106°
	Extension	28°	109°
	Rotation	16°	360°
	Abduction	13°	10°
	Adduction	13°	10°
Knee Joint	Flexion	150°	107°
	Extension	4°	0°

Pendulum Test

A pendulum test was conducted to evaluate whether the PlayGait might prevent natural passive movement which is important during unimpaired gait, either through jerk during the swing phase of walking or overall reductions in tibial accelerations. Although the device is passive, it was important to ensure that the patient would not be working against the device while walking. The test was conducted by attaching an accelerometer to the ankle of PlayGait while it was weighted to simulate either a 3 year or 6 year old patient, by adding weights of approximately 1.5 lbs and 3.6 lbs, respectively. Including testing equipment, the total weights added were 1.43 lbs and 3.88 lbs. The hip and thigh were secured in a horizontal position; the lower leg was extended into a straightened position and released to swing freely (Figure B-1). With the positioning of the acceleration, the x -axis measured proximal/distal motion, the y-axis measured anterior/posterior motion, and the z-axis measured medial/lateral motion.

(a)

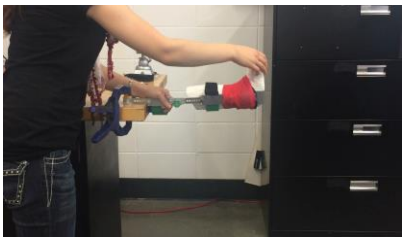

(b)

(c)

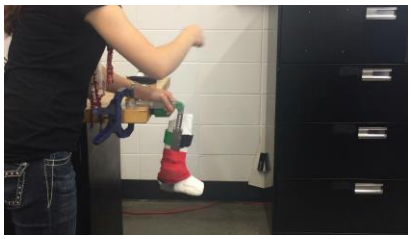

(d)

Figure B-1: Pendulum test. (a) Testing configuration with the thigh strut fixed to the table and the foot and tibia free to swing about the knee joint. (b) The leg completely extended, preparing to release. (c) The foot freely swinging. (d) The foot at rest after the pendulum test.

In Table B.3 below, the peak tibial accelerations recorded during the pendulum test are provided along with the design specifications as determined by an adult male walking in shod conditions [2]. The anterior-posterior peak accelerations shown for the 3 and 6 year old bottom out at -2g which is most likely an issue with the accelerometer and not actually the true acceleration values.

The anterior-posterior peak accelerations show that PlayGait weighted with a 3- and 6-year-old foot meets design specification of -2.09g. PlayGait weighted with a 3-year-old foot allow motion greater than needed but not when weighted with a 6 year old foot. The axial accelerations of allowed by the PlayGait are slightly restricted compared to the 1.70g in the design specification. Though this test does not fully demonstrate that the PlayGait promotes fluid movement by not impeding the acceleration of typical gait, this was a limitation of the test setup

rather than the device. Only motion of the lower leg was evaluated, but walking requires a complex combination of movements that are difficult to replicate under the time and budget restraints of this project. These results alone do not support the core function, but are a strong indication that the device would perform as needed under further testing.

Table B.3: Tibial acceleration results from the pendulum test.

	Anterior-Posterior Peak Negative Accel (g's) (Y)	Lateral Peak Positive Accel (g's) (Z)	Axial Peak Accel (g's) (X)
Adult male (design specification)	-2.09	0.90	1.7
Three year old	-2	1.4	1.3
Six year old	-2	0.54	1.3

3-Point Bend Test

As a Class I medical device, the FDA requires demonstration of mechanical failure testing, although there is no standard. The joint most likely to experience high bending forces perpendicular to its axis of motion is the knee joint. As such, this joint was tested until failure in a three-point bend test with an Instron (Instron 5585H 250 kN) (Figure B-2). The test was conducted on a partially assembled leg consisting of the knee joint, thigh strut, and calf strut. Supports were located 65 mm to the right and left of the knee joint's axis of rotation. This

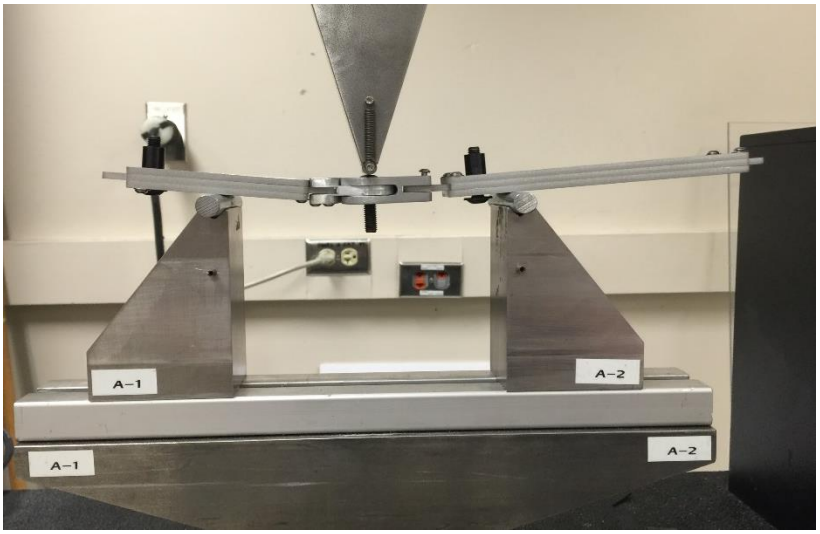

Figure B-2: The three-point bend test conducted on the knee joint.

placement was close to the knee rather than at the ends of the struts, which would result in testing the bending strength of the struts themselves, rather than the connection between the struts and the knee. The load was applied at 3 mm per minute until failure for three specimens.

Figure B-3 depicts the results of this bend test and demonstrates both snapping failure and plastic deformation. The lowest point of failure out of three trials occurred just over 900 N which exceeds expected forces from a pediatric user in this direction. Failure occurred at the small tabs used to screw the knee joint to the struts rather than in the joint itself. Variability in the maximum load achieved may be due to inconsistencies in manufacturing of the three knee joints.

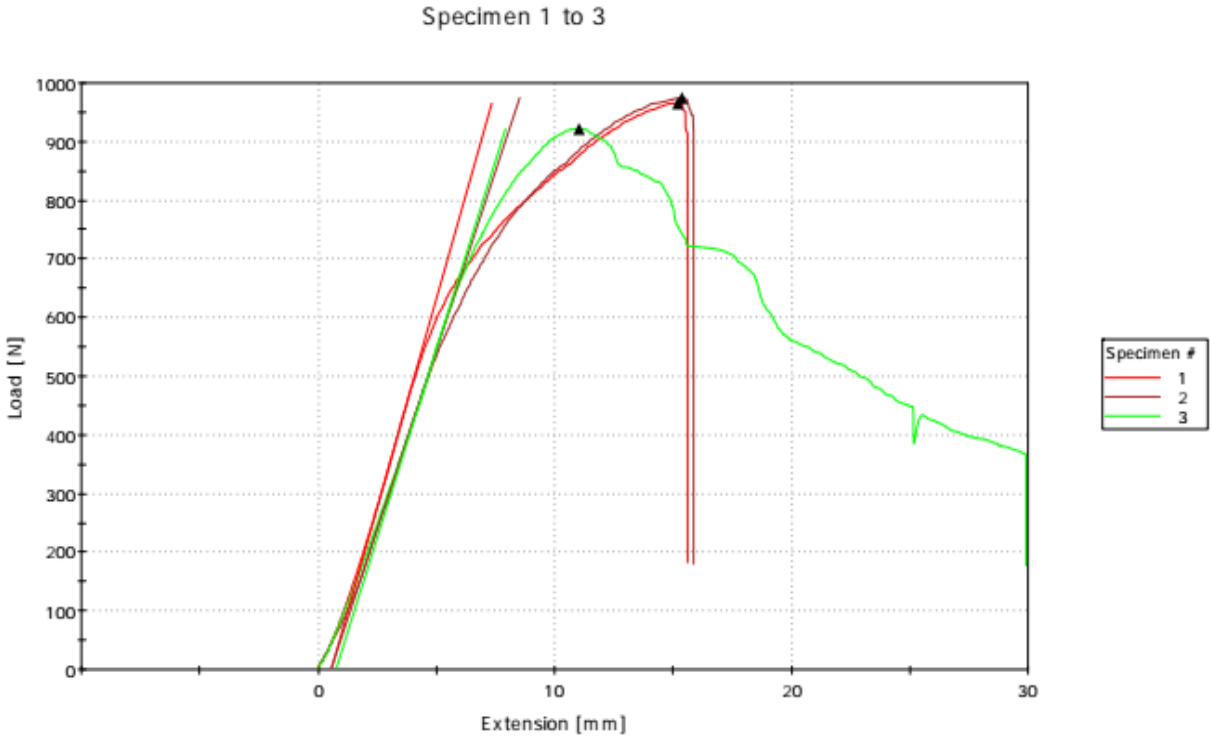

Figure B-3: The load vs. extension curve produced by the three-point bend test indicates variability in load response.

References:

[1] Ounpuu, S., J. R. Gage, and R. B. Davis. "Three-Dimensional Lower Extremity Joint Kinetics In Normal Pediatric Gait". *Journal of Pediatric Orthopaedics* 11.3 (1991): 341-349. Web.

[2] Lafortune, Mario A. "Three-Dimensional Acceleration Of The Tibia During Walking And Running". *Journal of Biomechanics* 24.10 (1991): 877-886. Web.

Note: This material is from in the Engineering Innovations in Health final report created by Jessica Zistatsis, Kira Neuman, Alex Gong, Jeffrey Bergeson, and Daniel Parrish (2016).

Appendix C: Motion Capture Study Protocol

Equipment to bring:

- PlayGait and Kickstart
- DelSys (2 snap leads, 6 regular)
- Heart rate monitor & watch
- Load Cell + Data Logger
- Array of springs
- Cigna spray
- Coban and Athletic Tape
- Tight fitting clothing
- Consent, assent, and survey forms
- Clipboard
- Parking validation & reimbursement check
- Toy/stuffed animal
- Trial note sheet
- Body weight scale (AMP Lab office)
- Flexible measuring tape
- Small tape measure
- 2 Video cameras + tripods
- Allen wrench set
- Flat headed screw driver

Before participant arrives:

1. Turn on computers and connect them.
2. Charge Delsys system Garmin watch.
3. Camera and force plate calibration (45 min). Plug into the SS USB port.
4. Turn on heart rate monitor watch and verify it is collecting data. Set up activity online. Charge watch.
5. Tape on markers (place on cardboard) and EMG sensors.
6. Put low stiffness spring on Exoskeleton.
7. Set up EMG workspace. Start Analog then open Qualisys with Window layout 3. Verify it's setup to start on trigger, it's sampling at 2000 Hz, and the configuration is with snap leads. Connect the 3-prong cable to the control port of one camera.
8. Set up load cell data logger software (USB connection) and verify data is collecting. Verify all leads are connected.
9. Place tape on floor to mark end regions and width of walking track.
10. Set up video cameras for frontal and sagittal plane viewing with chargers plugged in.
11. Verify PlayGait hip joint is entirely screwed in.

Roles of assistants:

- Physical therapist and spotter: _____
- Photographer: _____
- Videographer: _____
- Note taker and audio recorder (for interviews): _____
- Biostamp monitor: _____
- Qualisys operator: _____Jessica_____

Once participant arrives, before data collection:

In exam room (bring Delsys & laptop):

12. CONSENT FORM / ASSENT FORM
13. If needed, have participant change into tight fitting clothing
14. See if child needs to use the bathroom
15. Participant info
    a. Paretic side: _____

Birthdate:		Height:	m
Gender:		Weight:	kg

    b. Determine spring stiffness using excel chart
        i. Low stiffness: _____ N/m
        ii. Medium stiffness: _____ N/m
        iii. High stiffness: _____ N/m
16. Place heart rate monitor. Wet contacts first.
17. Skin prep for EMG sensors:
    a. Shave area (can mark the regions with surgical marker: heart, 8 EMG locations)
    b. Alcohol wipe over the area.
    c. Cigna spray on a paper towel and wipe on the area and let air dry.
18. Place EMG sensors bilaterally (in the exam room)
    See next page for placement instructions.
    MAKE SURE KIDS ARE IN A COMFORTABLE POSITION
19. Test the sensors by:
    a. Biceps femorus: While standing, raise leg and push against my hand, which is pushing downward on the shank.
    b. Gastroc: standing on toes and standing on heels.
    c. Rectus Femoris: Sit down and raise knee to my hand or do squats.
    d. Ant tib: Heel on ground with toes elevated and rotated medially. Flex foot proximal-distal

Muscle	EMG sensor number	Sensor Position	Finding muscle*	Picture* * Quotes and pictures come from http://seniam.org/
Biceps femoris long head	L # 9, R #10	50% on the line between the ischial tuberosity and the lateral epicondyle of the tibia. Lateral side of leg.	"Press against the leg proximal to the ankle in the direction of knee extension."	
Gastrocnemius (medial)	L #11, R # 12 (SNAP LEADS, wrap with coban)	Electrodes need to be placed on the most prominent bulge of the muscle.	"Plantar flexion of the foot with emphasis on pulling the heel upward more than pushing the forefoot downward. For maximum pressure in this position it is necessary to apply pressure against the forefoot as well as against the calcaneus."	
Rectus femoris	L # 13, R # 14	The electrodes need to be placed at 50% on the line from the anterior spina iliaca superior to the superior part of the patella.	"Extend the knee without rotating the thigh while applying pressure against the leg above the ankle in the direction of flexion." Lift leg up to ceiling and kick out. Apply extension force to ankle in sagittal plane.	
Anterior tibialis	L # 15, R#16	The electrodes need to be placed at 1/3 on the line between the tip of the fibula and the tip of the medial malleolus.	"Support the leg just above the ankle joint with the ankle joint in dorsiflexion and the foot in inversion without extension of the great toe. Apply pressure against the medial side, dorsal surface of the foot in the direction of plantar flexion of the ankle joint and eversion of the foot." Find tibia. Just to the lateral.	

20. Place reflective markers on body. Wrap coban under segment markers. Hold up exoskeleton for placement of pelvic markers before placing PSIS and ASIS.

R Acrom - L Acrom:	cm		
A. Pelvis (LASIS - RASIS):	cm	P. Pelvis (LPSIS-RPSIS):	cm
R ASIS-R Med Knee:	cm	L ASIS-L Med Knee:	cm
R ASIS-R Lat Knee:	cm	L ASIS-L Lat Knee:	cm
R Knee (Med - Lat Con):	cm	L Knee (Med - Lat Con):	cm
R Lat Knee-R Lat Mal:	cm	L Lat Knee-L Lat Mal:	cm
R Ank (Med - Lat Mal):	cm	L Ank (Med - Lat Mal):	cm
R 5MT-R Toe:	cm	L 5MT-L Toe:	cm
R Heel-R Toe (wrap lat under mal):	cm	L Heel-L Toe (wrap lat under mal):	cm
R Heel-R 5MT (wrap lat under mal):	cm	L Heel-L 5MT (wrap lat under mal):	cm

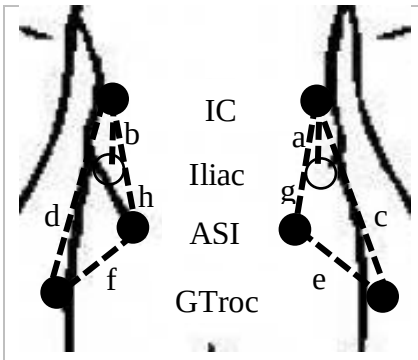

a: _____ cm (directly vertical L iliac crest to L_IC)

b: _____ cm (directly vertical R iliac crest to R_IC)

c: _____ cm (L_IC to L GTroch)

d: _____ cm (R_IC to R GTroch)

e: _____ cm (L ASIS to L GTroch)

f: _____ cm (R ASIS to R GTroch)

g: _____ cm (L_IC to L ASIS)

h: _____ cm (R_IC to R ASIS)

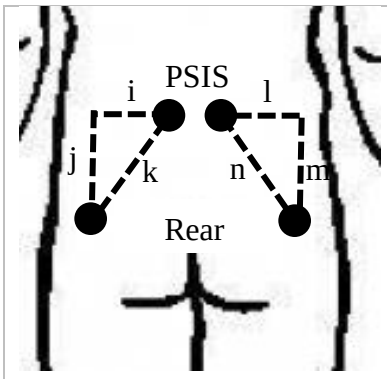	i: _____ cm j: _____ cm k: _____ cm l: _____ cm m: _____ cm n: _____ cm o: _____ cm (depth difference btwn L_PSIS and L_Rear) p: _____ cm (depth difference btwn R_PSIS and R_Rear)

Data Collection:

- Instruct participants how to walk on force plates. Start walking far behind treadmill to reach steady state when entering motion capture space.
- Turn on heart rate monitor.

Before each trial:

- ***Zero force plates***
- ***Set up video camera***

For typically developing:

21. Shod, no device:
    a. Static calibration trial and take photo (every 45° of upper and lower body) of marker placement. Arms separated from sides, feet shoulder width apart, palms facing anteriorly.
    b. Motion to gather joint centers
    c. Walk back and forth on runway two times.

rest

22. Put on exoskeleton and allow participant to practice walking. Add markers onto exoskeleton at hip, thigh, knee, shank, and ankle. TURN ON DATA LOGGER BEFORE TENSIONING EXOTENDON.
    a. Thigh setting: hole # _____
    b. Shank setting: hole # _____

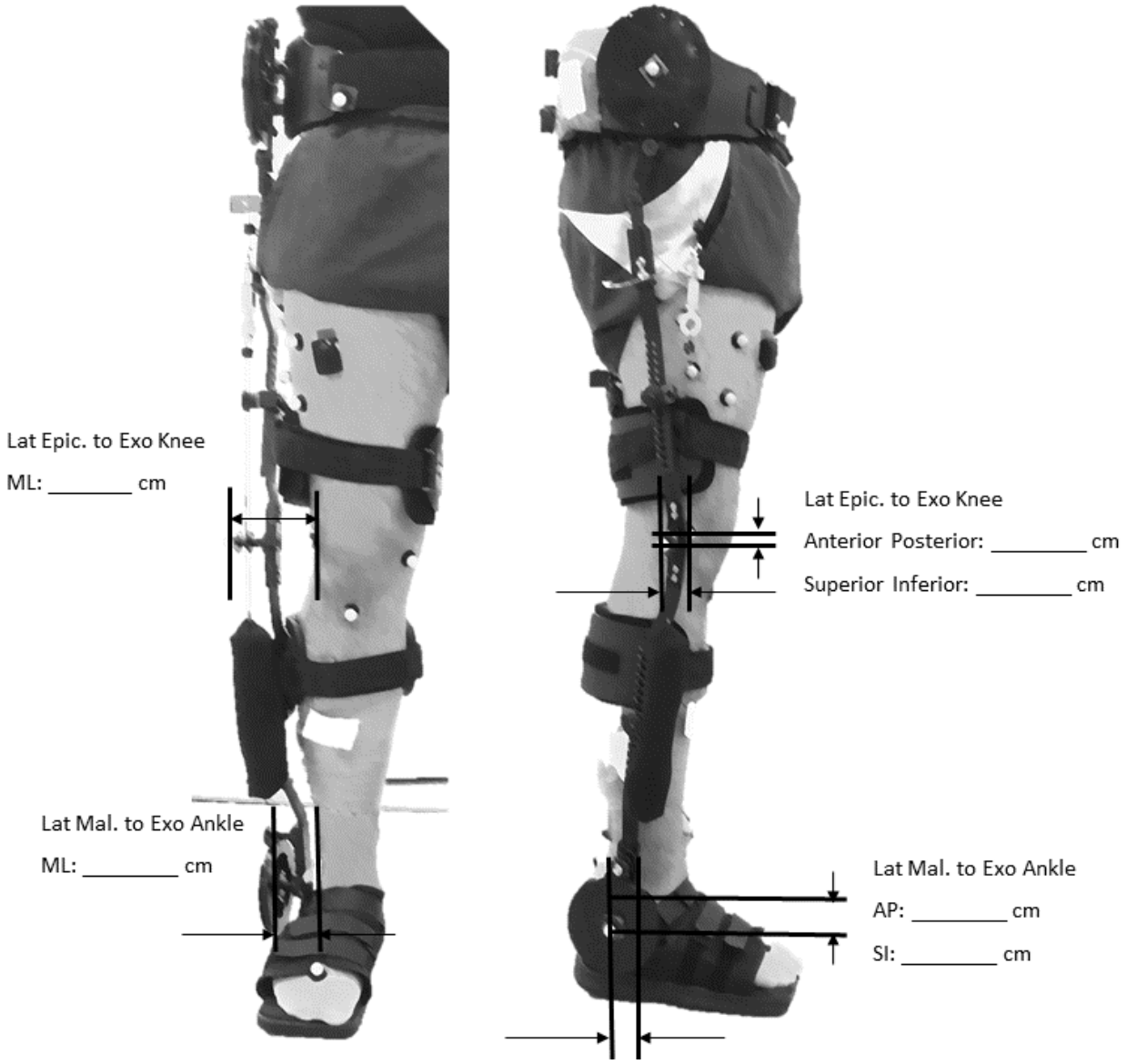

23. With Exoskeleton:
    a. Static calibration trial and take photos of marker placement.
    b. Two good trials walking trials with each stiffness.

For children with CP:

24. With AFO (baseline):
    a. Static calibration trial and take photo of marker placement (if any markers have to change, such as malleolus)
    b. Walk back and forth on runway

rest

25. With AFO + Exoskeleton low stiffness (repeat a. and b. from step 25)

rest

26. With AFO + Exoskeleton medium stiffness (repeat b. from step 25)

rest

27. With AFO + Exoskeleton high stiffness (repeat b. from step 25)

rest

28. No AFO and no Exoskeleton (baseline)
    a. Static calibration trial and take photo of marker placement (if any markers have to change, such as malleolus)
    b. Walk back and forth on runway
29. No AFO + Exoskeleton low stiffness (repeat a. and b. from step 25)

rest

30. No AFO + Exoskeleton medium stiffness (repeat b. from step 25)

rest

31. No AFO + Exoskeleton high stiffness (repeat b. from step 25)

rest

Post Motion Capture

32. Remove PlayGait, markers, and sensors
33. Interview questions with caregiver and child & survey with child (AUDIO RECORD)
34. **Provide reimbursement (check and parking)** and toy/stuffed animal. Check number: _____ Coupon number: _____

After participant leaves

35. Clean up
    a. Rub PlayGait and EMG sensors with alcohol prep wipes
    b. Rinse heart rate monitor chest strap with water after removing cover plate.
    c. Remove tape from markers
36. Save Qualisys data onto thumb drive
    a. Export .tsv and .mat after gap filling and applying AIM model
37. Export load cell data to .csv.

Appendix D: OpenSim Musculoskeletal Modeling and Simulation

The full-body OpenSim musculoskeletal model developed by Rajogopal 2016 was used for kinematic analysis (Rajagopal et al. 2016). This model features boney geometry for the full body. The model has 37 degrees of freedom across the entire body including 6 degrees of freedom for the pelvis and 7 per leg [1]. To scale the model according to the pipeline in Figure D-1, we developed a marker set consisting of 62 markers corresponding to the experimental protocol (Figure D-2). To improve scaling for each participant, anatomical landmark markers on the elbow, wrist, pelvis, knee, and ankle with a high degree of experimental placement accuracy were fixed in position for scaling (Table D.1). The No Exo static trials were used to scale the model for each participant (Table D.2). Scaling adjusts each body segment of the model (hand, pelvis, etc.) independently to create a subject-specific model that matches experimental data from the No Exo static trial. The markers on the unscaled model are compared to the experimental markers, and the distance between the model and experimental markers is minimized through a weighted least squares algorithm of measurement pairs for each body segment. Marker weights were specified on a 0 to 20 scale, where zero indicated the experimental marker had extremely low positional accuracy compared to the markers on the unscaled model (such as for segment markers placed on the thigh, humerus, and radius) and 20 indicated very high positional accuracy (such as for markers placed on bony landmarks). Segment marker trajectories experience high displacements due to skin motion artifacts, where the fleshy skin moves relative to the bone, and thus have low positional accuracy.

As body segments are three-dimensional objects, each segment was scaled independently in the x, y, and z directions, when possible [2]. When the experimental markers on a body were not on the same axis, virtual markers were created by projecting the experimental markers along

a specific axis, and measurement pairs were then created for markers along this axis. For instance, when scaling the tibia vertically, it is more accurate to scale based on the knee joint center and the ankle joint center than using the medial or lateral knee and ankle markers as they are not aligned vertically. A description of the virtual markers created for static scaling is provided in Table D.3. Markers placed on bony landmarks have a higher degree of certainty for positional accuracy, and thus they were weighted higher than markers placed on fleshy body segments. A sample of scaling factors (Figure D-3), measurement sets (Figure D-4), and marker weights (Figure D-5) for static scaling is depicted at the end of this Appendix.

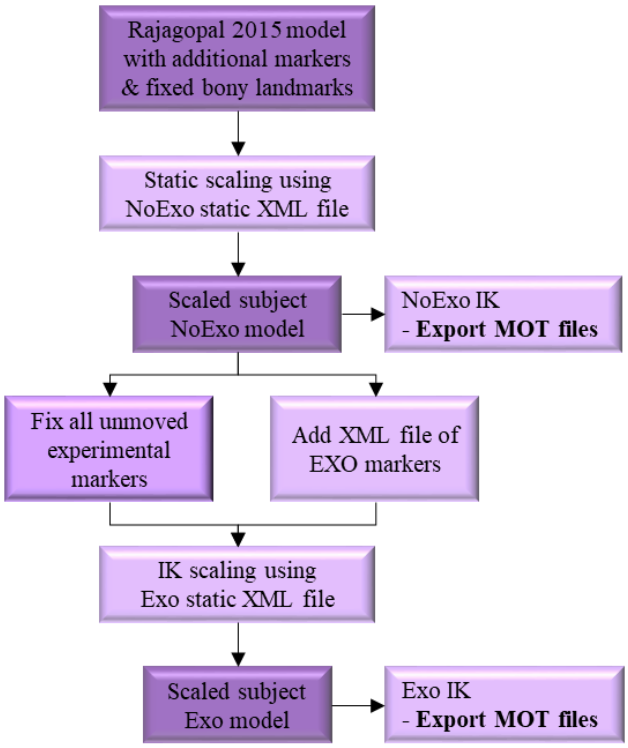

Figure D-1: OpenSim data processing pipeline with models highlighted in dark purple and outputs bolded.

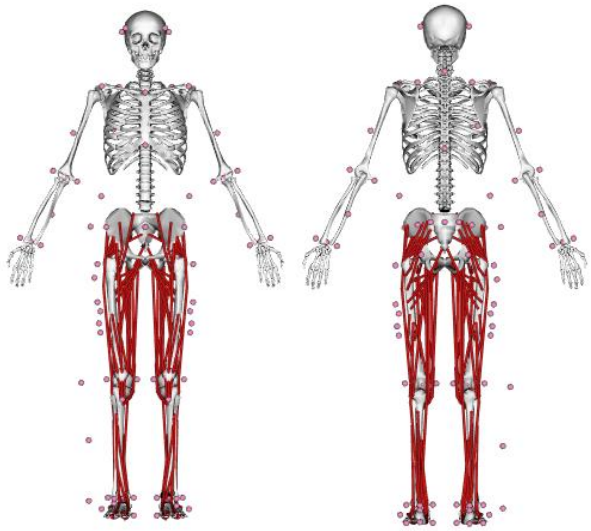

Figure D-2: Unscaled Rajagopal model with the adapted experimental marker set.

Table D.1: Markers fixed in the adapted Rajagopal 2016 model before static scaling for specific subjects.

Marker name (applies to left and right side of body)	Description
HME	Medial epicondyle (elbow)
HLE	Lateral epicondyle (elbow)
RSP	Radial styloid process (wrist)
USP	Ulnar styloid process (wrist)
ASIS	Anterior superior iliac spine (pelvis)
FLE	Lateral femoral epicondyle (knee)
FME	Medial femoral epicondyle (knee)
AnkL	Lateral malleolus (ankle)
AnkM	Medial malleolus (ankle)

Table D.2: Inputs and outputs for each OpenSim process.

OpenSim Process	Inputs	Outputs
Static Scaling	TRC file of static marker trajectories, subject weight, Rajagopal model, Static marker weights	Subject-specific model
Inverse Kinematics	Subject-specific model, TRC file of dynamic marker trajectories, Dynamic marker weights	Joint angles (MOT files)

Table D.3: Description of virtual markers used for static scaling.

Virtual Marker	Associated Scale Factor(s)	Description
RWJC, LWJC	hand	Right and left wrist joint centers
RPm, LPm	torso_x, torso_y, thigh_R_y, thigh_L_y	Right and left mid-pelvis (mid in the anterior – posterior direction)
RSHv, LSHv	torso_x,	Right and left shoulder
ASIm	pelvis_x	Mid-point of the right and left ASIS markers
PSIm	pelvis_x	Mid-point of the right and left PSIS markers
RKJC, LKJC	thigh_R_y, thigh_L_y, tibia_R_y, tibia_L_y	Right and left knee joint centers
RAJC, LAJC	tibia_R_y, tibia_L_y	Right and left ankle joint centers
RATv, LATv	foot_x	Right and left projection of the toe marker to the ankle vertical position
RAHv, LAHv	foot_x	Right and left projection of the heel marker to the ankle vertical position

To generate a model for use with the exoskeleton trials, the OpenSim Scaling Tool was used to add the 5 additional markers applied on the exoskeleton. Before scaling, all of the model's markers that did not change position between the No Exo and Exo conditions were fixed. The unfixed markers included the left and right ASIS, PSIS, and thigh markers as they were removed or moved to accommodate wearing the exoskeleton. All scale factors were set to one to ensure the size of the model would not change, and measurement pairs and marker weights remained the same to identify the relative position of the additional exoskeleton markers.

Inverse kinematics was run on the No Exo and Exo models using the marker trajectory data from each walking trial and a different set of marker weights (Figure D-6). Again, weighted least squares optimization was used to minimize the difference between experimental markers and the scaled model markers. As this study's outcome measures focus on hip, knee, and ankle movement, the bony landmark markers on the pelvis, knee, and foot were weighted highest. Maximum errors between model and experimental markers are recommended as 2-4 cm [2], but we saw larger errors in the upper body markers since study participants moved their head drastically which could not be accommodated by the model's rigid torso.

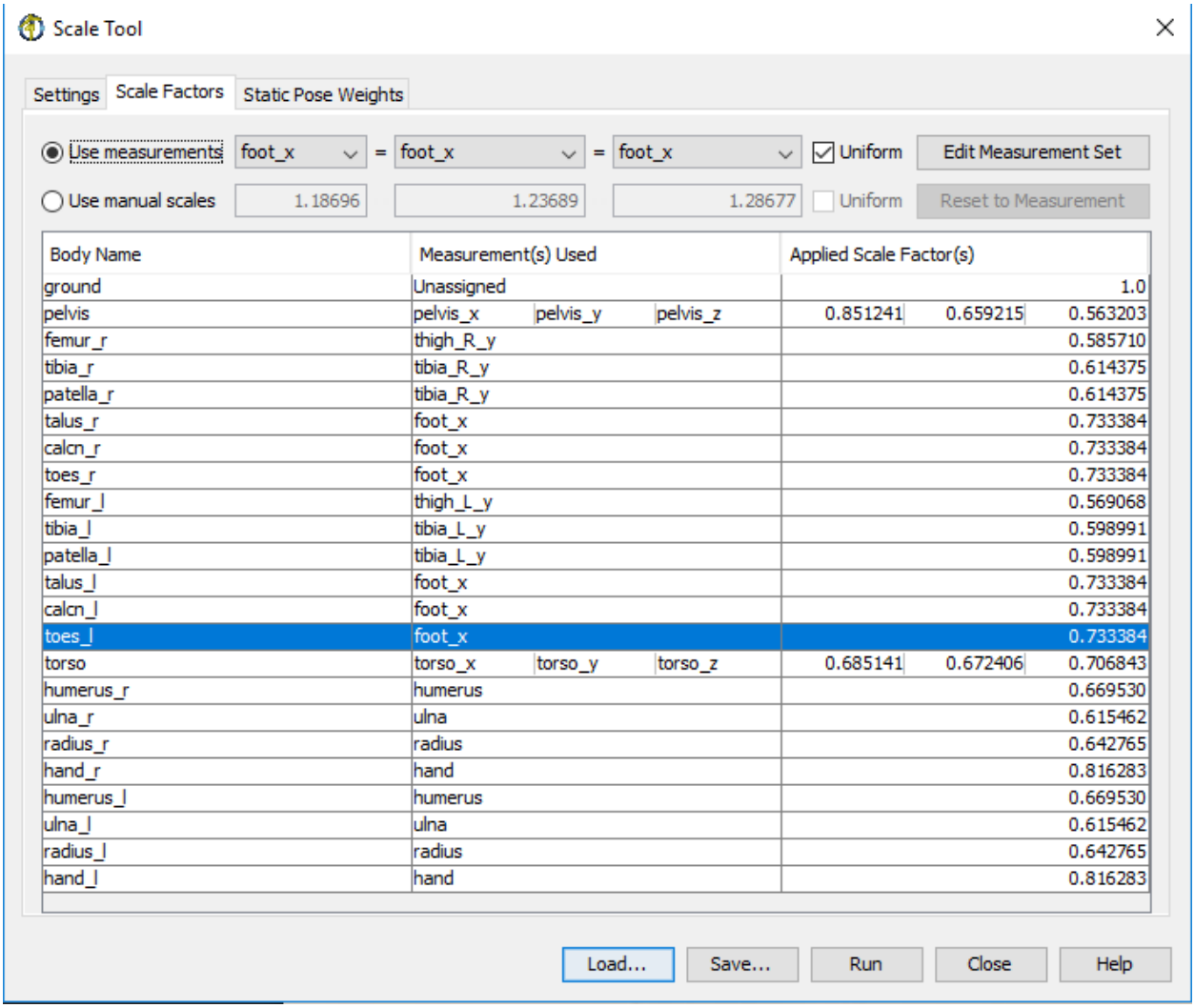

Body Name	Measurement(s) Used			Applied Scale Factor(s)		
ground	Unassigned					1.0
pelvis	pelvis_x	pelvis_y	pelvis_z	0.851241	0.659215	0.563203
femur_r	thigh_R_y					0.585710
tibia_r	tibia_R_y					0.614375
patella_r	tibia_R_y					0.614375
talus_r	foot_x					0.733384
calcn_r	foot_x					0.733384
toes_r	foot_x					0.733384
femur_l	thigh_L_y					0.569068
tibia_l	tibia_L_y					0.598991
patella_l	tibia_L_y					0.598991
talus_l	foot_x					0.733384
calcn_l	foot_x					0.733384
toes_l	foot_x					0.733384
torso	torso_x	torso_y	torso_z	0.685141	0.672406	0.706843
humerus_r	humerus					0.669530
ulna_r	ulna					0.615462
radius_r	radius					0.642765
hand_r	hand					0.816283
humerus_l	humerus					0.669530
ulna_l	ulna					0.615462
radius_l	radius					0.642765
hand_l	hand					0.816283

Figure D-3: Sample scale factors used for static scaling

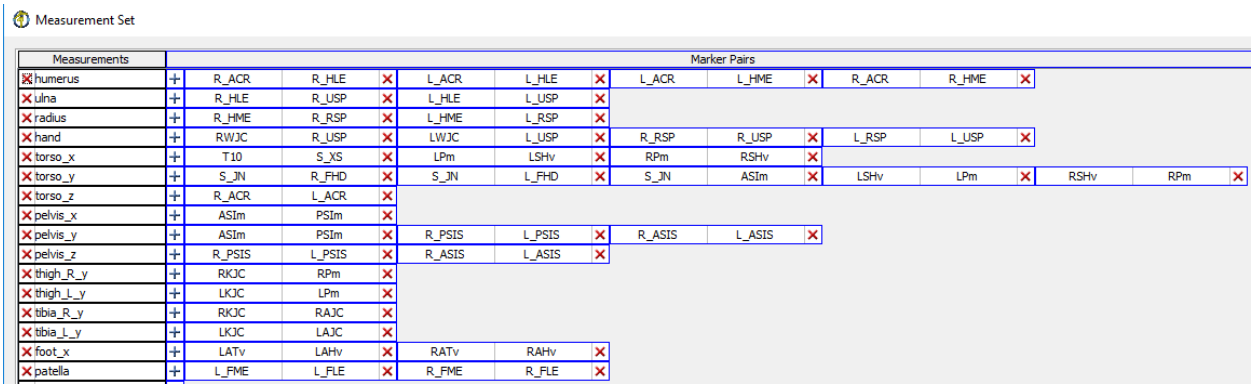

Measurements	Marker Pairs											
humerus	R_ACR	R_HLE	L_ACR	L_HLE	L_ACR	L_HME	R_ACR	R_HME				
ulna	R_HLE	R_USP	L_HLE	L_USP								
radius	R_HME	R_RSP	L_HME	L_RSP								
hand	RWJC	R_USP	LWJC	L_USP	R_RSP	R_USP	L_RSP	L_USP				
torso_x	T10	S_XS	LPm	LSHv	RPm	RSHv						
torso_y	S_JN	R_FHD	S_JN	L_FHD	S_JN	ASIm	LSHv	LPm	RSHv	RPm		
torso_z	R_ACR	L_ACR										
pelvis_x	ASIm	PSIm										
pelvis_y	ASIm	PSIm	R_PSIS	L_PSIS	R_ASIS	L_ASIS						
pelvis_z	R_PSIS	L_PSIS	R_ASIS	L_ASIS								
thigh_R_y	RKJC	RPm										
thigh_L_y	LKJC	LPm										
tibia_R_y	RKJC	RAJC										
tibia_L_y	LKJC	LAJC										
foot_x	LATv	LAHv	RATv	RAHv								
patella	L_FME	L_FLE	R_FME	R_FLE								

Figure D-4: Marker pairs used to generate measurement sets

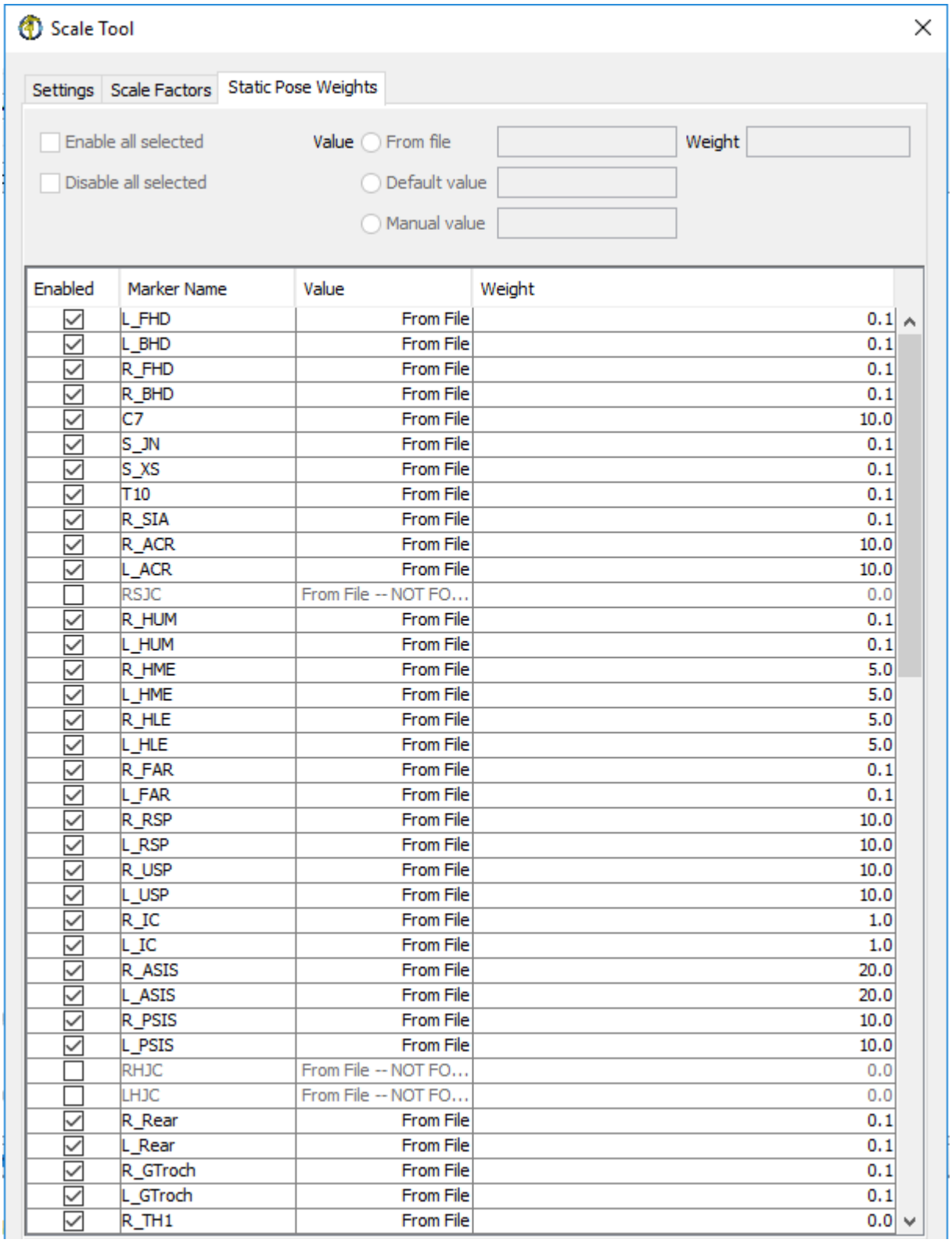

Enabled	Marker Name	Value	Weight
☑	L_FHD	From File	0.1
☑	L_BHD	From File	0.1
☑	R_FHD	From File	0.1
☑	R_BHD	From File	0.1
☑	C7	From File	10.0
☑	S_JN	From File	0.1
☑	S_XS	From File	0.1
☑	T10	From File	0.1
☑	R_SIA	From File	0.1
☑	R_ACR	From File	10.0
☑	L_ACR	From File	10.0
☐	RSJC	From File -- NOT FO...	0.0
☑	R_HUM	From File	0.1
☑	L_HUM	From File	0.1
☑	R_HME	From File	5.0
☑	L_HME	From File	5.0
☑	R_HLE	From File	5.0
☑	L_HLE	From File	5.0
☑	R_FAR	From File	0.1
☑	L_FAR	From File	0.1
☑	R_RSP	From File	10.0
☑	L_RSP	From File	10.0
☑	R_USP	From File	10.0
☑	L_USP	From File	10.0
☑	R_IC	From File	1.0
☑	L_IC	From File	1.0
☑	R_ASIS	From File	20.0
☑	L_ASIS	From File	20.0
☑	R_PSIS	From File	10.0
☑	L_PSIS	From File	10.0
☐	RHJC	From File -- NOT FO...	0.0
☐	LHJC	From File -- NOT FO...	0.0
☑	R_Rear	From File	0.1
☑	L_Rear	From File	0.1
☑	R_GTroch	From File	0.1
☑	L_GTroch	From File	0.1
☑	R_TH1	From File	0.0

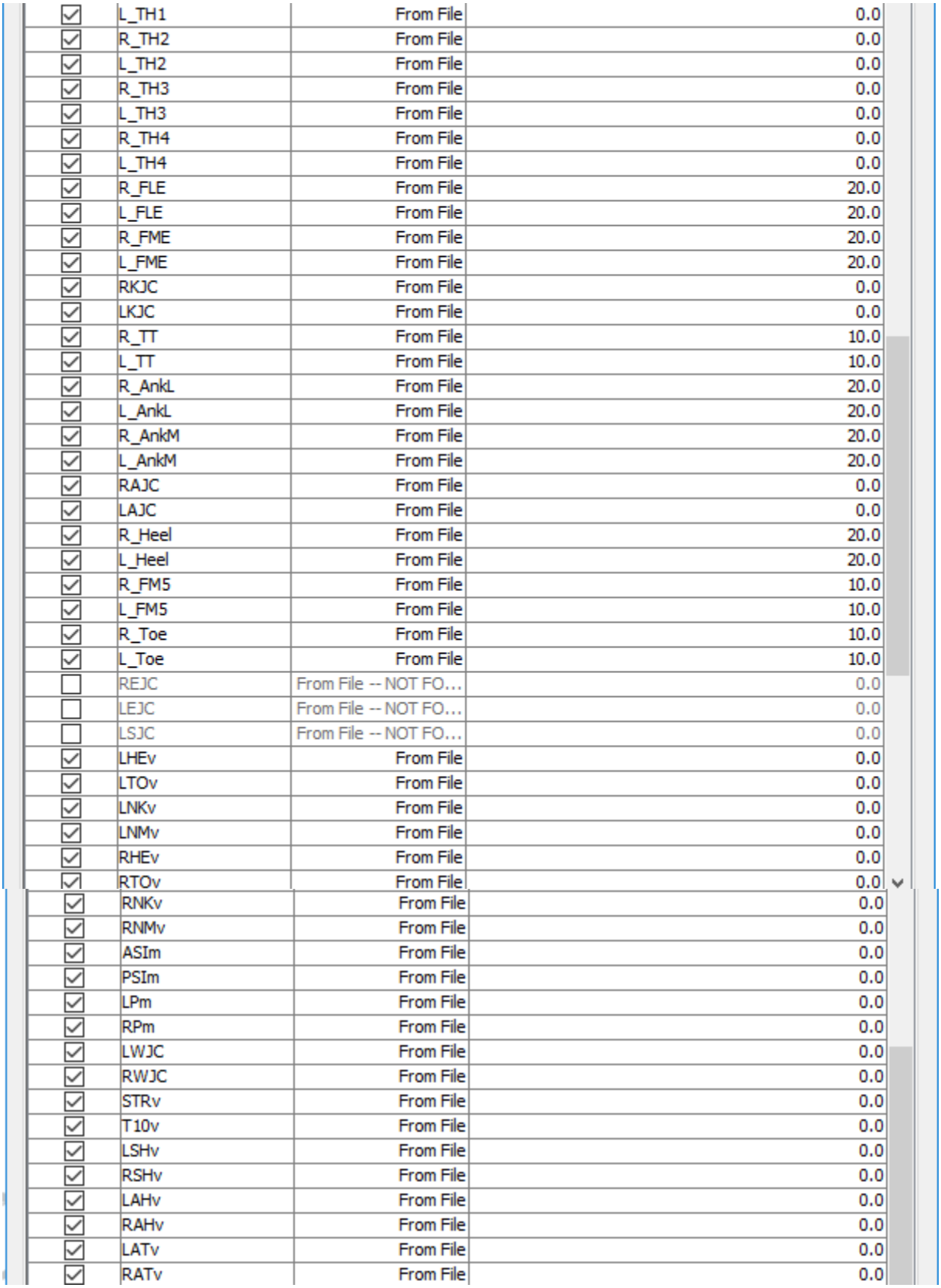

☑	L_TH1	From File	0.0
☑	R_TH2	From File	0.0
☑	L_TH2	From File	0.0
☑	R_TH3	From File	0.0
☑	L_TH3	From File	0.0
☑	R_TH4	From File	0.0
☑	L_TH4	From File	0.0
☑	R_FLE	From File	20.0
☑	L_FLE	From File	20.0
☑	R_FME	From File	20.0
☑	L_FME	From File	20.0
☑	RKJC	From File	0.0
☑	LKJC	From File	0.0
☑	R_TT	From File	10.0
☑	L_TT	From File	10.0
☑	R_AnkL	From File	20.0
☑	L_AnkL	From File	20.0
☑	R_AnkM	From File	20.0
☑	L_AnkM	From File	20.0
☑	RAJC	From File	0.0
☑	LAJC	From File	0.0
☑	R_Heel	From File	20.0
☑	L_Heel	From File	20.0
☑	R_FM5	From File	10.0
☑	L_FM5	From File	10.0
☑	R_Toe	From File	10.0
☑	L_Toe	From File	10.0
☐	REJC	From File -- NOT FO...	0.0
☐	LEJC	From File -- NOT FO...	0.0
☐	LSJC	From File -- NOT FO...	0.0
☑	LHEv	From File	0.0
☑	LTOv	From File	0.0
☑	LNKv	From File	0.0
☑	LNMv	From File	0.0
☑	RHEv	From File	0.0
☑	RTOv	From File	0.0
☑	RNKv	From File	0.0
☑	RNMv	From File	0.0
☑	ASIm	From File	0.0
☑	PSIm	From File	0.0
☑	LPm	From File	0.0
☑	RPm	From File	0.0
☑	LWJC	From File	0.0
☑	RWJC	From File	0.0
☑	STRv	From File	0.0
☑	T10v	From File	0.0
☑	LSHv	From File	0.0
☑	RSHv	From File	0.0
☑	LAHv	From File	0.0
☑	RAHv	From File	0.0
☑	LATv	From File	0.0
☑	RATv	From File	0.0

Figure D-5: Marker weights based on a 0-20 scale for static scaling

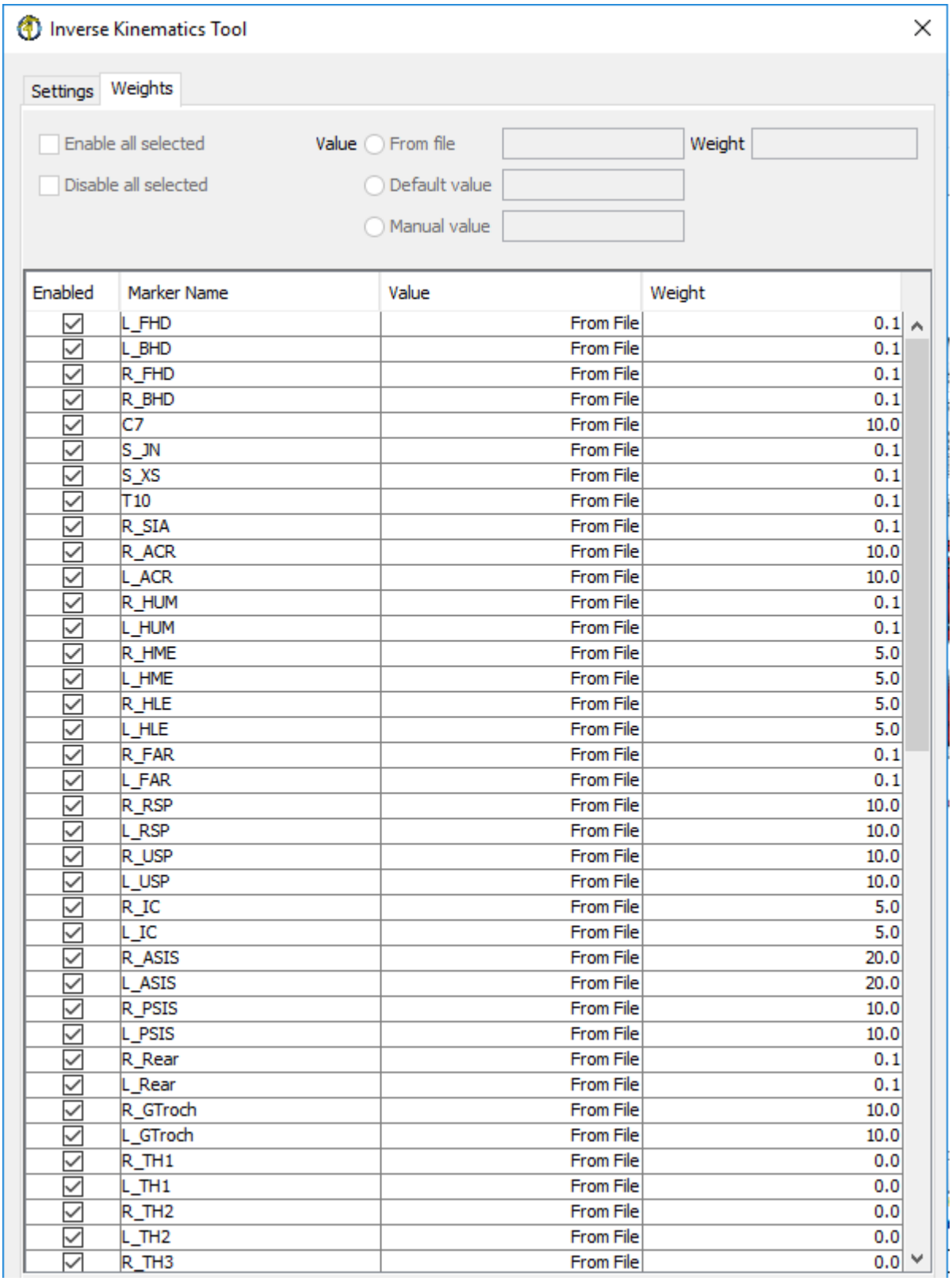

Enabled	Marker Name	Value	Weight
☑	L_FHD	From File	0.1
☑	L_BHD	From File	0.1
☑	R_FHD	From File	0.1
☑	R_BHD	From File	0.1
☑	C7	From File	10.0
☑	S_JN	From File	0.1
☑	S_XS	From File	0.1
☑	T10	From File	0.1
☑	R_SIA	From File	0.1
☑	R_ACR	From File	10.0
☑	L_ACR	From File	10.0
☑	R_HUM	From File	0.1
☑	L_HUM	From File	0.1
☑	R_HME	From File	5.0
☑	L_HME	From File	5.0
☑	R_HLE	From File	5.0
☑	L_HLE	From File	5.0
☑	R_FAR	From File	0.1
☑	L_FAR	From File	0.1
☑	R_RSP	From File	10.0
☑	L_RSP	From File	10.0
☑	R_USP	From File	10.0
☑	L_USP	From File	10.0
☑	R_IC	From File	5.0
☑	L_IC	From File	5.0
☑	R_ASIS	From File	20.0
☑	L_ASIS	From File	20.0
☑	R_PSIS	From File	10.0
☑	L_PSIS	From File	10.0
☑	R_Rear	From File	0.1
☑	L_Rear	From File	0.1
☑	R_GTroch	From File	10.0
☑	L_GTroch	From File	10.0
☑	R_TH1	From File	0.0
☑	L_TH1	From File	0.0
☑	R_TH2	From File	0.0
☑	L_TH2	From File	0.0
☑	R_TH3	From File	0.0

Enabled	Marker Name	Value	Weight
☑	R_TH3	From File	0.0
☑	L_TH3	From File	0.0
☑	R_TH4	From File	0.0
☑	L_TH4	From File	0.0
☑	R_FLE	From File	20.0
☑	L_FLE	From File	20.0
☐	R_FME	From File -- NOT FOUND!	0.0
☐	L_FME	From File -- NOT FOUND!	0.0
☐	RKJC	From File -- NOT FOUND!	0.0
☐	LKJC	From File -- NOT FOUND!	0.0
☑	R_TT	From File	20.0
☑	L_TT	From File	20.0
☑	R_AnkL	From File	10.0
☑	L_AnkL	From File	10.0
☑	R_AnkM	From File	10.0
☑	L_AnkM	From File	10.0
☐	RAJC	From File -- NOT FOUND!	0.0
☐	LAJC	From File -- NOT FOUND!	0.0
☑	R_Heel	From File	10.0
☑	L_Heel	From File	10.0
☑	R_FM5	From File	5.0
☑	L_FM5	From File	5.0
☑	R_Toe	From File	5.0
☑	L_Toe	From File	5.0

Figure D-6: Sample marker weights on a 0-20 scale for inverse kinematics

References:

[1] Rajagopal, A., C. L. Dembia, M. S. DeMers, D. D. Delp, J. L. Hicks and S. L. Delp (2016). "Full-body musculoskeletal model for muscle-driven simulation of human gait." IEEE Transactions on Biomedical Engineering 63(10): 2068-2079.

[2] OpenSimVideos (2017). OpenSim Webinar: Tips and Tricks for Data Collection, Scaling and Inverse Kinematics in OpenSim, YouTube.

Appendix E: Inverse Kinematics and Correlation Plots for all Conditions

TD1

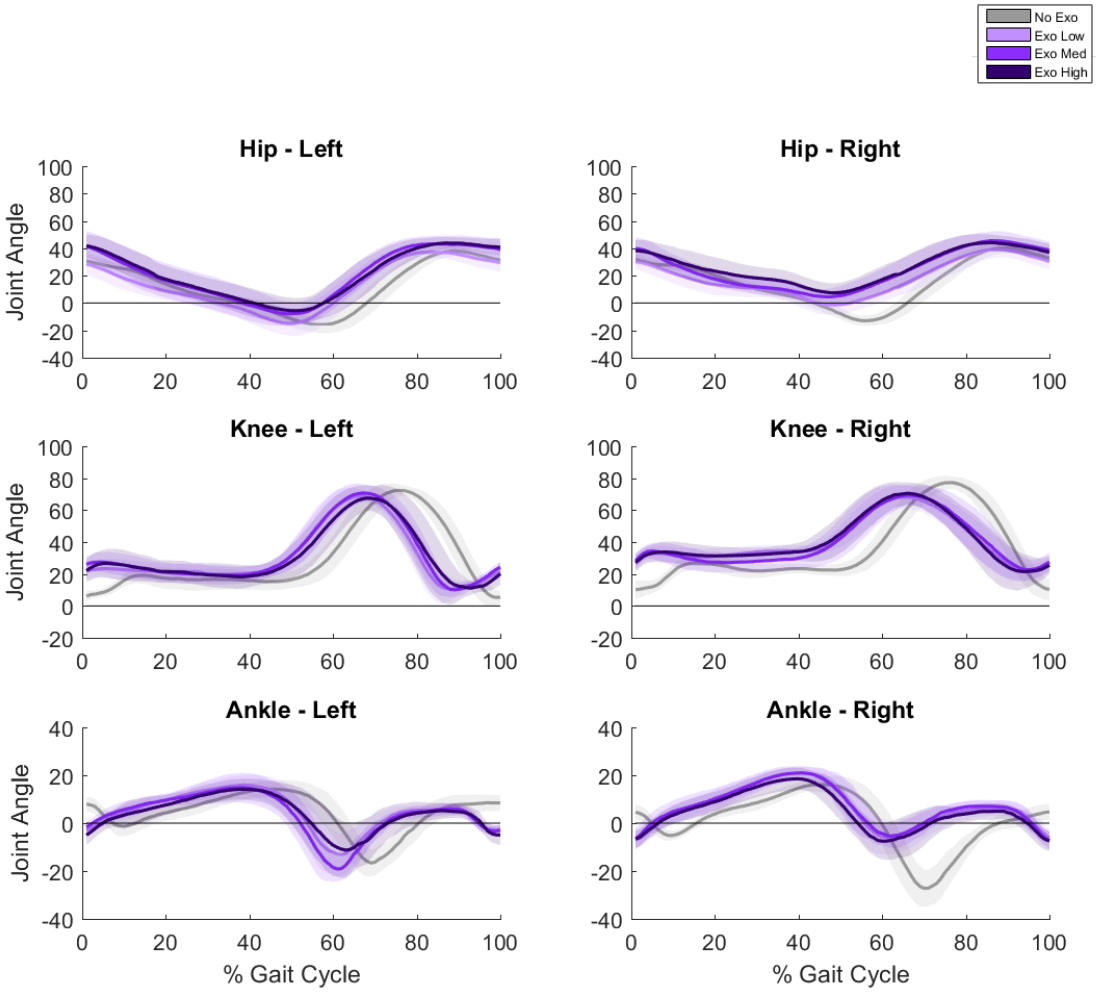

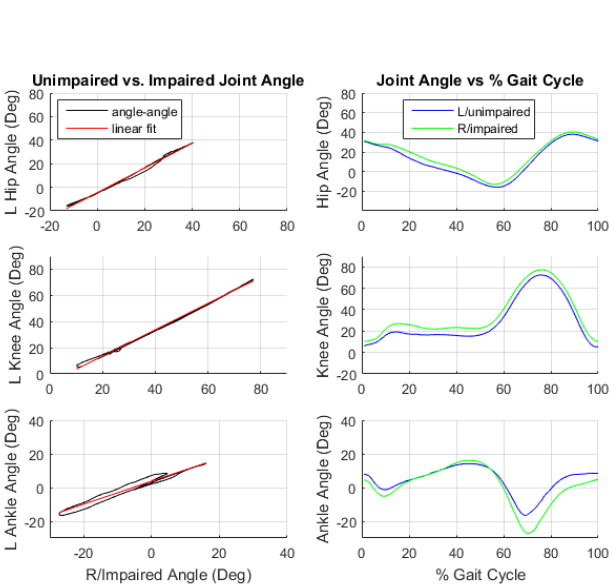

No Exo

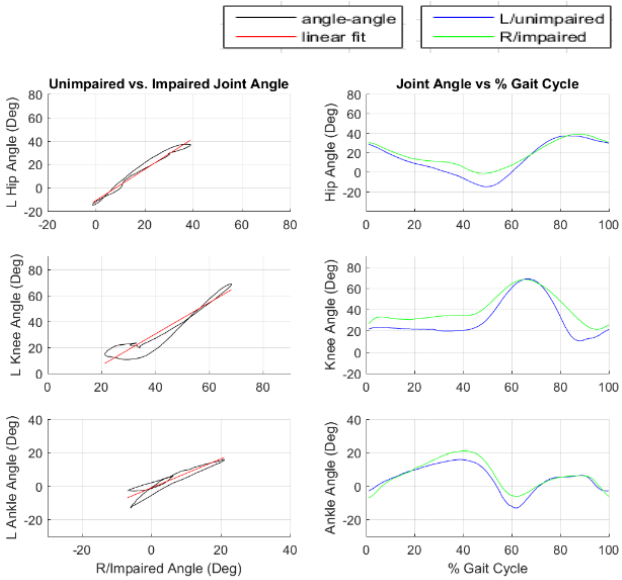

Exo Low

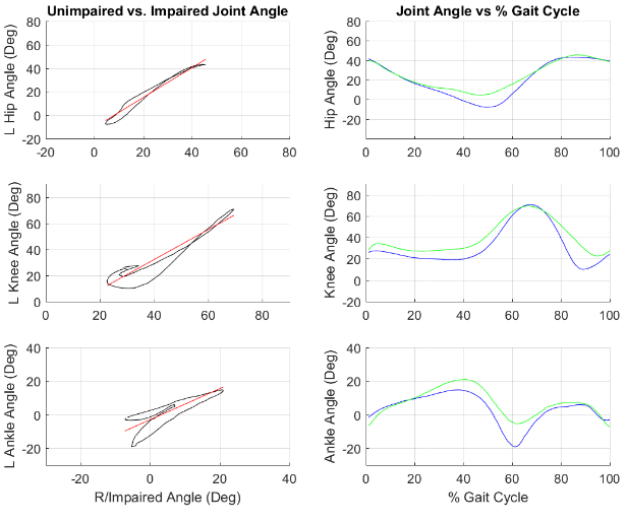

Exo Med

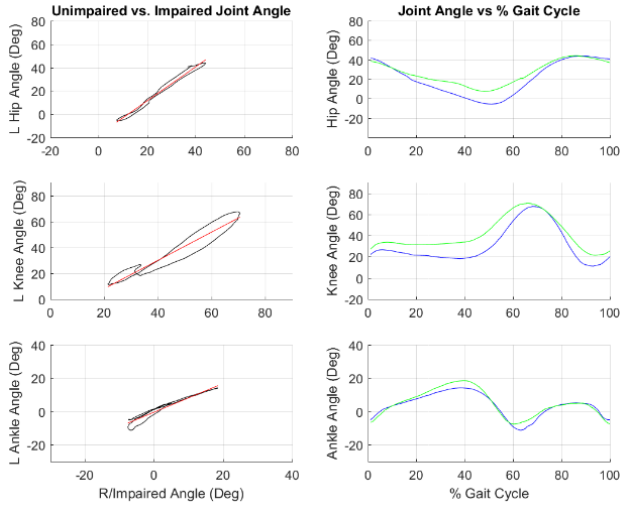

Exo High

TD 2

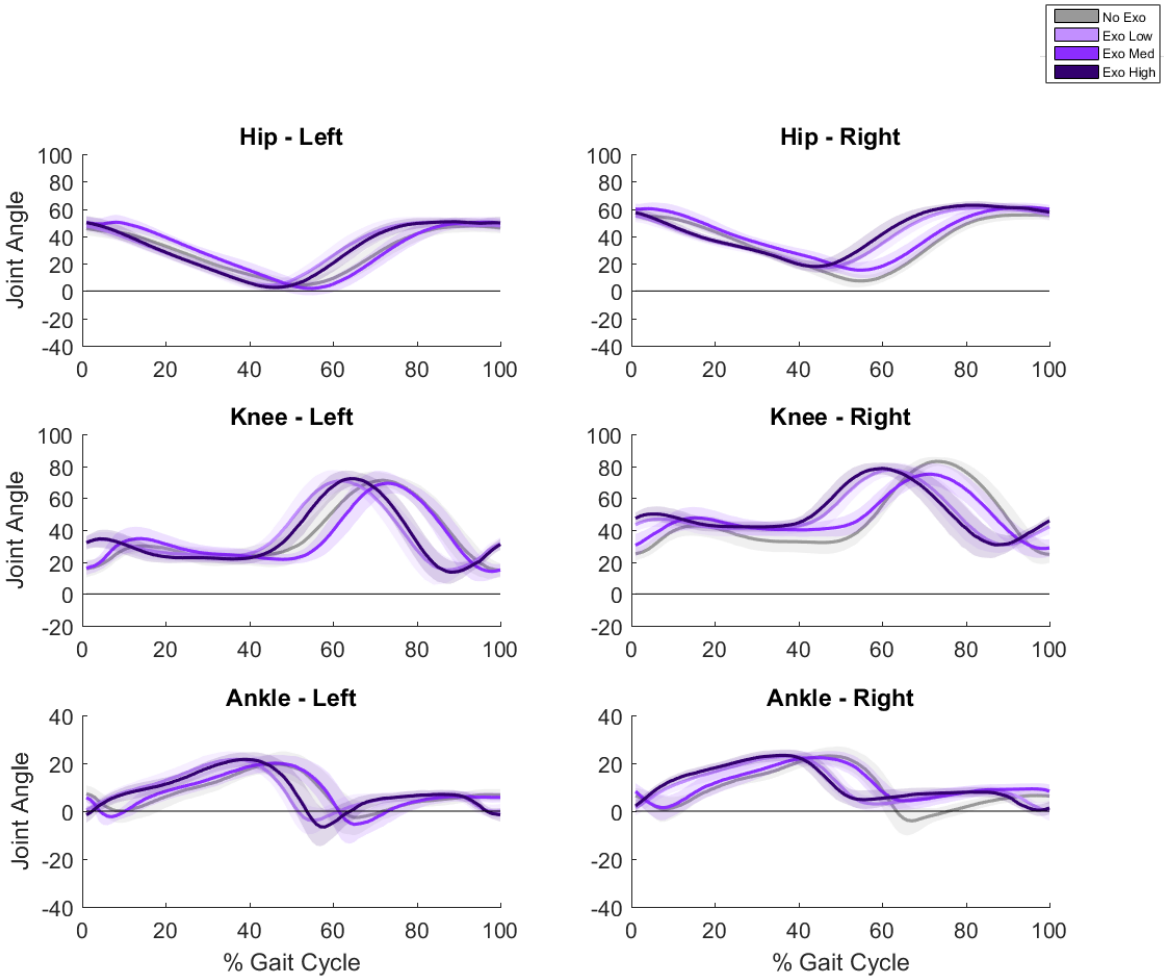
No Exo
Exo Low
Exo Med
Exo High
Hip - Left
Hip - Right
Knee - Left
Knee - Right
Ankle - Left
Ankle - Right
Joint Angle
% Gait Cycle

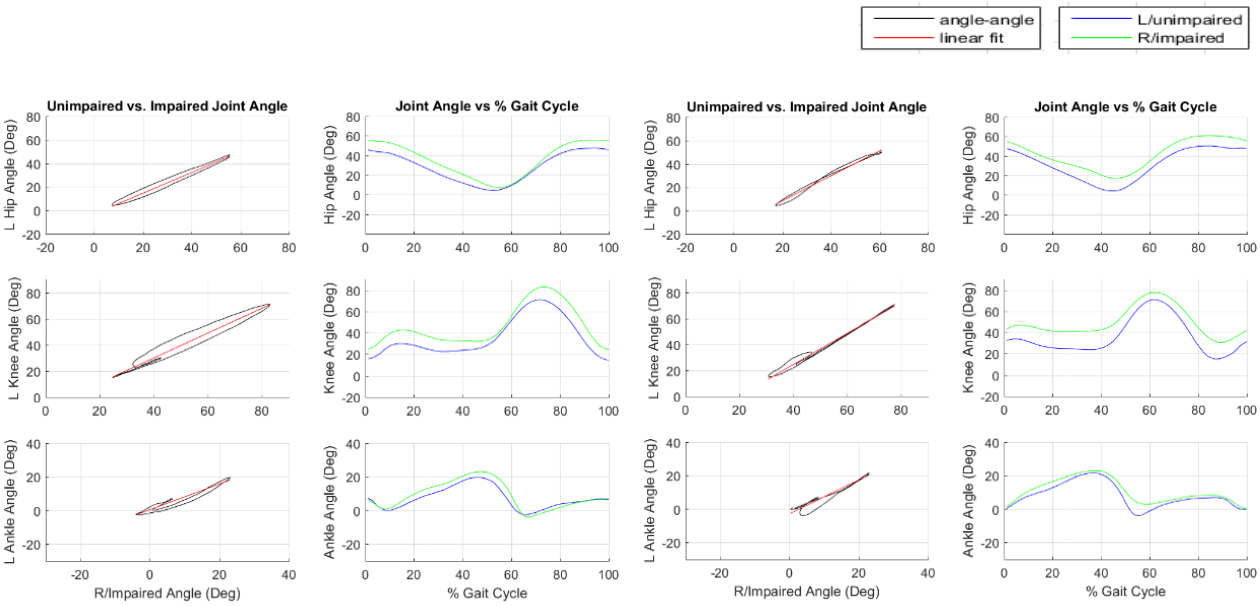

No Exo

Exo Low

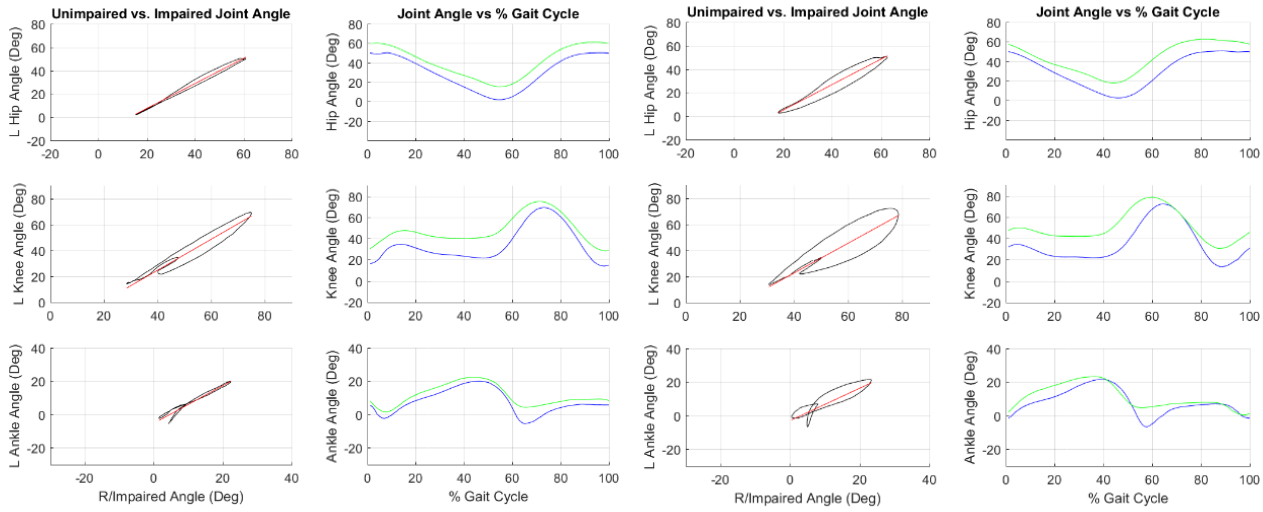

Exo Med

Exo High

TD3

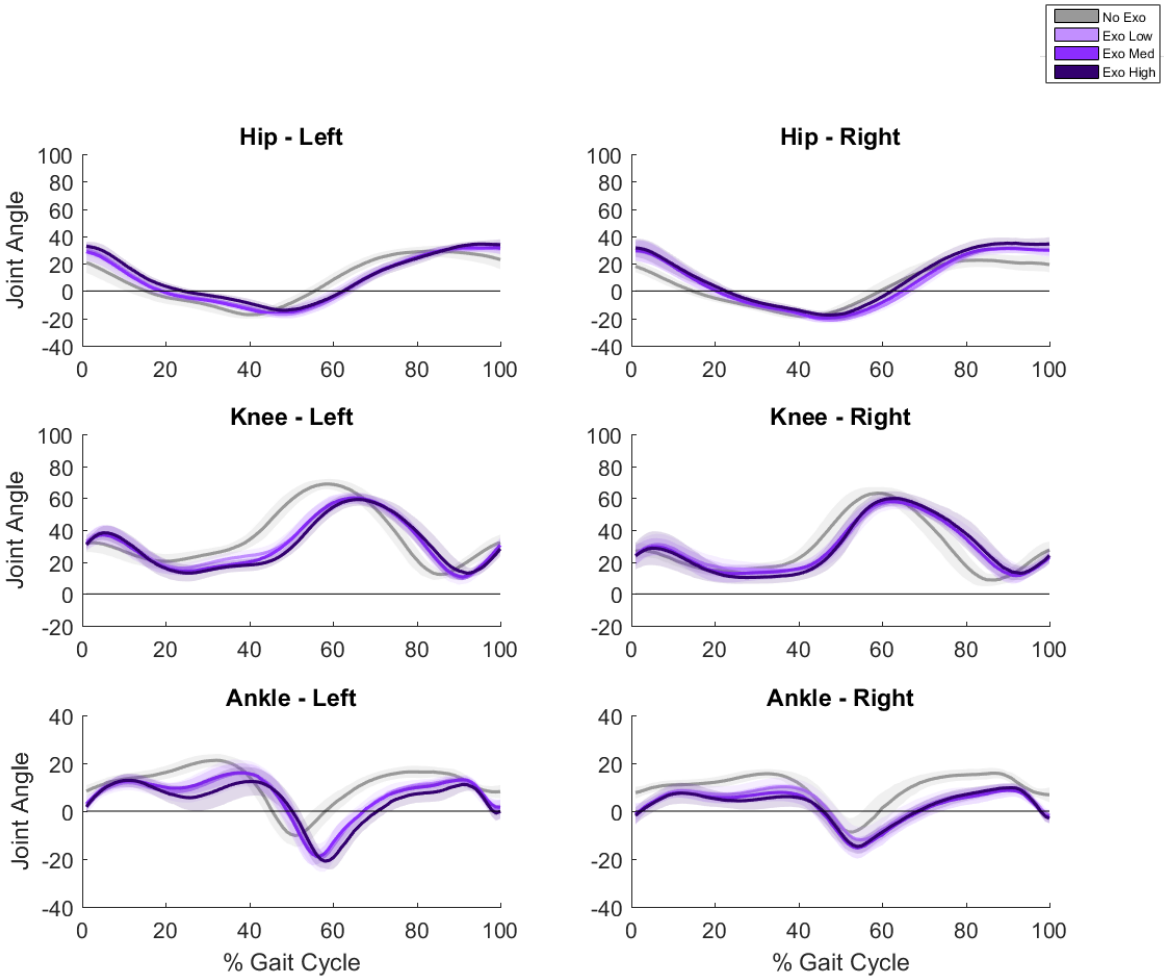
No Exo
Exo Low
Exo Med
Exo High
Hip - Left
Hip - Right
Knee - Left
Knee - Right
Ankle - Left
Ankle - Right
Joint Angle
% Gait Cycle

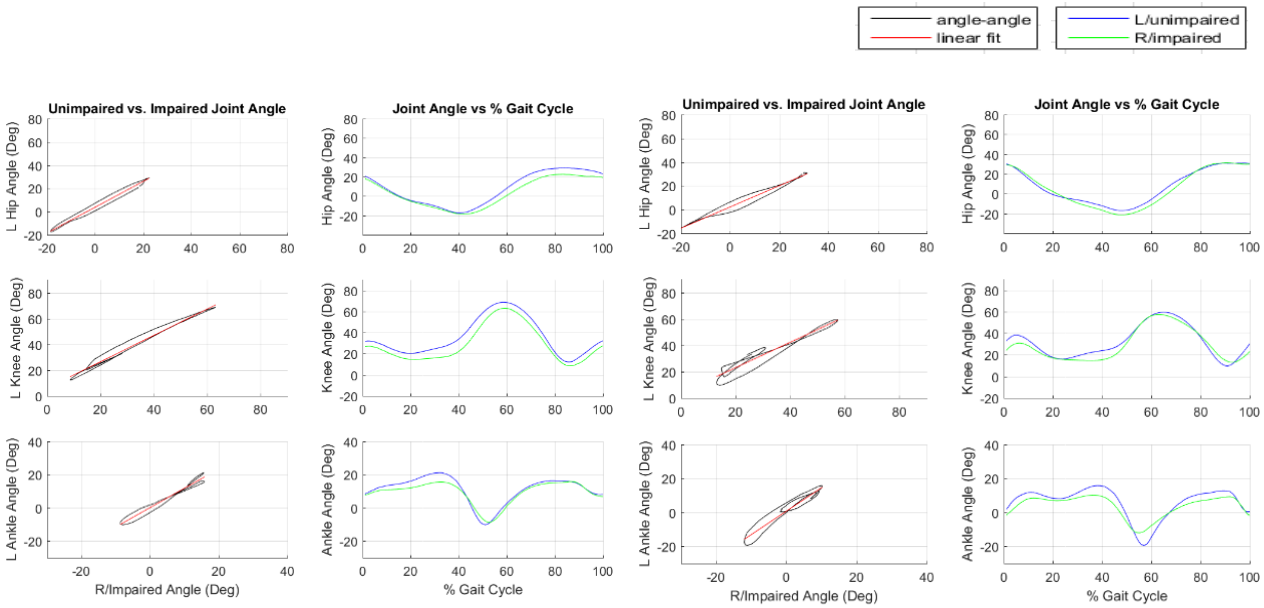

No Exo

Exo Low

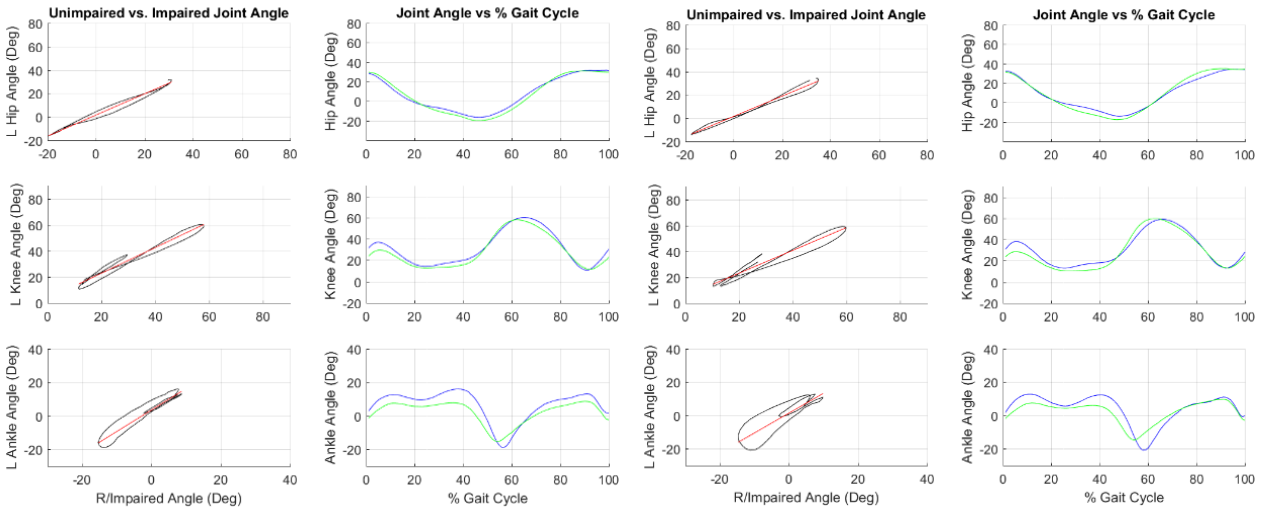

Exo Med

Exo High

H1

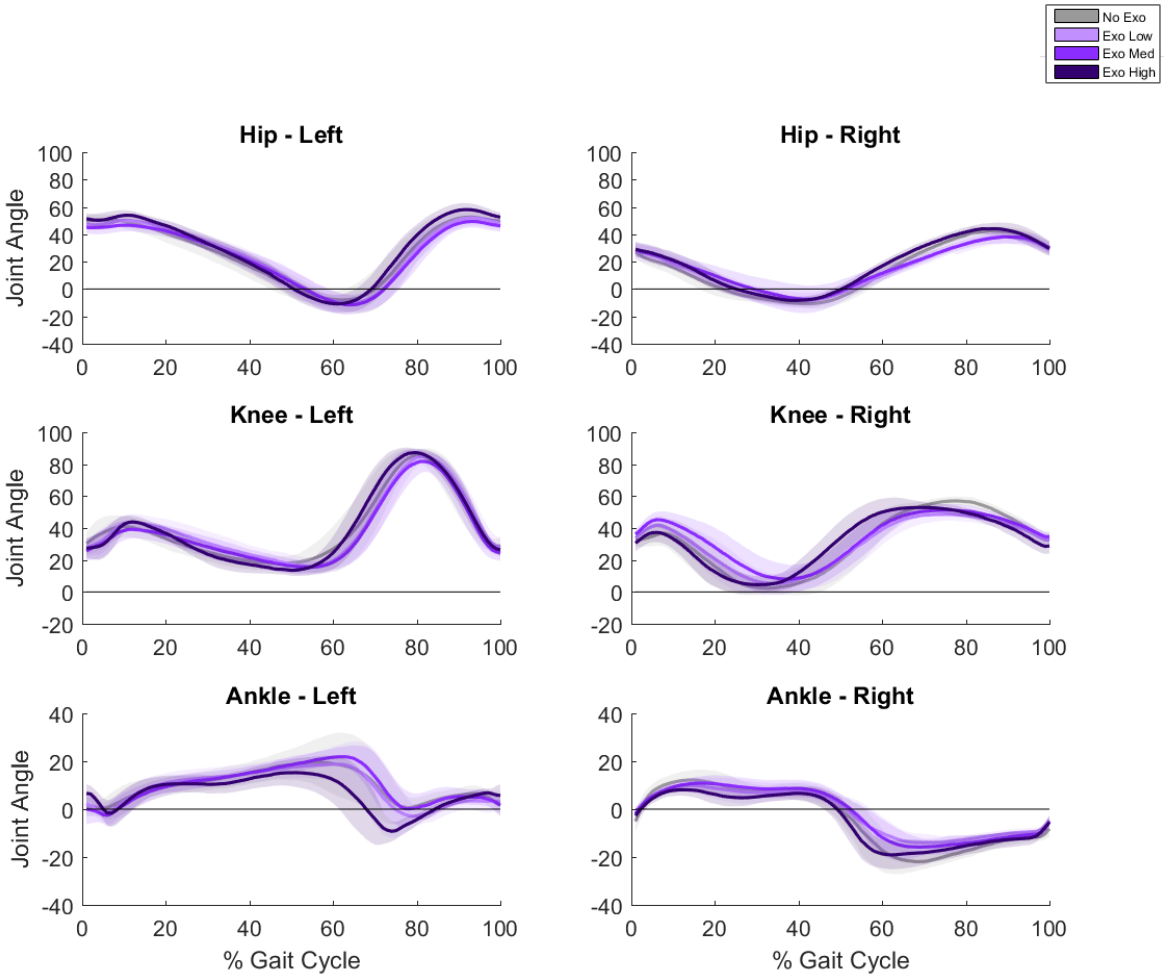
No Exo
Exo Low
Exo Med
Exo High
Hip - Left
Hip - Right
Knee - Left
Knee - Right
Ankle - Left
Ankle - Right
Joint Angle
% Gait Cycle

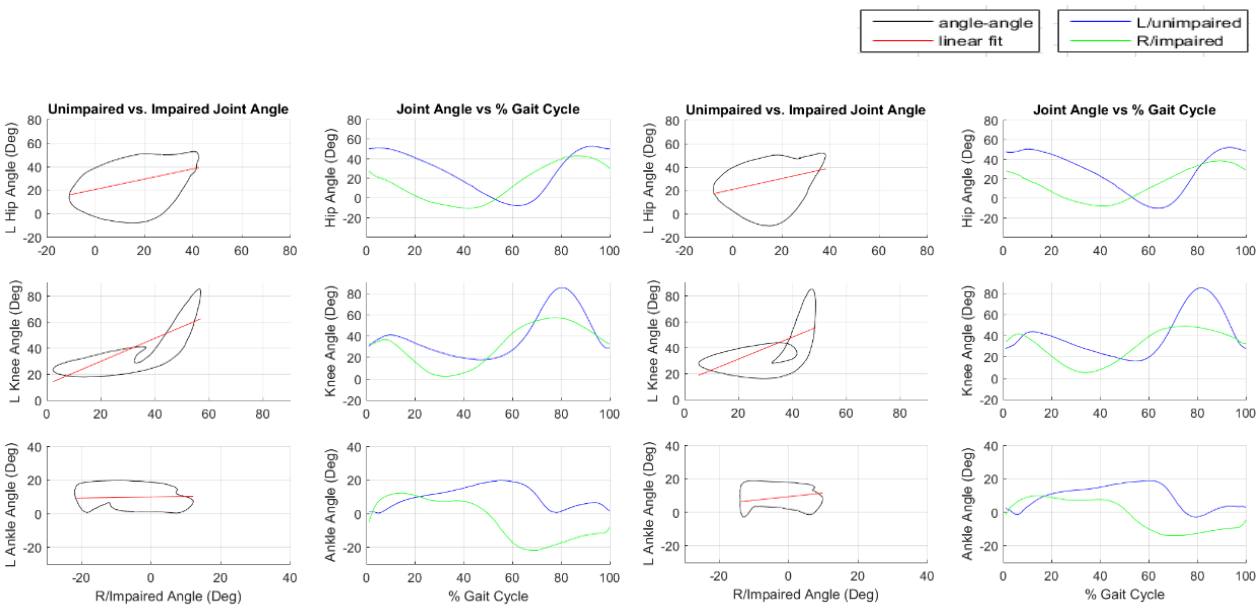

No Exo

Exo Low

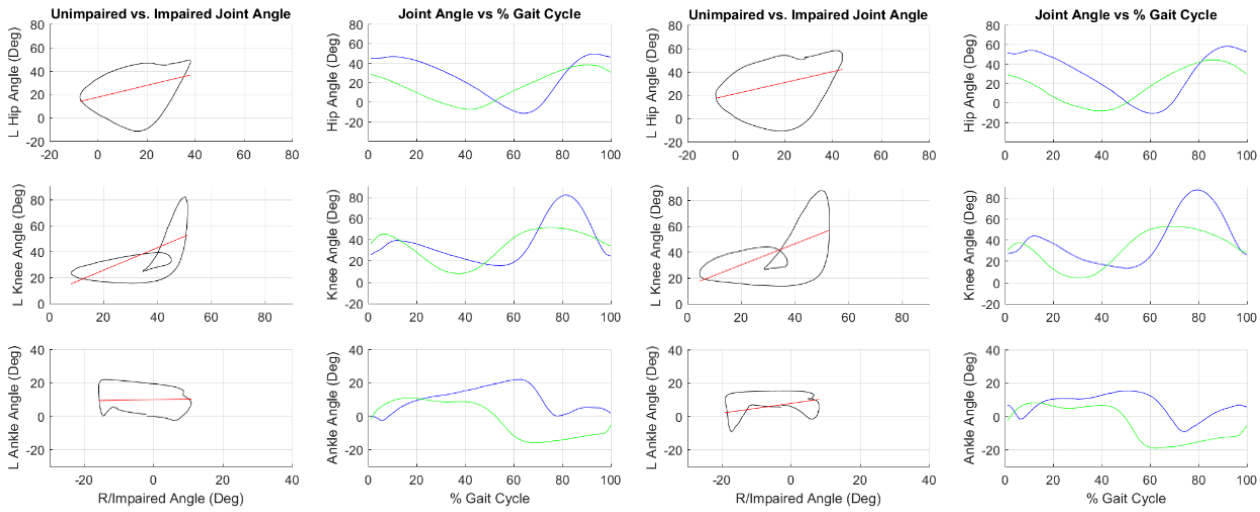

Exo Med

Exo High

H2

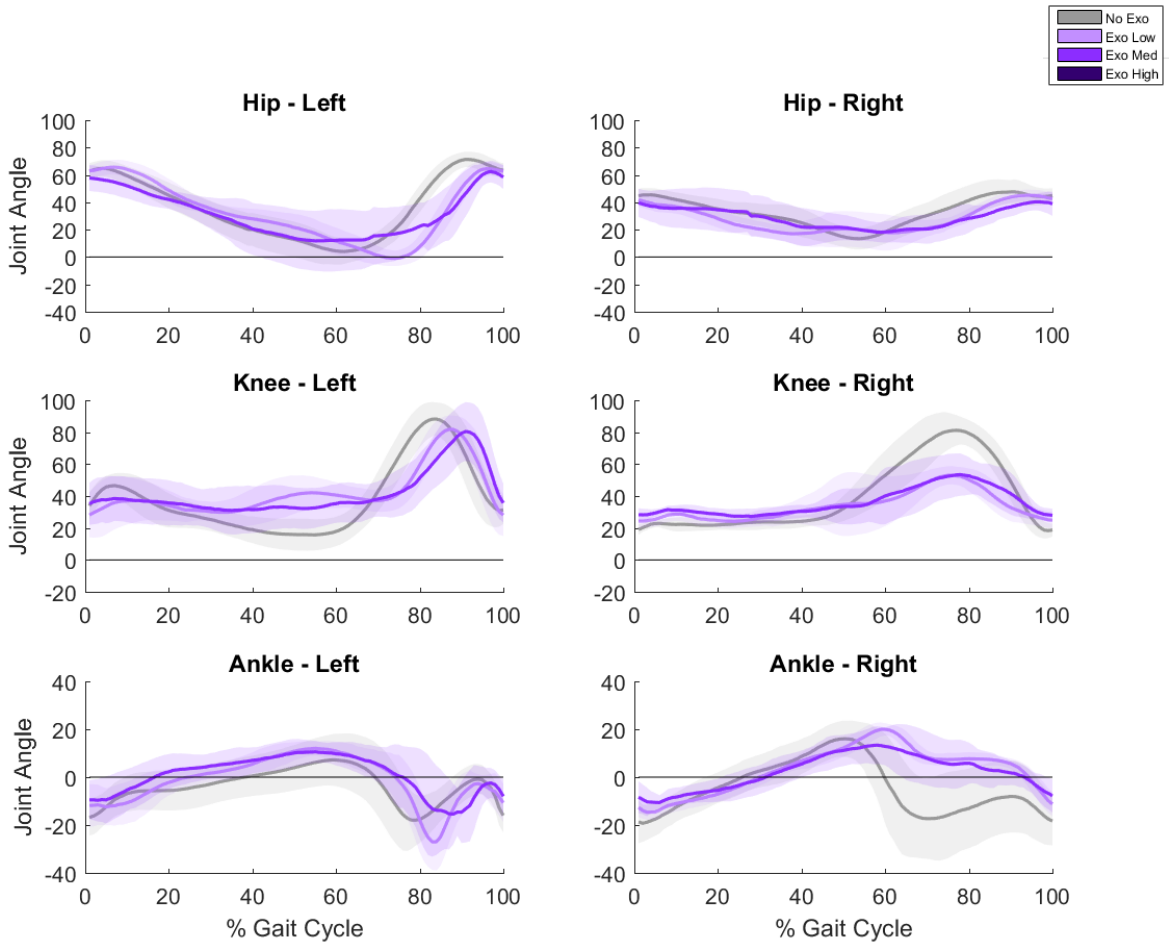
No Exo
Exo Low
Exo Med
Exo High
Hip - Left
Hip - Right
Knee - Left
Knee - Right
Ankle - Left
Ankle - Right
Joint Angle
% Gait Cycle

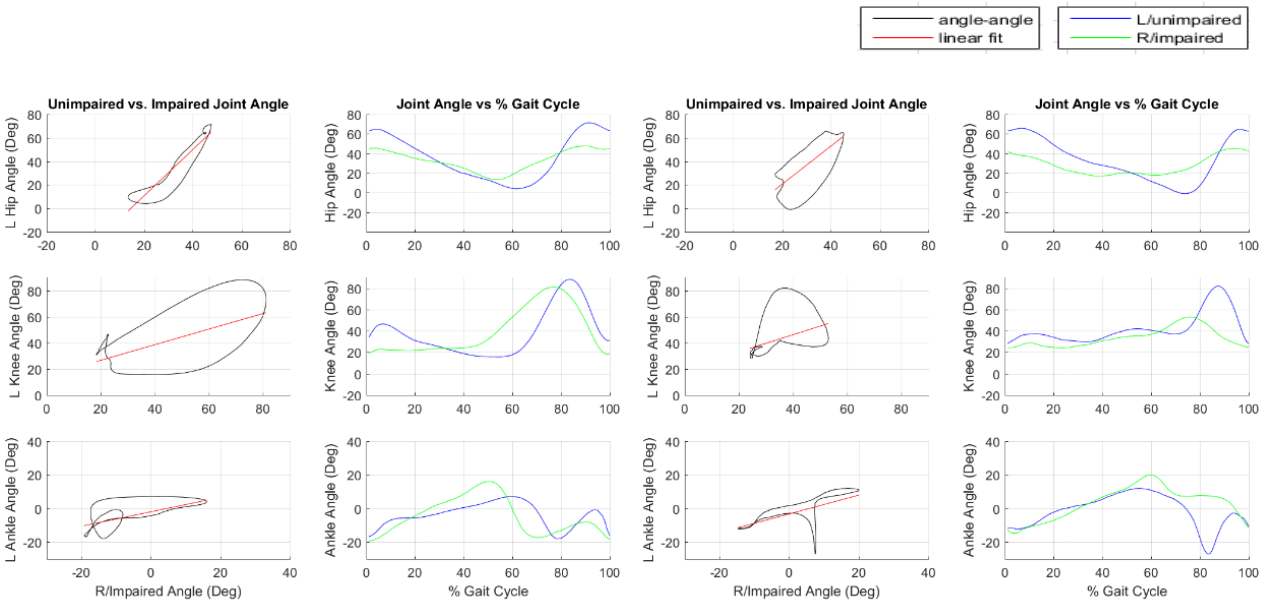

No Exo

Exo Low

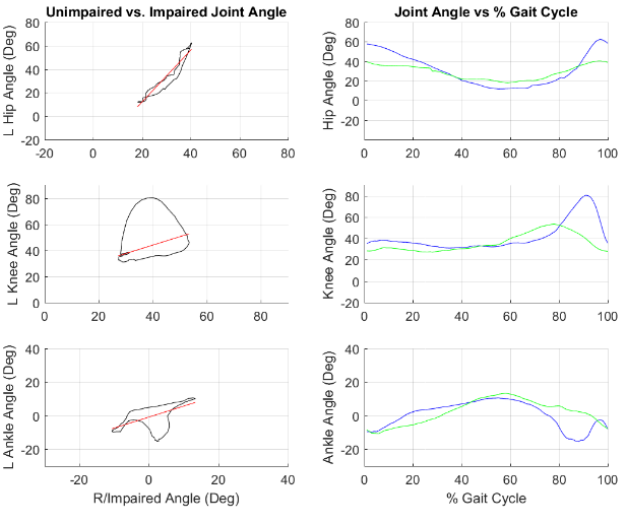

Exo Med

No Exo High data

Appendix F: Electromyography Results

TD1 – Right Leg

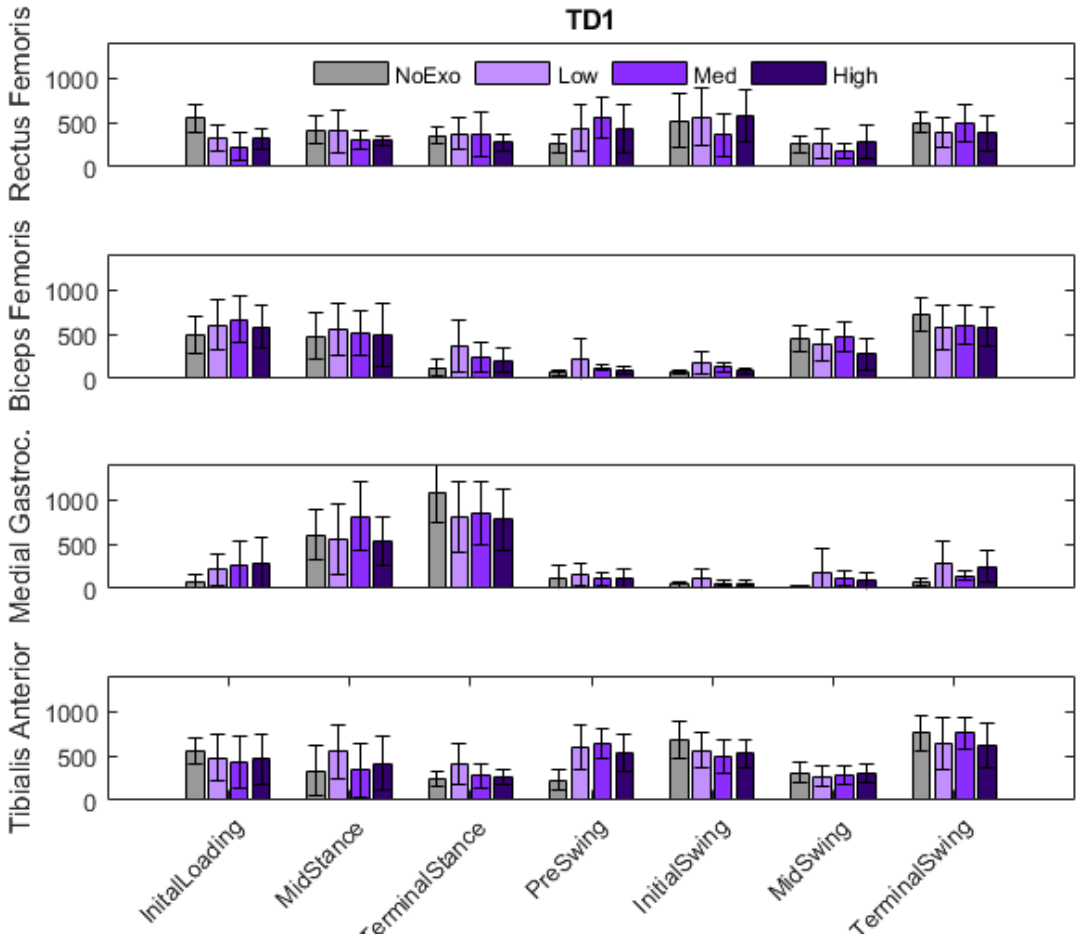

TD1 – Left Leg

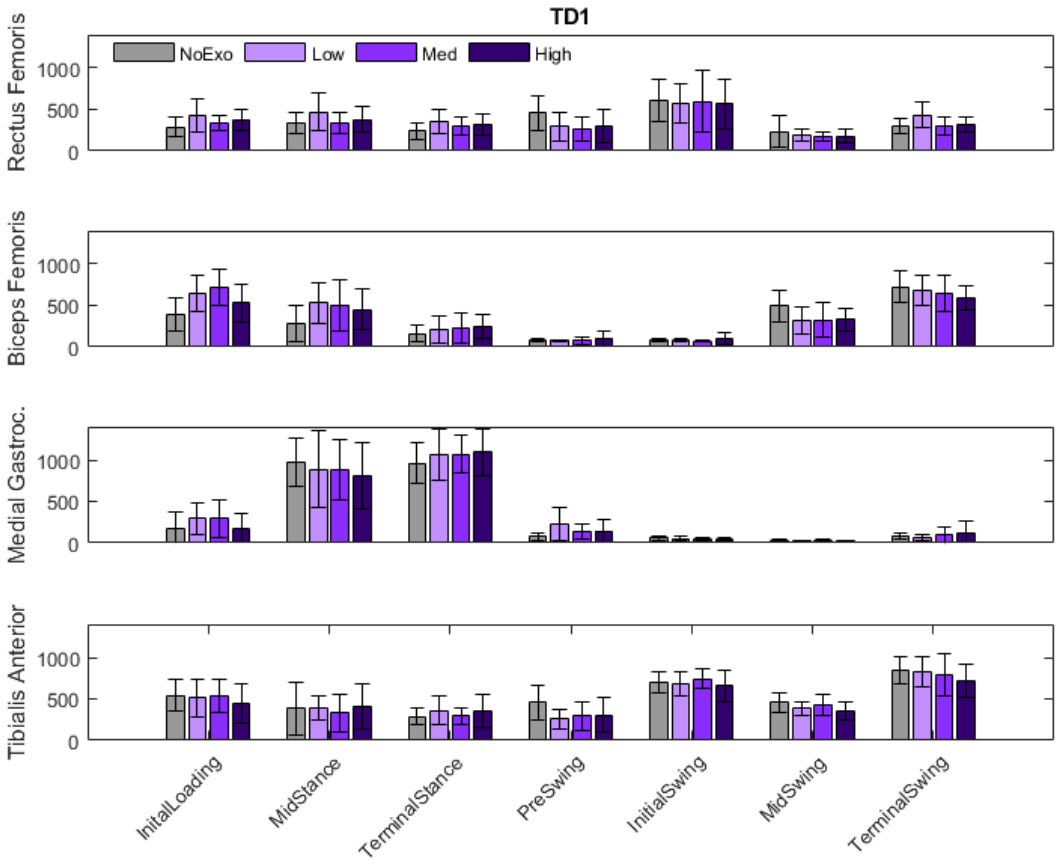
TD1
NoExo
Low
Med
High
Rectus Femoris
Biceps Femoris
Medial Gastroc.
Tibialis Anterior
1000
500
0
InitalLoading
MidStance
TerminalStance
PreSwing
InitialSwing
MidSwing
TerminalSwing

TD2 – Right Leg

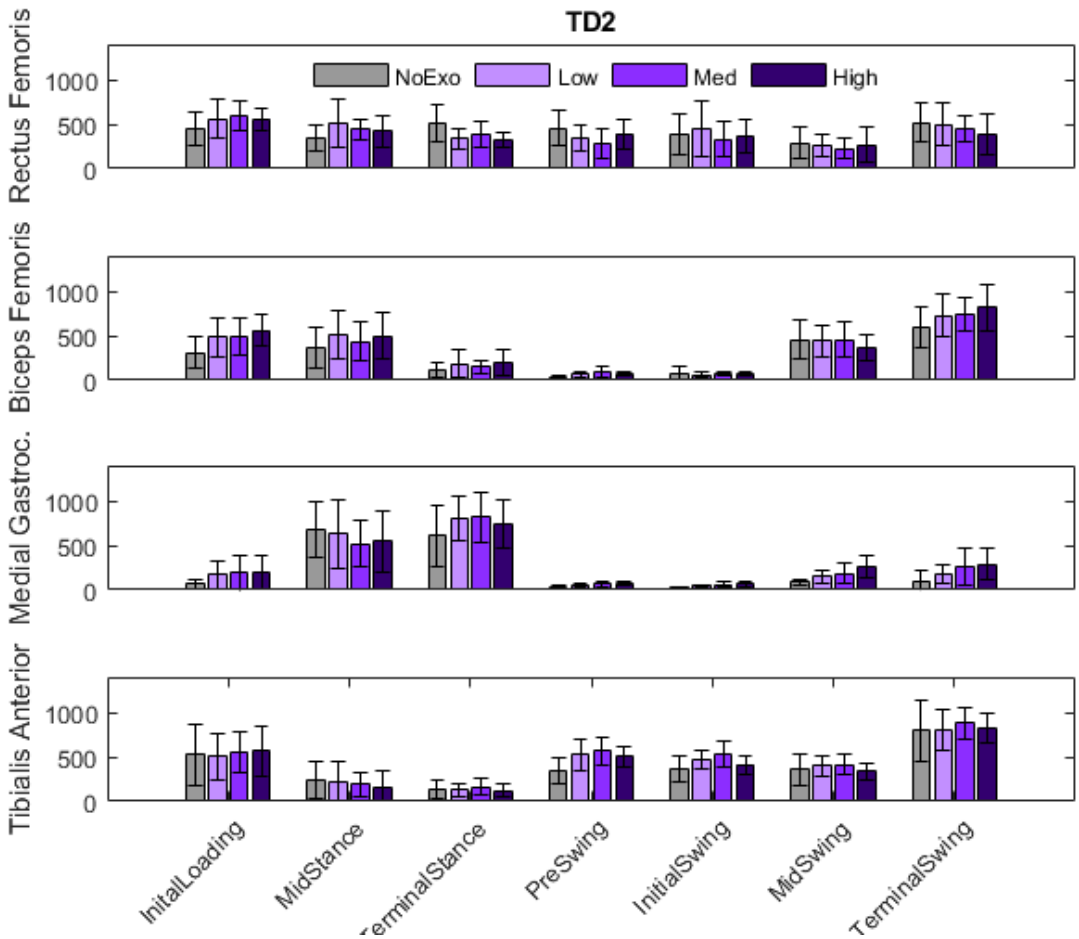

TD2 – Left Leg

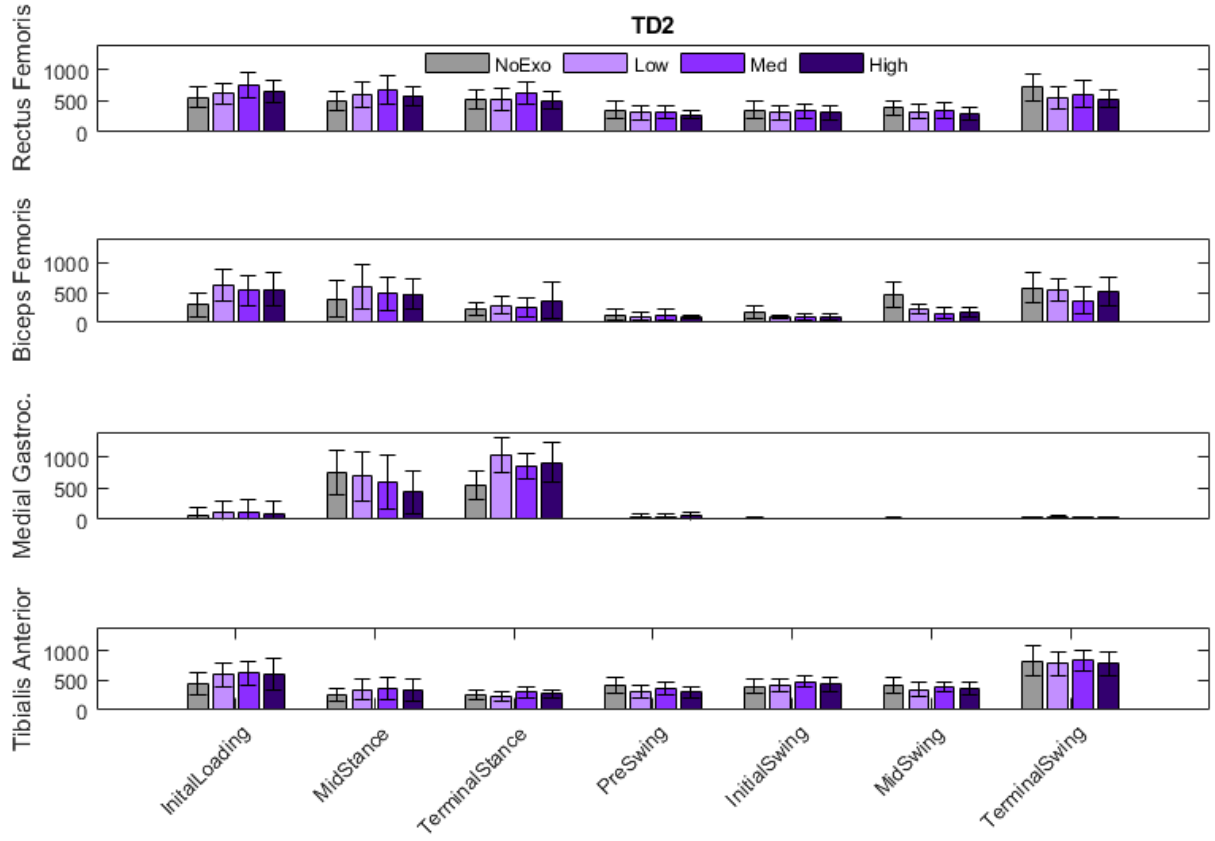
TD2
NoExo
Low
Med
High
Rectus Femoris
Biceps Femoris
Medial Gastroc.
Tibialis Anterior
1000
500
0
InitalLoading
MidStance
TerminalStance
PreSwing
InitialSwing
MidSwing
TerminalSwing

TD3 – Right Leg

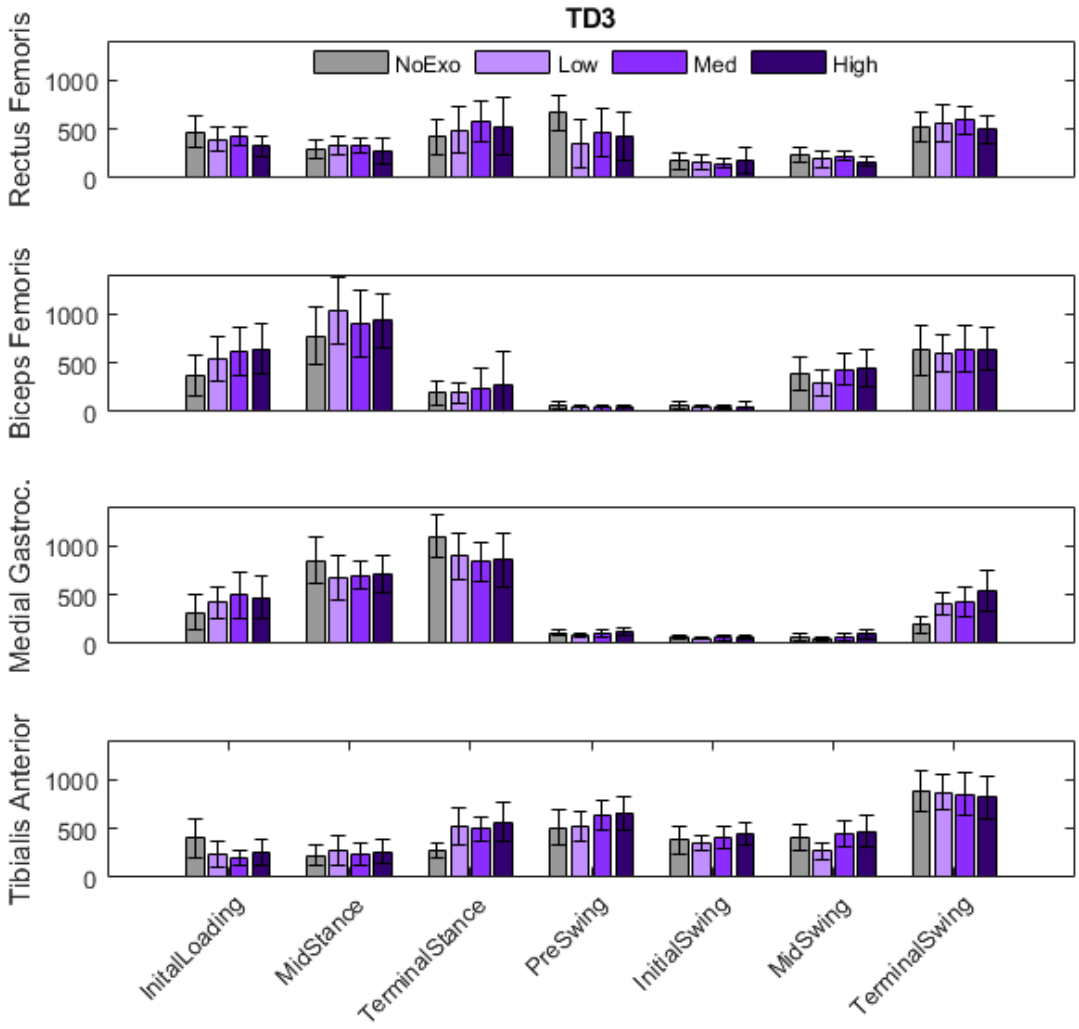

TD3 – Left Leg

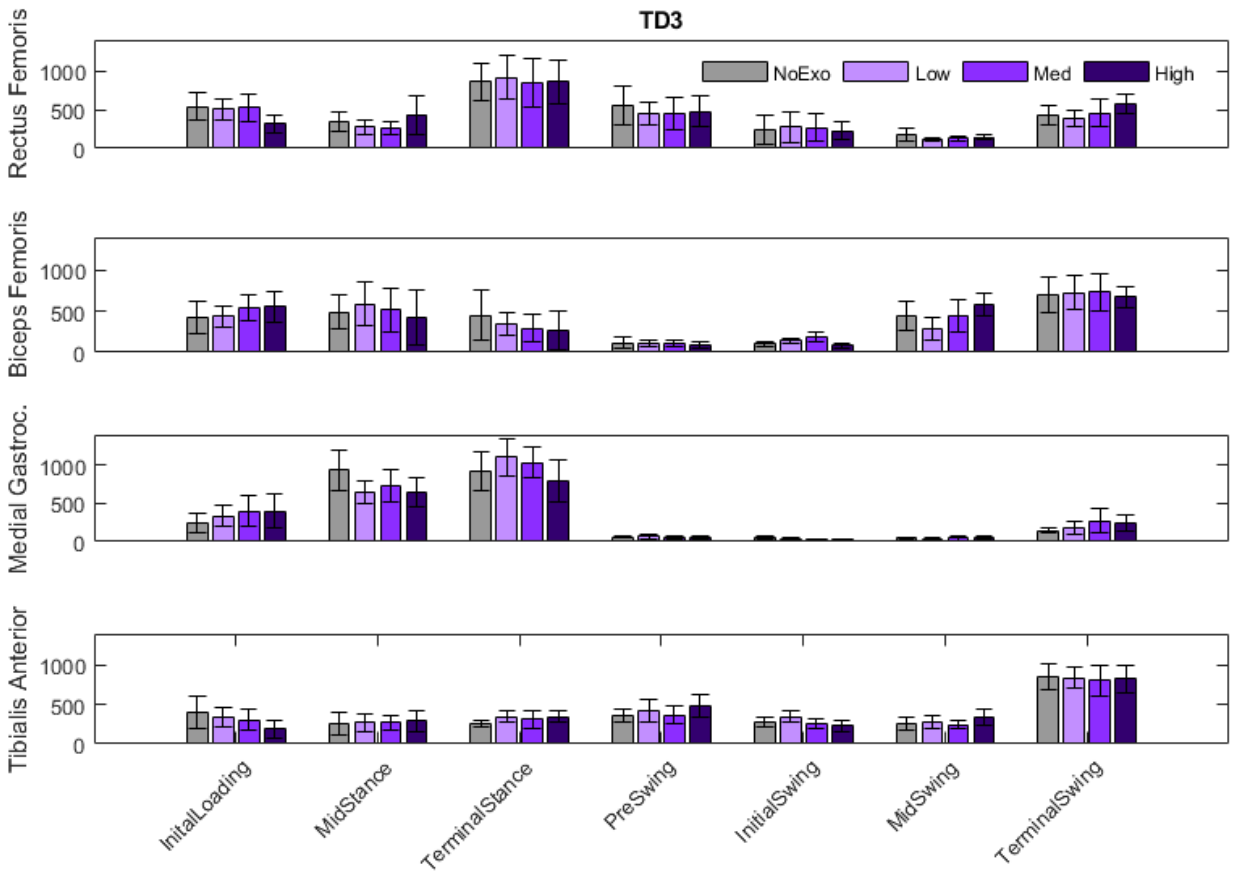
TD3
NoExo
Low
Med
High
Rectus Femoris
Biceps Femoris
Medial Gastroc.
Tibialis Anterior
1000
500
0
InitalLoading
MidStance
TerminalStance
PreSwing
InitialSwing
MidSwing
TerminalSwing

H1 – Right Leg

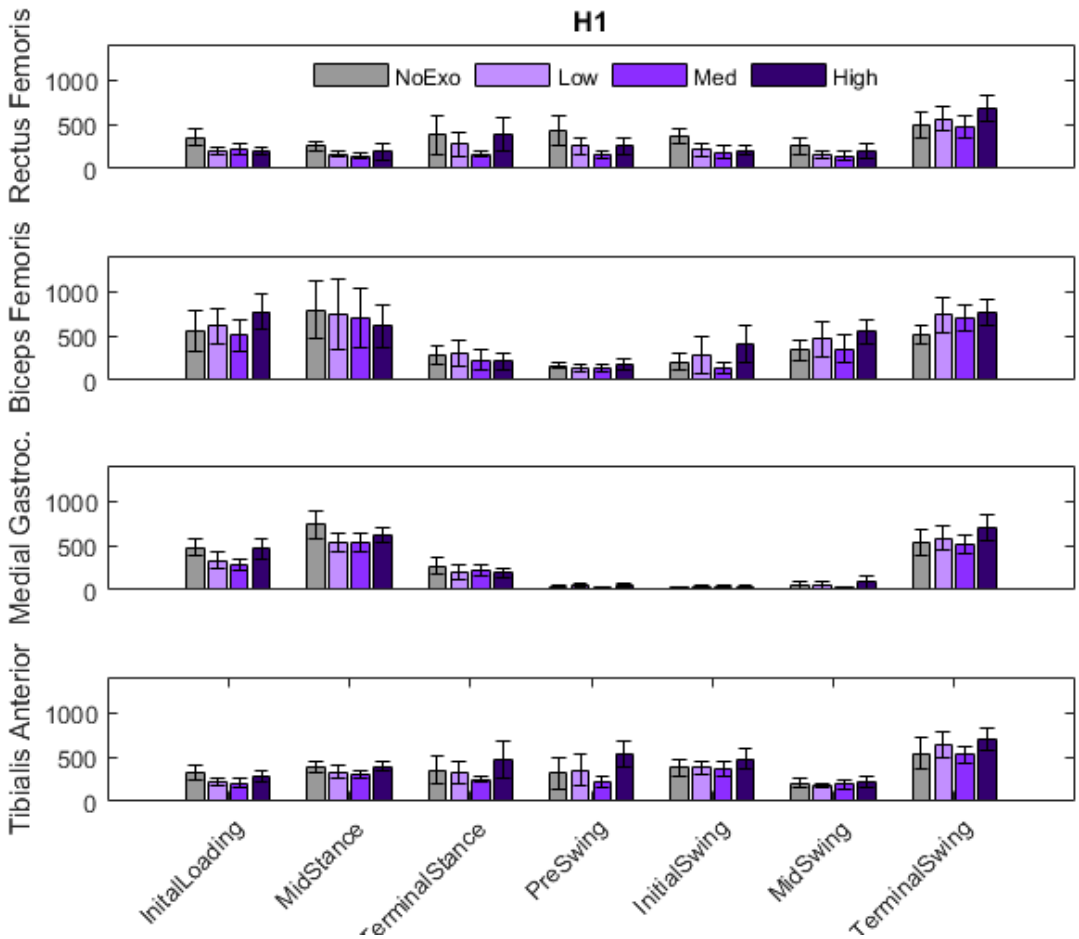
H1
NoExo
Low
Med
High
Rectus Femoris
Biceps Femoris
Medial Gastroc.
Tibialis Anterior
1000
500
0
InitalLoading
MidStance
TerminalStance
PreSwing
InitialSwing
MidSwing
TerminalSwing

H1 – Left Leg

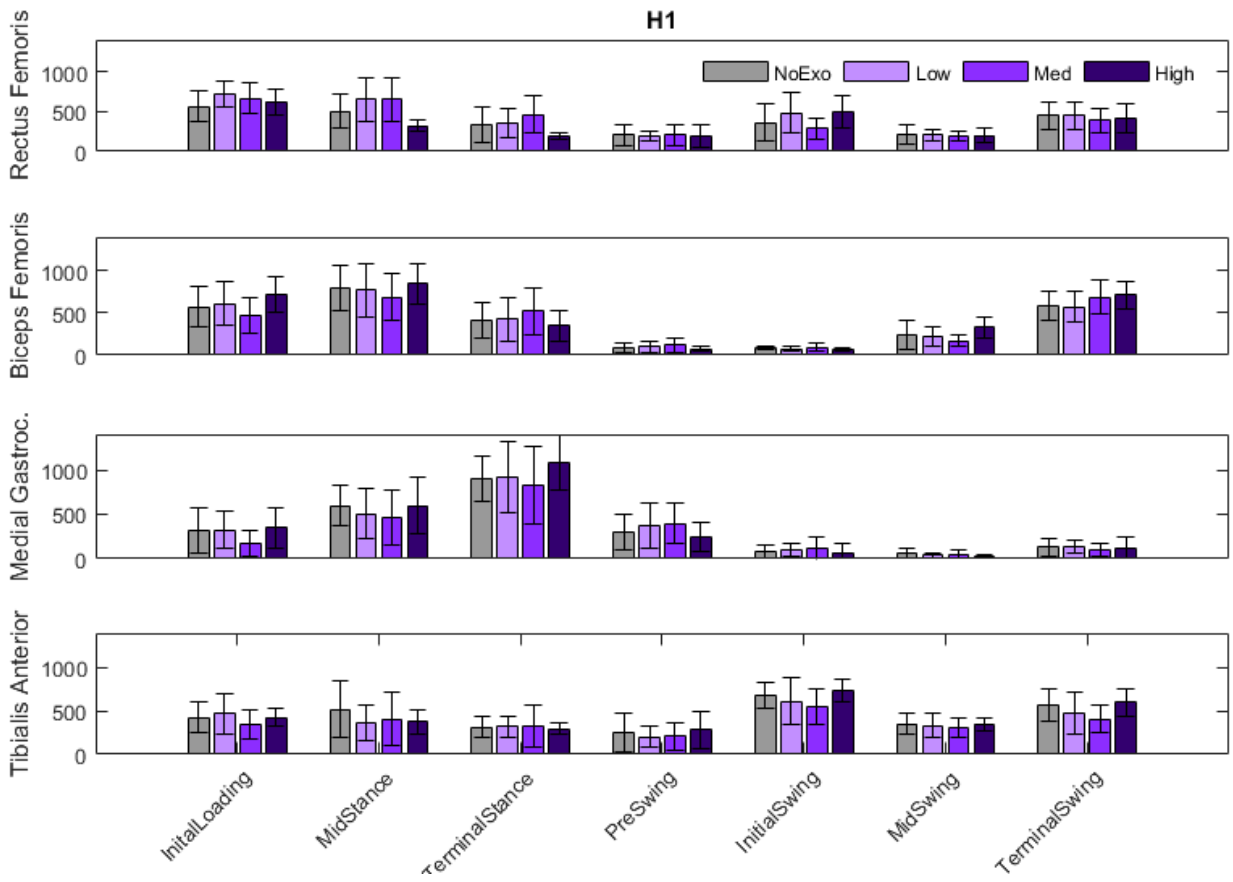
H1
NoExo
Low
Med
High
Rectus Femoris
Biceps Femoris
Medial Gastroc.
Tibialis Anterior
1000
500
0
InitalLoading
MidStance
TerminalStance
PreSwing
InitialSwing
MidSwing
TerminalSwing

H2 – Right Leg

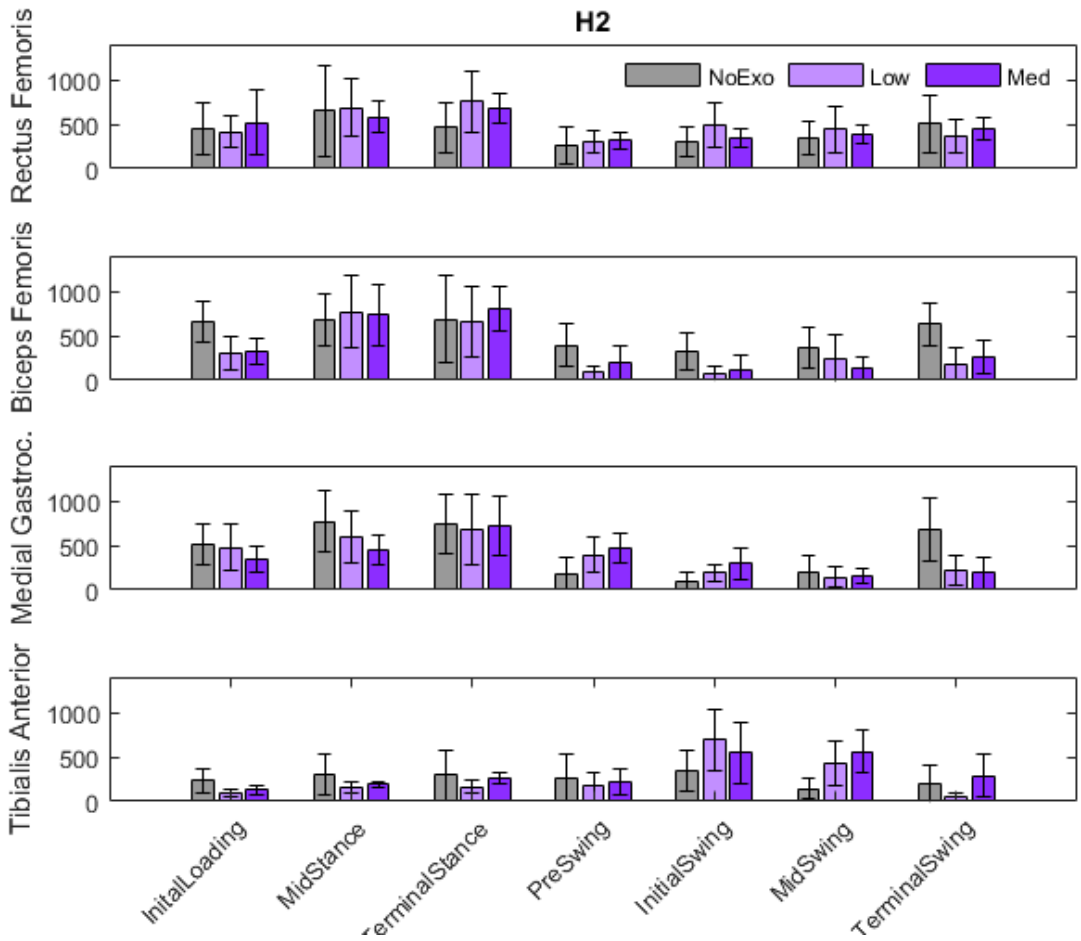
H2
NoExo
Low
Med
Rectus Femoris
Biceps Femoris
Medial Gastroc.
Tibialis Anterior
1000
500
0
InitalLoading
MidStance
TerminalStance
PreSwing
InitialSwing
MidSwing
TerminalSwing

H2 – Left Leg

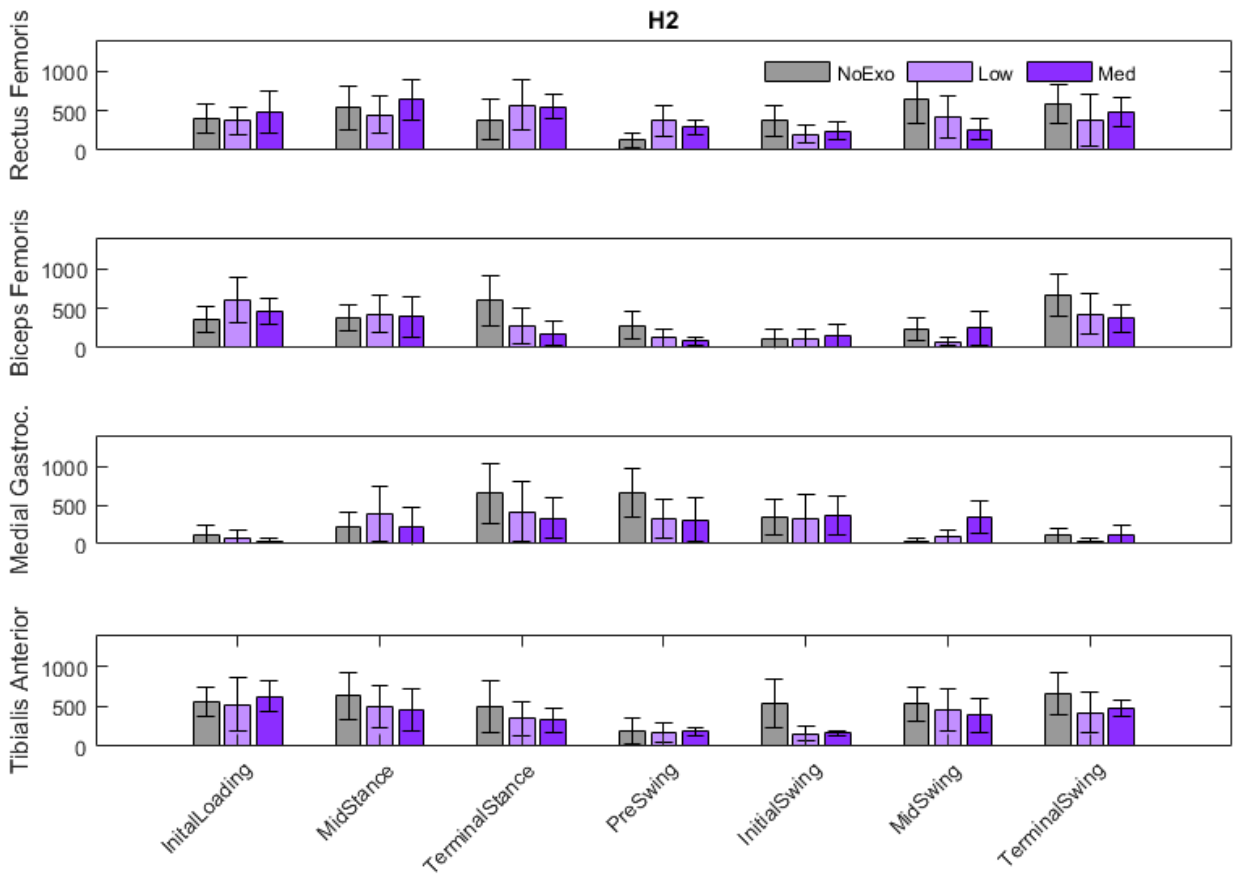
H2
NoExo
Low
Med
Rectus Femoris
Biceps Femoris
Medial Gastroc.
Tibialis Anterior
1000
500
0
InitalLoading
MidStance
TerminalStance
PreSwing
InitialSwing
MidSwing
TerminalSwing